Oklahoma Department of Transportation
200 NE 21st Street, Oklahoma City, OK 73105-3204

FINAL REPORT ~ FHWA-OK-22-01

DEMONSTRATION OF THE APPLICABILITY OF THE NEW CPTU/SCPTU CORRELATIONS WITH SOIL PARAMETER EVALUATION

Gerald A. Miller, Ph.D., P.E.
Tareq Abuawad, Ph.D. Candidate

School of Civil Engineering and Environmental Science (CEES)
The University of Oklahoma
Norman, Oklahoma

James Nevels, Ph.D., P.E.

J.N. In Situ, Inc.

January 2022

OKLAHOMA Transportation

PUBLIC DISCLAIMER

The Oklahoma Department of Transportation (ODOT) ensures that no person or groups of persons shall, on the grounds of race, color, sex, religion, national origin, age, disability, retaliation or genetic information, be excluded from participation in, be denied the benefits of, or be otherwise subjected to discrimination under any and all programs, services, or activities administered by ODOT, its recipients, sub-recipients, and contractors. To request an accommodation please contact the ADA Coordinator at 405-521-4140 or the Oklahoma Relay Service at 1-800-722-0353. If you have any ADA or Title VI questions email ODOT-ada-titlevi@odot.org.

DISCLAIMER

The contents of this report reflect the views of the author(s) who is responsible for the facts and the accuracy of the data presented herein. The contents do not necessarily reflect the views of the Oklahoma Department of Transportation or the Federal Highway Administration. This report does not constitute a standard, specification, or regulation. While trade names may be used in this report, it is not intended as an endorsement of any machine, contractor, process, or product.

DEMONSTRATION OF THE APPLICABILITY OF THE NEW CPTU/SCPTU CORRELATIONS WITH SOIL PARAMETER EVALUATION

FINAL REPORT ~ FHWA-OK-22-01

ODOT SPR ITEM NUMBER 2308

Submitted to:

Office of Research and Implementation

Oklahoma Department of Transportation

Submitted by:

Gerald A. Miller, Ph.D., P.E.
Tareq Abuawad, Ph.D. Candidate
School of Civil Engineering and Environmental Science (CEES)
The University of Oklahoma
James Nevels, Ph.D., P.E.
J.N. In Situ, Inc.

OKLAHOMA
Transportation

January 2022

TECHNICAL REPORT DOCUMENTATION PAGE

<table>
<tr><td colspan="2">1. REPORT NO.
FHWA-OK-22-01</td><td>2. GOVERNMENT ACCESSION NO.</td><td colspan="2">3. RECIPIENT'S CATALOG NO.</td></tr>
<tr><td colspan="3">4. TITLE AND SUBTITLE
DEMONSTRATION OF THE APPLICABILITY OF THE NEW CPTU/SCPTU CORRELATIONS WITH SOIL PARAMETER EVALUATION</td><td colspan="2">5. REPORT DATE
Jan 2022
6. PERFORMING ORGANIZATION CODE</td></tr>
<tr><td colspan="3">7. AUTHOR(S)
Gerald A. Miller, PE, PhD, Tareq Z. Abuawad, PhD (Candidate), James Nevels, PE, PhD</td><td colspan="2">8. PERFORMING ORGANIZATION REPORT</td></tr>
<tr><td colspan="3">9. PERFORMING ORGANIZATION NAME AND ADDRESS
University of Oklahoma
School of Civil Engineering and Environmental Science
202 West Boyd Street, Room 334
Norman, OK 73019</td><td colspan="2">10. WORK UNIT NO.
11. CONTRACT OR GRANT NO.
ODOT SPR Item Number 2308</td></tr>
<tr><td colspan="3">12. SPONSORING AGENCY NAME AND ADDRESS
Oklahoma Department of Transportation
Office of Research and Implementation
200 N.E. 21st Street, Room G18
Oklahoma City, OK 73105</td><td colspan="2">13. TYPE OF REPORT AND PERIOD COVERED
Final Report
Oct 2018 - Dec 2021
14. SPONSORING AGENCY CODE</td></tr>
<tr><td colspan="5">15. SUPPLEMENTARY NOTES</td></tr>
<tr><td colspan="5">16. ABSTRACT
Nine test sites across the state of Oklahoma were investigated using the Seismic Cone Penetration Test with pore water pressure measurement (SCPTu). Field testing was conducted during wet and dry periods to observe the effect of moisture conditions on the data collected from the field. Disturbed and undisturbed samples were collected at each site to conduct laboratory tests and determine the properties of the soils tested. Using the field and laboratory data, correlations proposed in the literature to predict various soil properties were tested for their applicability to Oklahoma Soils. Results showed that some existing and new correlations may provide reasonable first approximations of soil properties. However, there is considerable uncertainty with these correlations based on scatter observed in the comparisons to SCPTu and laboratory test data gathered in this current study. Additionally, it was observed that the moisture conditions at the time of SCPTu has a considerable influence on predicted soil properties.</td></tr>
<tr><td colspan="2">17. KEY WORDS
Cone testing, unsaturated soils, shear wave velocity, soil properties, correlations</td><td colspan="3">18. DISTRIBUTION STATEMENT
No restrictions. This publication is available from the Office of Research and Implementation, Oklahoma DOT.</td></tr>
<tr><td colspan="2">19. SECURITY CLASSIF. (OF THIS REPORT)
Unclassified</td><td>20. SECURITY CLASSIF. (OF THIS PAGE)
Unclassified</td><td>21. NO. OF PAGES
Incl. cover & roman numeral pages 184</td><td>22. PRICE
N/A</td></tr>
</table>

SI CONVERSION FACTORS

SI* (MODERN METRIC) CONVERSION FACTORS

APPROXIMATE CONVERSIONS TO SI UNITS

SYMBOL	WHEN YOU KNOW	MULTIPLY BY	TO FIND	SYMBOL
		LENGTH		
in	inches	25.4	millimeters	mm
ft	feet	0.305	meters	m
yd	yards	0.914	meters	m
mi	miles	1.61	kilometers	km
		AREA		
in^2	square inches	645.2	square millimeters	mm^2
ft^2	square feet	0.093	square meters	m^2
yd^2	square yard	0.836	square meters	m^2
ac	acres	0.405	hectares	ha
mi^2	square miles	2.59	square kilometers	km^2
		VOLUME		
fl oz	fluid ounces	29.57	milliliters	mL
gal	gallons	3.785	liters	L
ft^3	cubic feet	0.028	cubic meters	m^3
yd^3	cubic yards	0.765	cubic meters	m^3
	NOTE: volumes greater than 1000 L shall be shown in m^3			
		MASS		
oz	ounces	28.35	grams	g
lb	pounds	0.454	kilograms	kg
T	short tons (2000 lb)	0.907	megagrams (or "metric ton")	Mg (or "t")
		TEMPERATURE (exact degrees)		
°F	Fahrenheit	5 (F-32)/9 or (F-32)/1.8	Celsius	°C
		ILLUMINATION		
fc	foot-candles	10.76	lux	lx
fl	foot-Lamberts	3.426	candela/m^2	cd/m^2
		FORCE and PRESSURE or STRESS		
lbf	poundforce	4.45	newtons	N
lbf/in^2	poundforce per square inch	6.89	kilopascals	kPa

APPROXIMATE CONVERSIONS FROM SI UNITS

SYMBOL	WHEN YOU KNOW	MULTIPLY BY	TO FIND	SYMBOL
		LENGTH		
mm	millimeters	0.039	inches	in
m	meters	3.28	feet	ft
m	meters	1.09	yards	yd
km	kilometers	0.621	miles	mi
		AREA		
mm^2	square millimeters	0.0016	square inches	in^2
m^2	square meters	10.764	square feet	ft^2
m^2	square meters	1.195	square yards	yd^2
ha	hectares	2.47	acres	ac
km^2	square kilometers	0.386	square miles	mi^2
		VOLUME		
mL	milliliters	0.034	fluid ounces	fl oz
L	liters	0.264	gallons	gal
m^3	cubic meters	35.314	cubic feet	ft^3
m^3	cubic meters	1.307	cubic yards	yd^3
		MASS		
g	grams	0.035	ounces	oz
kg	kilograms	2.202	pounds	lb
Mg (or "t")	megagrams (or "metric ton")	1.103	short tons (2000 lb)	T
		TEMPERATURE (exact degrees)		
°C	Celsius	1.8C+32	Fahrenheit	°F
		ILLUMINATION		
lx	lux	0.0929	foot-candles	fc
cd/m^2	candela/m^2	0.2919	foot-Lamberts	fl
		FORCE and PRESSURE or STRESS		
N	newtons	0.225	poundforce	lbf
kPa	kilopascals	0.145	poundforce per square inch	lbf/in^2

*SI is the symbol for the International System of Units. Appropriate rounding should be made to comply with Section 4 of ASTM E380. (Revised March 2003)

Acknowledgement

The authors are grateful to the various ODOT residencies and county governments that assisted with identification and access to field test sites. Thanks is also due to Scott Garland and Chris Clarke of ODOT Materials Division for their review and constructive suggestions. This research was funded by the Oklahoma Department of Transportation and this support is gratefully acknowledged.

Table of Contents

List of Tables

APPENDIX D TABLES

List of Figures

APPENDIX A FIGURES

APPENDIX B FIGURES

APPENDIX C FIGURES

1 Introduction

1.1 General

In recent years, cone penetration testing has become one of the more common soil profiling testing methods for geotechnical applications in different construction projects. In transportation projects, cone penetration tests (CPTs) can be used for subsurface exploration for new projects, rehabilitation projects and forensic investigations. One of the significant advantages of cone testing is the ability to produce a continuous soil profile. Despite all the advantages of the CPT, the inability to obtain soil samples from the field is one of the biggest disadvantages using this testing method. It is common for engineers to use CPT correlations found in the literature to predict different soil parameters (e.g. shear strength, OCR, friction angle, etc.). However, there is significant uncertainty surrounding the CPT correlations because they rely on empiricism, and because local site conditions may be different from those used to develop the correlations.

A primary purpose of this study was to collect data from field testing and laboratory testing of Oklahoma soils and compare them to existing correlations found in the literature. The goal was to determine if the data collected from field and the laboratory tests on Oklahoma soils would fit the CPT correlations proposed by other researchers (e.g. Mayne and Kemper 1899, Mayne 2014, Robertson 2016).

Another goal of this study was to examine the effect of variations in moisture content of the soil, due to the seasonal changes, on the measured cone testing parameters. As the moisture content changes the stress state (in terms of soil suction)

is changed. The importance of the stress state of the soil lies in the role it plays in the soil's strength and stiffness.

The field and laboratory testing program utilized nine sites across the state of Oklahoma. The nine sites included various soil types according to the USCS classification system as follows:

- Site #1 (ML),
- Site #2 (CL and CH),
- Site #3 (CH),
- Site #4 (CH),
- Site #5 (CL and CH),
- Site #6 (ML, CL and CH),
- Site #7 (ML and SM),
- Site #8 (CL and CH), and
- Site #9 (ML and SM).

Soil samples were collected from the field during site visits to prepare laboratory specimens for testing.

For field testing, Seismic Cone Penetration Tests with pore pressure measurements (SCPTu) were conducted at each site. During each visit, cone parameters including tip resistance (q_c), sleeve friction (f_s), and pore pressure (u_2) were measured nearly continuously with depth and shear wave velocity (V_s) was determined at discrete depths. Drilling and sampling were also performed at each of the testing sites to collect disturbed and undisturbed soil samples for laboratory testing.

In addition to field testing, laboratory testing was conducted to examine the strength, stress-strain behavior, physical and index properties (Atterberg limits, unit weight, natural water content, etc.), and total suction of the soil collected from the testing sites.

Correlations were examined involving cone testing parameters, shear wave velocity, and the soil's mechanical properties. Modifications were applied to the existing correlations as needed to account for differences in the soils tested in Oklahoma and new correlations were proposed for some soil parameters.

1.2 Objectives and tasks

This is the final research report for the project titled “Demonstration of the Applicability of the New CPTu/SCPTu Correlations with Soil Parameter Evaluation”. The purpose of research described in this report is captured broadly by the following three objectives:

1. To demonstrate the applicability of various cone testing correlations to a broad range of Oklahoma soil types and as needed, develop specific correlations for Oklahoma soil based on laboratory test results and SCPTu data collected.
2. To better understand the behavior of the SCPTu parameters in unsaturated soils and the effect of degree of saturation on various correlations for predicting soil properties.
3. To produce comprehensive recommendations for the application of CPT, CPTU, and SCPTu tests for geotechnical engineers in Oklahoma.

To achieve these objectives, the following tasks were completed:

1. Selected nine testing sites that represent different soil types and profiles across Oklahoma.
2. Conducted field testing using SCPTu, and different sampling methods to gather data for laboratory testing, analysis and comparison.
3. Conducted laboratory testing on soil obtained from field test sites to estimate different physical, index, and mechanical soil properties.
4. Established graphical and/or mathematical relationships between SCPTu parameters and various soil properties.

1.3 Layout of the report

There are five chapters following the introductory chapter. Chapter 2 provides a literature review of past research related to the project's topics and helpful correlations that were used during this study. Chapter 3 describes the testing program followed by the results in Chapter 4. Chapter 5 presents the empirical correlations along with SCPTu data and corresponding laboratory determined soil properties from this study. Finally, Chapter 6 provides some conclusions and recommendations for practice and further research.

2 Literature Review

2.1 Introduction

In this chapter, previous research on CPT, CPTu and SCPTu testing and some of the numerous correlations existing in the published literature are discussed.

2.2 Overview

The cone penetration test (CPT) is a mechanical test used to evaluate the properties of soil subjected to deep penetration. Early on it was used in 1935 by the Laboratory of Soil Mechanics at Delft; a historical overview of the development of the CPT was described by Massarsch (2014). CPTs are known for their unique advantages for in situ testing, which include fast and continuous profiling, easy repeatability of the test, high reliability in terms or operator dependency, economical and less time consuming, and there are many methods for interpretation. Disadvantageous include lack of soil samples and determination of soil properties relies on empirical methods which inherently involve considerable uncertainty.

A friction cone penetrometer (CPT) is a steel probe that is pushed vertically into a soil profile and used to measure the forces generated by the soil at the tip and along a friction sleeve during penetration. The tip resistance (q_c), and sleeve friction (f_s) at a point in the soil profile is computed by dividing the tip force by the cross-sectional area and the sleeve friction force by the sleeve area, respectively. Friction Ratio (FR) is the sleeve friction divided by the tip resistance, and expressed as a percentage. Friction Ratio is commonly used to estimate the type of soil that is tested. The principles and techniques of friction cone and piezocone testing have been thoroughly studied to improve their effectiveness, and the standardized procedure for conducting the test is

referenced in ASTM D5778-12, Standard Test Method for Electronic Friction Cone and Piezocone Penetration Testing of Soils.

During piezocone testing (CPTu), pore water pressure measurements are collected using an additional sensor attached to the steel probe, usually just behind the tip (known as the u_2 pore pressure measurement location). This test is very useful in saturated soils for analyzing soil type and properties. However, when conducting the CPTu in unsaturated soils, desaturation of the pore pressure measuring system is possible, which would affect the sensor's response and the reliability of the data.

An example of SCPTu results from the current study is shown in Figure 1; it includes the soil stratigraphy, tip resistance (q_c), sleeve friction (f_s), pore water pressure (u), and shear wave velocity (V_s). The figure shows the changes in the cone parameters through the soil profile and the variation of q_c, f_s, u_o, and V_s with depth. The data in Figure 1 are from the SCPTu tests conducted during a field visit to Site #6 in Wewoka, Oklahoma.

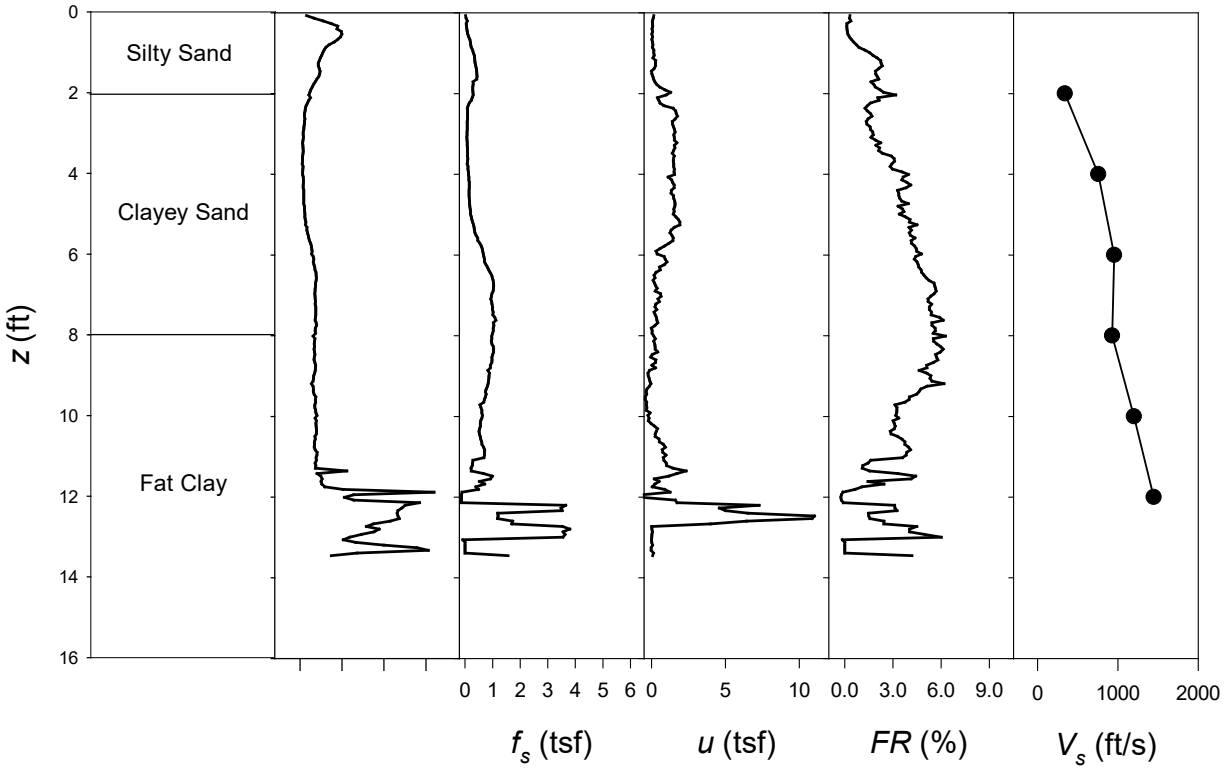

Figure 1. Results for SCPTu tests at Site 6 (Wewoka) showing depth against soil stratigraphy, q_c, f_s, u, FR, and V_s

2.3 Cone penetration testing in saturated soils

The literature on CPT, CPTu and SCPTu testing in saturated soils is vast. Data collected from the CPT and CPTu, and SCPTu tests have been used to interpret soil properties such as soil type, unit weight, relative density, friction angle, shear strength and consolidation properties. Schmertmann (1978), Lunne et al. (1997), Gui et al (1998), and Robertson and Cabal (2015), among others, have proposed general guidelines on cone applications for engineering practice.

Different approaches are proposed to determine soil properties in coarse- and fine-grained soils (e.g. Robertson and Campanella 1983a and 1983b, Mayne and Kemper 1988, Mayne 2006a, Mayne 2014, Robertson 2009, Saye et al. 2013,

Robertson 2016). For coarse-grained soils (gravel and sands), relative density (D_r), elastic modulus (E), and friction angle (ϕ') are of primary interests, while for fine-grained soils, undrained shear strength, coefficient of consolidation (c_v), overconsolidation ratio (OCR), and coefficient of compressibility (m_v) or consolidation parameters are of primary interest.

Multiple theories and approaches have been proposed for interpreting CPTs in saturated soils such as, theory of bearing capacity (Durgunoglu and Mitchell 1975, Robertson and Campanella 1983), cavity expansion theory (Vesic 1972) and studies involving CPTs in calibration chambers (Houlsby and Hitchman 1988). Using these theories and studies, many methods have been proposed to analyze CPT data.

More recently, cone penetrometers have been equipped for determination the shear wave velocity of the soil. These tests are done by equipping the steel cone with an accelerometer or geophones to detect the shear waves generated in the soil profiles by an excitation at the ground surface. Comprehensive guides and recommendations for the application and analysis of seismic cone data are also available in numerous publications (e.g. Robertson et al. 1986, Mayne and Rix 1995, Mayne 2006b, Hegazy and Mayne 2006, Wair et al. 2012, Robertson and Cabal 2015).

2.4 Cone penetration testing in unsaturated soils

Although the literature on cone penetration testing in saturated or dry soils is vast, there are relatively fewer studies that deal with the interpretation of cone test results from unsaturated soil profiles. The behavior of unsaturated soils varies significantly to that of saturated and dry soils. As discussed in this section, some researchers have investigated the influence of saturation on cones parameters, mainly tip resistance.

Hryciw and Dowding (1987) studied cone penetration in partially saturated sands and found that saturation had a significant influence on the tip resistance. Results showed that the tip resistance values were higher in low saturation soil than dry soil while increasing the saturation between 70 to 90% showed lower tip resistance compared to fully saturated soils.

The results from Hryciw and Dowding study led other researchers to investigate the effects of saturation and suction on cone parameters (Houston et al. 1995, Lehane et al. 2004, Nevels 2006, Collins and Miller 2014, Collins 2016, Rocha et al. 2016, Tang et al. 2017, Miller et al. 2018, Lo Presti et al. 2018, Miller et al. 2021). Changes in soil's suction is associated with changing the saturation, which affects the stress state of the soil. Results showed that as saturation decreased and matric suction increased in the soil, this generally led to an increase in the tip resistance values.

Empirical methods for estimating the bearing capacity in unsaturated soils using cone parameters have been presented by some authors (Mohammad and Vanpalli 2015, Miller et al. 2021) and some studies have attempted to develop and validate numerical and analytical methods for estimating the properties of soil from cone penetration tests conducted in unsaturated soils (Yang and Russel 2015, Tang et al. 2017). These methods are largely based on empirical data and are not yet widely used. While they provide a step-by-step approach to interpret CPT results in unsaturated soils, they are not yet widely used because of the limitations of the number of soils that have been tested.

2.5 Existing correlations for estimating soil properties based on cone parameters

Various correlations have been proposed to interpret soil types and properties using results of cone penetration tests. In this section a few common correlations used in geotechnical engineering practice are presented.

2.5.1 Soil type interpretation

Robertson et al. (1986) presented a CPT-based method to estimate soil type based on suggested charts, these charts were developed using the tip resistance and friction ratio of the cone. The charts known as the Soil Behavior Type (SBT) charts are popular because of the simplicity in plotting the cone results. Robertson (1990) proposed a modified version of the SBT chart using normalized cone parameters, which allows for more accurate and reliable interpretations since effective stress is taken into consideration. Jeffries and Davis (1993) identified the SBT index "I_c" used in normalized SBT charts. I_c is used to identify the radius of concentric circles that define the soil type within the classification chart. Robertson and Wride (1998) modified the definition of I_c to apply for the proposed normalized SBT charts. Equation 1 is used to calculate I_c.

$$I_c = \sqrt{(3.47 - logQ_{tn})^2 + (1.22 + \log F_r)^2} \quad (1)$$

Where Q_{tn} is the normalized tip resistance corrected for the penetration induced pore water pressure and F_r is the normalized sleeve friction. An example of the normalized SBT-I_c chart is shown in Figure 2.

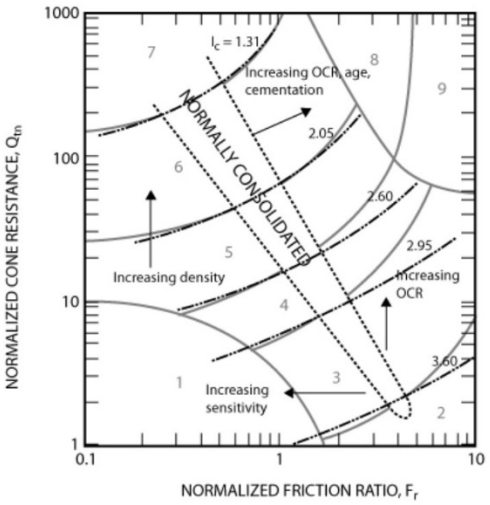

Zone	*Soil Behavior Type*	I_c
1	*Sensitive, fine grained*	N/A
2	*Organic soils – clay*	> 3.6
3	*Clays – silty clay to clay*	2.95 – 3.6
4	*Silt mixtures – clayey silt to silty clay*	2.60 – 2.95
5	*Sand mixtures – silty sand to sandy silt*	2.05 – 2.6
6	*Sands – clean sand to silty sand*	1.31 – 2.05
7	*Gravelly sand to dense sand*	< 1.31
8	*Very stiff sand to clayey sand**	N/A
9	*Very stiff, fine grained**	N/A

** Heavily overconsolidated or cemented*

Figure 2. Normalized SBT (Robertson 1990), updated by Robertson (2010)

2.5.2 Soil property interpretations

Multiple correlations have been proposed to estimate physical and mechanical soil properties using cone data. Below, a description of some common correlations used in CPT analysis is presented.

2.5.2.1 Unit weight

For total unit weight a trend between unit weight and sleeve friction has been identified by Mayne and Peuchen (2012). The relationship between total unit weight and sleeve friction is presented using two empirical correlations represented by Equations 2 and 3.

$$\gamma_t = 26 - \frac{14}{1+(0.5*\log(f_s+1))^2} \quad (2)$$

And

$$\gamma_t = 12 - 1.5 * \ln(f_s + 1) \tag{3}$$

In Figure 3, the results presented by Mayne and Peuchen (2012) for different types of soils are shown.

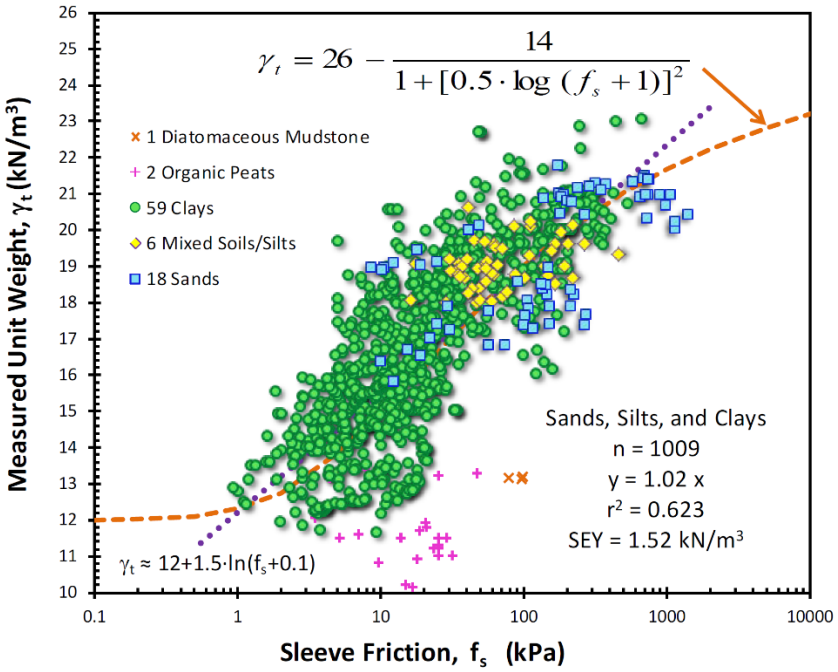

Figure 3. Correlation between CPT sleeve friction and total unit weight (Mayne and Peuchen 2012)

2.5.2.2 Undrained shear strength

The undrained shear strength represents the shearing resistance of soil in the presence of shear induced excess pore water pressures. It depends on the loading, soil anisotropy and strain rate. Equation 4 represents a semi-empirical correlation, based on bearing capacity theory, between s_u and the tip resistance Lunne et al. (1997).

$$s_u = \frac{q_c - \sigma_{vo}}{N_{kt}} \tag{4}$$

Where N_{kt} is an empirical factor that depends on the plasticity and sensitivity of the soil. Typically, N_{kt} varies from 10 to 18 with an average of 14 (Lunne et al. 1997). However, Marsland and Quarterman (1982) have observed higher N_{kt} values in the mid 20's to mid 30's for overconsolidated and fissured clays.

2.5.2.3 Overconsolidation ratio and preconsolidation stress

The overconsolidation ratio (*OCR*) is the ratio of preconsolidation stress (σ'_p) and the current effective overburden stress (σ'_{vo}) at a point in the soil profile, where σ'_p is determined using a one-dimensional consolidation test. Robertson (2009) suggested a correlation represented by Equation 5 to estimate the *OCR* for overconsolidated clay soils using the normalized tip resistance.

$$OCR = 0.25 * Q_t^{1.25} \tag{5}$$

Mayne et al. (2009) proposed Equation 6 for the relationship between the net tip resistance and yield stress, σ'_y (note $\sigma'_p = \sigma'_y$). It includes empirical exponent m' which appears to be a function of the mean grain size of the soil.

$$\sigma'_y = 0.33(q_t - \sigma_{vo})^{m'} \tag{6}$$

In Figure 4, data collected by Mayne for many different soil types are shown along with lines representing Equation 6 and different values of exponent m', which appears to be strongly correlated to soil type.

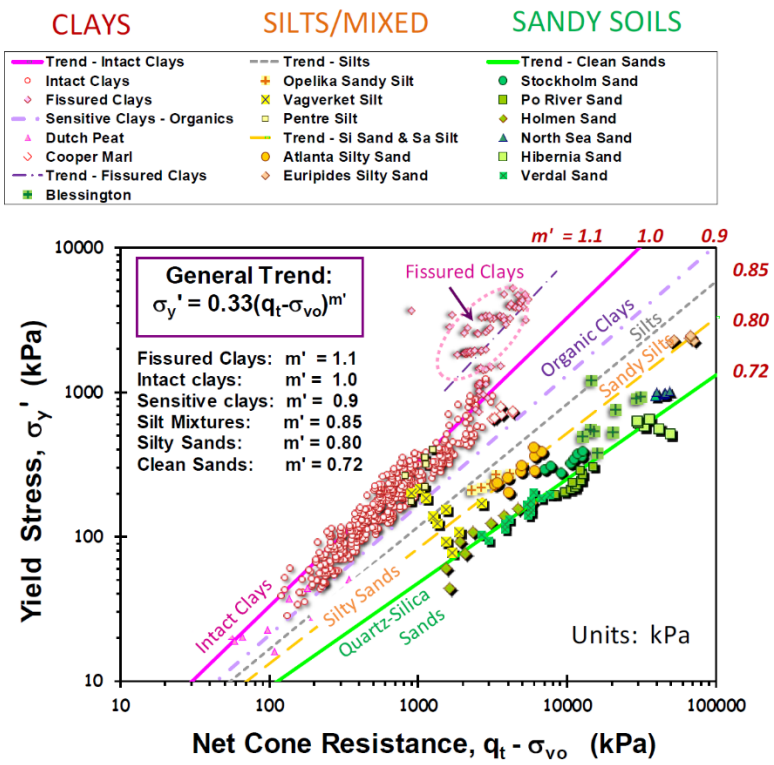

Figure 4. Net cone resistance versus yield stress (Mayne et al 2009)

2.5.2.4 Shear wave velocity

Robertson and Cabal (2015) used I_c to correlate the cone's normalized tip resistance to the normalized shear wave velocity as show by Equation 7.

$$V_s = (\alpha_{vs} * (q_t - \sigma_{vo})/p_a)^{0.5} \; where \; \alpha_{vs} = 10^{0.55I_c + 1.68} \tag{7}$$

Rix and Mayne (1995) proposed an empirical relationship between shear wave velocity and tip resistance given by Equation 8 for intact and fissured clays, while Hegazy and Mayne (2006) presented Equation 9 involving sleeve friction for both cohesive and cohesionless soils.

$$V_s = 1.75 * q_c^{0.627} \tag{8}$$

$$V_s = 78.11 * (f_s)^{0.2475} \tag{9}$$

These equations are represented in Figures 5 and 6, respectively. respectively, where predicted shear wave velocities are compared against those directly measured with the seismic cone for the same sounding.

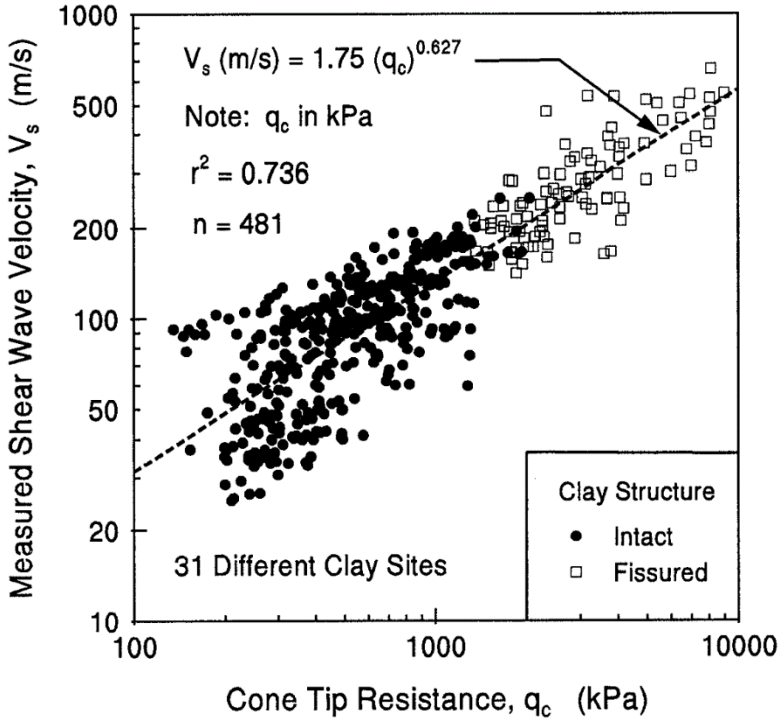

Figure 5. Tip Resistance versus shear wave velocity (Mayne and Rix 1995)

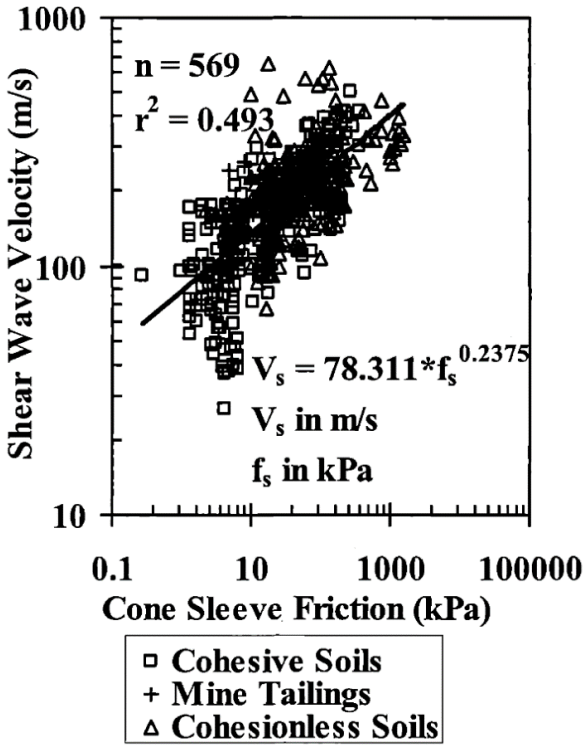

Figure 6 Sleeve Friction versus Shear Wave Velocity (Hegazy and Mayne 2006)

2.5.2.5 Friction angle

Research was conducted on coarse-grained soils to determine the correlation between the cone parameters and the friction angle (ϕ'). In most studies, direct shear tests and triaxial tests were used to measure ϕ' in the lab. Several empirical correlations have been proposed for uncemented quartz sands (e.g. Robertson and Campanella 1983, Kulhawy and Mayne 1990, Uzielli et al 2013).

Fewer studies have looked at friction angle correlations for clays and silts. In some studies, CPT tip resistance was correlated to friction angle using different proposed factors and excess pore water pressure (e.g. Sanven and Want 1995, Mayne 2006).

In this research, correlations proposed by Kulhawy and Mayne (1990) and Uzielli et al. (2013) were used. These correlations given by Equations 10 and 11, respectively, utilize the stress normalized tip resistance corrected for penetration induced pore water pressure (q_{t1}) (note q_{t1}= Normalized q_t). A comparison of these equations to friction angles obtained from triaxial testing on low plasticity soils are shown in Figure 7.

$$\phi' = 25°(q_{t1})^{0.1} \tag{10}$$

$$\phi' = 17.6° + 11 * log(q_{t1}) \tag{11}$$

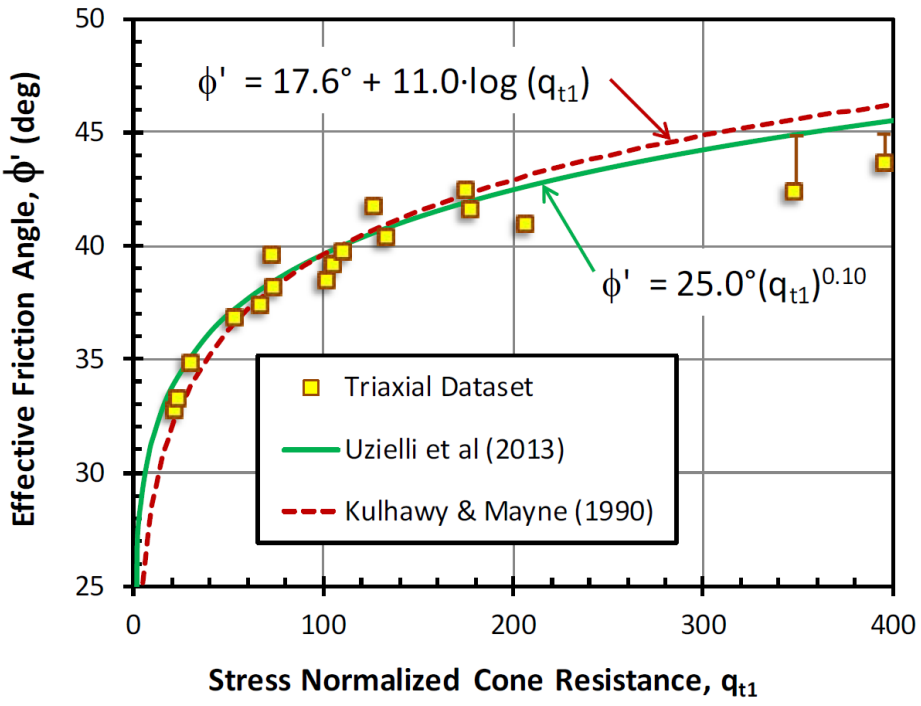

Figure 7. Stress Normalized Tip Resistance versus Effective Friction Angle (Mayne 2014)

3 Methods and Materials

3.1 Introduction

This chapter describes the test site soils and the testing methods used in this research to determine the various field and laboratory soil parameters investigated.

3.2 Test sites

Nine sites were tested around the State of Oklahoma. The locations were chosen to ensure that a good representation of the Oklahoma soils was tested. A list of the test sites and the corresponding geological origin, soil type and location are shown in Table 1. The approximate locations of the field-testing sites is shown in Figure 8.

3.3 Field testing

3.3.1 Introduction

Field testing including SCPTu and soil sampling were performed at the chosen sites. Each site was visited twice; an attempt was made to visit each site during a wet period and dry period. During each visit, four SCPTu testing locations, approximately five feet apart, were used to ensure that profiles were obtained in the same general location. At each testing location a cone sounding was taken to refusal. In addition, seismic velocity readings were obtained during each sounding at discrete depths.

For soil sampling, continuous disturbed and undisturbed samples were collected within the active zone (depth ranging between 8-12 feet depending on the soil profile). These depths represent the general active zone of the soil profiles in Oklahoma.

Table 1. List of tested sites and locations

Location Number	Geological Origin	Soil Types	Location	Latitude	Longitude
1	Eolian	Wind blown silts and silty sands (SPT Calibration Site)	Curtis	36°26'4.79"N	99° 8'4.48"W
2	Residual	Clay soils	Lake Hefner	35°33'37.97"N	97°36'51.83"W
3	Alluvial	Mixed clay soils	Muskoge e	35°56'42.16"N	96° 0'39.45"W
4	Alluvial	Clay soils	Wagoner	35°57'5.38"N	95°32'5.19"W
5	Residual	Clay soils	Hobart	34°59'24.71"N	99° 3'9.87"W
6	Alluvial / Residual	Paleoterrace, clayey and loamy colluvium or alluvium over clayey residuum weathered from shale	Wewoka	35°10'59.54"N	96°28'53.89"W
7	Alluvial	Fine sand	Norman	35°12'1.02"N	97°29'2.69"W
8	Residual	Mixed clay soils	Fairview	36°15'9.03"N	98°28'47.13"W
9	Residual	Mixed clays, sands and silty clays	Fears Lab-University of Oklahom a	35°11'26.54"N	97°26'14.54"W

3.3.2 Seismic cone penetration testing

The SCPTu was performed at each testing location generally according to the procedure given in the American Society for Testing and Materials (ASTM) Standard D5778 "Standard Test Method for Electronic Friction Cone and Piezocone Penetration Testing of Soils" (ASTM 2012).

For each cone sounding the cone was pushed into the soil and the tip resistance (q_c), sleeve friction (f_s), friction ratio (FR), and pore pressure (u_2) were recorded with depth. To measure the shear wave velocities (V_s) at discrete depths, the procedure provided in the American Society for Testing and Materials (ASTM) D7400/D7400M-19

“Standard Test Methods for Downhole Seismic Testing” (ASTM 2017) was followed. Measurements were taken at a two to three foot intervals depending on the soil profile tested. A 5 lb hammer was used to hit the right and left metal plates placed under the cone truck. The hammer excitation generates shear waves that are recorded using the geophones embedded in the cone.

3.3.3 Soil sampling

Soil samples were collected for laboratory testing as described below.

3.3.3.1 Disturbed samples

For collecting disturbed samples, one of the following methods were performed at each test site. In general accordance with the American Society for Testing and Materials (ASTM) D1452-16 “Standard Practice for Soil Exploration and Sampling by Auger Borings” ASTM (2009), and (ASTM) D6282-14 “Standard Guide for Direct Push Soil Sampling for Environmental Site Characterizations” (ASTM 2014). The first method was used during the first visit to the testing sites and the second method was used during the second visit.

3.3.3.2 Undisturbed samples

Undisturbed sampling was performed according to the American Society for Testing and Materials (ASTM) D1587-15 “Standard Practice for Thin-Walled Tube Sampling of Fine-Grained Soils for Geotechnical Purposes” (ASTM 2015). For each site, thin wall tube sampling was performed to collect soil samples in the active zone if possible.

3.4 Classification and physical property testing

3.4.1 Particle size analysis

A particle size analysis was performed on soil collected from the field test sites. For sites 1 through 6, and 8 the particle size analysis data were obtained from previous ODOT testing conducted at the same site location in the field. For sites 7 and 9 testing was conducted in the University of Oklahoma laboratory using disturbed samples collected in the field. Testing was performed in general accordance with the American Society for Testing and Materials (ASTM) D 6913-17 “Standard Test Methods for Particle-Size Distribution (Gradation) of Soils Using Sieve Analysis ” (ASTM 2017).

3.4.2 Atterberg limits testing

Atterberg limit tests were performed on soils collected from the field testing sites. For sites 1 through and 8 the Atterberg limits data were obtained from previous ODOT testing conducted at the same site location in the field. For sites 7 and 9 testing was conducted in the University of Oklahoma laboratory using disturbed samples collected in the field. The Atterberg Limits tests were performed in accordance with ASTM D 4318-21 “Standard Test Method for Liquid Limit, Plastic Limit, and Plasticity Index of Soils” (ASTM 2009).

3.4.3 Unit weight

The unit weight measurements on the undisturbed soil samples were performed in general accordance with the ASTM D7263−09 “Standard Test Methods for Laboratory Determination of Density and Unit Weight of Soil Specimens” (ASTM 2018).

3.4.4 WP4 total suction testing

Total suction measurements were performed on collected soil samples from the field. Testing was performed in general accordance with the “WP4 and WP4-T operator’s manual” (Version 5, 2007) provided by the Decagon device, Inc

3.5 Mechanical property testing

3.5.1 One dimensional consolidation testing

To determine the consolidation behavior of soils collected from the field, one dimensional consolidation testing was performed. This testing was done in general accordance with ASTM D2435/D2435M−11 “Standard Test Methods for One-Dimensional Consolidation Properties of Soils Using Incremental Loading” (ASTM 2011).

In order to simulate the field conditions of the soil, this test was also performed under unsaturated conditions. The testing procedures followed for the saturated and unsaturated state are described below.

3.5.1.1 Saturated testing

Samples were prepared by trimming the intact soils samples extruded from the Shelby tubes and placing the trimmed sample into a 2.5” diameter x 1” height metal ring. The weight of the sample and the ring were taken before starting the test to aid in the determination of soil phase properties. The excess soil from the trimmed sample was used to measure the natural water content. The trimmed sample was then placed in a consolidometer with porous stones and filter papers placed on top and bottom of the sample. After assembling the soil sample into the consolidometer, the sample was

loaded to the initial overburden pressure and inundated with water. A Load Increment Ratio (LIR) of one was used during testing to provide sufficient number of testing points. For each load increment the axial deformation readings were taken at 0.5, 1, 2, 4, 8, 15, 30, 60, 120, 240, 480 and 1440 minutes, measured from the time of each load application. When reaching the load increment of 4 tons per square foot (tsf) the sample was unloaded to 0.5 tsf and then reloaded to 8 tsf following the same load increment ratio.After applying the final load, the sample was unloaded and weighed to determine the final water content of the soil sample.

3.5.1.2 Unsaturated testing

For unsaturated one dimensional consolidation testing, the same steps followed during the saturated testing for preparing the soil sample were followed. After assembling the sample, the loading started without inundating the sample with water. A LIR of 1 was used during this test, each load was left for 24 hours and readings were taken at similar time intervals. After the loading was finished the sample was unloaded and weighed before putting it into the oven for drying.

3.5.2 Triaxial compression testing

To determine the shear strength of soils at the chosen sites, a multistage consolidated undrained triaxial compression test (CU) was performed. This testing was done with reference to ASTM D4767-11 “Standard Test Method for Consolidated Undrained Triaxial Compression Test for Cohesive Soils” (ASTM 2011). Specimens were prepared by trimming the thin-walled tube samples to obtain a height to diameter ratio of approximately 2. The prepared samples were sealed to the top cap and pedestal using a rubber membrane and placed in the triaxial cell. Assembled cells were filled with water

and a low initial confining stress was applied. Back pressure was applied incrementally to the top and bottom of the specimen to achieve saturation. Saturation was checked by measuring the B value of the specimen. Once adequate saturation was reached, cell pressure was increased to achieve an effective confining pressure equal to the assumed field overburden pressure, with the drainage lines open, and the sample was then left overnight to consolidate.

After the sample had consolidated, it was sheared at a rate of 1% per hour until the maximum shear stress was approached. After finishing the first stage and unloading the deviator stress, the effective confining pressure was doubled and the sample was left to consolidate. Shearing was repeated for the second stage at the same rate until the maximum shearing stress was approached. For the third stage the effective confining pressure was doubled again and the sample was left to consolidate overnight. For stage three the sample was again sheared at the rate of 1% per hour until ultimate shear failure occurred.

During testing the strain was determined for each stage using an LVDT gauge with a resolution of 0.0001 inches, the axial load applied was measured using a load cell with a resolution of 0.1 lbf and the pore water pressure was measured with a resolution of 0.01 psi. The values of the axial displacement, load, and pore water pressure were used to create the stress strain and p-q stress path curves, from which strength parameters could be determined.

4 Results and Discussion

4.1 Introduction

Nine sites were tested, some during wetter and drier periods to determine the effect of seasonal change on the data collected using the seismic cone penetration test (SCPTu). Disturbed and undisturbed samples were collected from each site for laboratory testing conducted to determine various soil properties. Results of field and laboratory measurements were analyzed and compared with goals of evaluating existing correlations between the SCPTu parameters and the soil properties. In this chapter the results from laboratory and field testing are presented.

4.2 Laboratory results

4.2.1 Index properties

The soils investigated in this study were tested to determine physical and index properties including grain size distribution (ASTM D 6913-17) and Atterberg Limits (ASTM D 4318-00). The results of these tests are presented in Tables 2 through 10. For each site the USCS classification, percent of fines and Atterberg limits are shown.

The data shown in the tables for Sites 1, 2, 3, 4, 5, 6, and 8 were obtained from records of previous studies by ODOT supplied by Dr. Nevels (see Oklahoma Department of Transportation References Nos. 34 to 40). The results were obtained from soils collected in the same location the CPT tests were conducted. For Sites 7 and 9, tests were conducted in the University of Oklahoma laboratory to determine soil properties needed for classification. The results indicate that soil profiles include various types of soils such as clays and clayey mixtures, silts and silty mixtures, and sand and

sandy mixtures. The sites investigated were primarily fine-grained; the exception being Site 1 (Curtis).

4.2.1.1 Site 1 (Curtis)

This site consists of eolian silts and silty sands, as shown in the Table 2. The top 4 feet of the soil profile is made of non-plastic silts while the bottom 6 feet is made of slightly plastic silts and silty sands mixtures.

Table 2. Soil index properties and classification for Site 1 (Curtis)

Depth (ft)	A-2-4	USC Group Class.	Percent Fines (%)	Liquid Limit (%)	Plastic Limit (%)	Plasticity Index (%)
1	A-2-4	SM	18	NP	NP	NP
2	A-2-4	SM	22	NP	NP	NP
3	A-2-4	SM	18	NP	NP	NP
4	A-4	SM	15	NP	NP	NP
5	A-6	SC	40	13	23	10
6	A-6	CL	63	16	40	24
7	A-2-4	CL	51	12	29	17
8	A-4	SM	25	NP	NP	NP
9	A-6	SC	34	14	22	8
10	A-2-4	SC	43	10	22	12

4.2.1.2 Site 2 (Lake Hefner)

This site is made of a shallow residual clay soil profile underlain by shale as shown in Table 3. The first few feet consist of fat clay soils while the lower part consists of lean clay.

Table 3. Soil index properties and classification for Site 2 (Lake Hefner)

Depth (ft)	AASHTO Group Class.	USC Group Class.	Percent Fines (%)	Liquid Limit (%)	Plastic Limit (%)	Plasticity Index (%)
1	A-7-6	CL	92	46	18	28
2	A-7-6	CH	95	56	15	41
3	A-7-6	CH	95	59	17	42
4	A-7-6	CH	97	67	19	48
5	A-6	CL	96	37	19	18
6	A-6	CL	95	34	19	15
7	A-6	CL	96	36	18	18

4.2.1.3 Site 3 (Muskogee)

As shown in Table 4, this site consists of alluvial mixed clay, the profile relatively uniform consisting of lean clay soil with a slight change at 2 feet to fat clay.

Table 4. Soil index properties and classification for Site 3 (Muskogee)

Depth (ft)	AASHTO Group Class.	USC Group Class.	Percent Fines (%)	Liquid Limit (%)	Plastic Limit (%)	Plasticity Index (%)
1	A-7-6	CL	86	46	19	27
2	A-7-6	CH	87	61	22	39
3	A-7-6	CL	86	47	25	22
4	A-6	CL	72	34	22	12
5	A-6	CL	87	38	21	17
6	A-6	CL	80	32	19	13
7	A-6	CL	82	34	19	15
8	A-6	CL	87	38	20	18
9	A-6	CL	86	37	20	17

4.2.1.4 Site 4 (Wagoner)

A uniform profile of alluvial fat clay soil is shown in Table 5. The plasticity index ranges from 49% at the highest and 40% at the lowest.

Table 5. Soil index properties and classification for Site 4 (Wagoner)

Depth (ft)	AASHTO Group Class.	USC Group Class.	Percent Fines (%)	Liquid Limit (%)	Plastic Limit (%)	Plasticity Index (%)
1	A-7-6	CH	89	66	26	40
2	A-7-6	CH	99	72	26	46
3	A-7-6	CH	99	73	28	45
4	A-7-6	CH	98	66	25	41
5	A-7-6	CH	98	74	26	48
6	A-7-6	CH	99	75	26	49
7	A-7-6	CH	98	71	24	47
8	A-7-6	CH	98	67	24	43
9	A-7-6	CH	98	68	24	44
10	A-7-6	CH	98	68	23	45
11	A-7-6	CH	99	65	23	42
12	A-7-6	CH	99	66	23	43
13	A-7-6	CH	98	64	23	41

4.2.1.5 Site 5 (Hobart)

This site is made of a mixture of residual clays, the soil varies between lean and fat clay throughout the soil profile as shown in Table 6.

Table 6. Soil index properties and classification for Site 5 (Hobart)

Depth (ft)	AASHTO Group Class.	USC Group Class.	Percent Fines (%)	Liquid Limit (%)	Plastic Limit (%)	Plasticity Index (%)
1	A-6	CL	96	37	19	18
2	A-7-6	CH	98	57	20	37
3	A-7-6	CH	95	58	26	32
4	A-7-6	CH	96	53	18	31
5	A-7-6	CH	93	52	20	32
6	A-7-6	CH	93	52	24	28
7	A-7-6	CL	94	46	18	28
8	A-7-6	CL	97	47	17	30
9	A-7-6	CL	98	49	25	24
10	A-7-6	CL	96	44	21	23
11	A-7-6	CL	97	42	21	21

4.2.1.6 Site 6 (Wewoka)

The alluvial soil in this profile is a mixture of non-plastic sand, silty sand and fat clay as shown in Table 7.

Table 7. Soil index properties and classification for Site 6 (Wewoka)

Depth (ft)	AASHTO Group Class.	USC Group Class.	Percent Fines (%)	Liquid Limit (%)	Plastic Limit (%)	Plasticity Index (%)
1	A-2-4	SM	33	NP	NP	NP
2	A-4	ML	40	19	16	3
3	A-6	SC-SM	48	26	14	12
4	A-6	CL	52	30	14	16
5	A-6	SC-SM	47	35	15	20
6	A-2-4	SM	21	NP	NP	NP
7	A-6	SC	49	37	18	19
8	A-7-6	CH	98	69	24	45
9	A-7-6	CH	98	57	27	30
10	A-7-6	CH	99	59	25	34
11	A-7-6	CH	95	52	23	29
12	A-7-6	CL	98	49	26	23
13	A-7-6	CH	99	60	26	34

4.2.1.7 Site 7 (Norman Maintenance Yard)

In this site the profile consists of alluvial fine sands mixtures. As the depth increases the plasticity of the soil changes from non-plastic to low plasticity as shown in Table 8.

Table 8. Soil index properties and classification for Site 7 (Norman MY)

Depth (ft)	AASHTO Group Class.	USC Group Class.	Percent Fines (%)	Liquid Limit (%)	Plastic Limit (%)	Plasticity Index (%)
1	A-3	SM	8	NP	NP	NP
5	A-3	SM	9	NP	NP	NP
7	A-2-4	SC	30	20	15	5
10	A-2-4	SC	32	20	16	4

4.2.1.8 Site 8 (Fairview)

The top 3 feet of this site consists of fat clay which then changes to lean clay for the depth of 4-11 feet, as shown in Table 9. This soil is classified as a residual clay soil.

Table 9. Soil index properties and classification for Site 8 (Fairview)

Depth (ft)	AASHTO Group Class.	USC Group Class.	Percent Fines (%)	Liquid Limit (%)	Plastic Limit (%)	Plasticity Index (%)
1	A-7-6	CH	95	58	16	42
2	A-7-6	CH	92	58	18	40
3	A-7-6	CH	95	52	16	36
4	A-7-6	CL	94	46	17	29
5	A-7-6	CL	91	43	16	27
6	A-7-6	CL	91	45	17	28
7	A-7-6	CL	99	45	18	27
8	A-7-6	CL	91	40	17	23
9	A-7-6	CL	90	41	14	27
10	A-7-6	CL	93	42	20	22
11	A-7-6	CL	97	44	26	19

4.1.2.9 Site 9 (Fears Lab)

This site consists of a diverse profile made of a mixture of silts, silty clay and silty sands, as shown in Table 10.

Table 10. Soil index properties and classification for Site 9 (Fears Lab)

Depth (ft)	USC Group Class.	Percent Fines (%)	Liquid Limit (%)	Plastic Limit (%)	Plasticity Index (%)
1	ML	57	NP	NP	NP
2	CL	70	26	16	10
3	ML	63	NP	NP	NP
4	ML	64	NP	NP	NP
5	ML	62	NP	NP	NP
6	CL	60	24	11	13
7	ML	61	NP	NP	NP
8	ML	55	NP	NP	NP
9	CL	58	22	14	8

4.2.3 Physical and mechanical properties

Laboratory testing was conducted to determine the total suction, total unit weight (ASTM D 7263-09), one dimensional consolidation (ASTM D2435-11) parameters, and shear strength via triaxial testing (ASTM D4767-11).

4.2.3.1 Unit weight results

The unit weight was determined for 24 undisturbed Shelby tube soil samples. Samples were trimmed to have a flat top and bottom surfaces. After sample preparation, the sample was weighed and measurements of diameter and height were used to calculate the sample volume. Results from unit weight testing are presented in Table 11, which provides the site number, name, depth of the sample, total unit weight (γ), natural water content (w_n), degree of saturation (S), and void ratio (e). To calculate the void ratio and degree of saturation, a solid specific gravity (G_s) of 2.70 was assumed.

Table 11. Soil unit weight and phase properties from tube samples

Site No	Site Name	Depth (ft)	Water content, w_n (%)	Total unit weight, γ (pcf)	Degree of Saturation, S (%)	Void ratio, e
2	Lake Hefner	0.8	17.1	128.4	86.1	0.54
2	Lake Hefner	1.4	24.4	119.3	87.1	0.76
2	Lake Hefner	2.0	21.1	125.3	90.7	0.63
3	Muskogee	4.7	22.3	109.1	67.8	0.89
3	Muskogee	6.3	24.1	110.0	72.2	0.90
3	Muskogee	8.6	16.6	111.2	58.5	0.77
4	Wagoner	2.3	28.1	103.4	69.9	0.85
4	Wagoner	4.2	26.2	105.1	69.2	0.88
4	Wagoner	6.4	23.4	106.1	65.9	0.96
4	Wagoner	8.2	27.7	108.2	75.7	0.99
5	Wewoka	2.6	23.4	111.2	66.2	0.82
5	Wewoka	8.8	21.2	130.8	95.7	0.53
6	Hobart	4.0	22.3	127.7	92.1	0.58
6	Hobart	6.3	22.8	127.4	93.0	0.59
7	Norman	6.6	8.8	125.1	51.1	0.47
7	Norman	8.0	15.5	127.4	79.4	0.53
8	Fairview	0.5	15.3	109.5	53.4	0.77
8	Fairview	2.2	20.1	128.7	94.8	0.57
8	Fairview	4.3	17.4	126.7	83.7	0.56
8	Fairview	6.5	22.1	125.5	93.4	0.64
8	Fairview	7.8	19.4	110.5	63.8	0.82
8	Fairview	8.1	18.1	115.7	67.9	0.72
9	Fears	0.2	12.5	118.1	55.8	0.60
9	Fears	7.1	17.8	122.7	77.8	0.62

As shown in Table 11, the unit weight for the upper ten feet of the soil profiles ranged from 103.4 to 130.8 pcf across eight of the test sites. Being predominantly cohesionless, tube samples could not be obtained at the Curtis Site 1. The water content and void ratio ranges were 8.8-28.1% and 0.47 to 0.99, with averages of 20.3 and 0.71, respectively. Degree of saturation range was 51-96%, with a median of 74%. At nearly all of the sites the water table was not encountered or encountered below 10 feet. This demonstrates the importance of considering the influence of the degree of saturation and suction on the interpretation of cone penetration test results.

4.2.3.2 One-dimensional consolidation test results

The one-dimensional consolidation test was conducted on undisturbed soil samples to determine the stress-strain behavior of the soil. The procedure followed for both saturated and unsaturated testing is described in Section 3.5.1. Unsaturated testing was conducted to represent the actual stress strain behavior for the soils in the field under constant water content conditions at the time of testing. Results from these test are compared to the saturated consolidation test to investigate and analyze the differences.

Tables 12 and 13 show the results for saturated and unsaturated consolidation testing. Site name, depth of sample tested, Overconsolidation Ratio (*OCR*), preconsolidation stress (σ'_p), recompression/swelling index (c_r=c_s), virgin compression index (c_c) and the corresponding water content before starting the test are presented. As expected, results showed some differences between saturated and unsaturated testing.

Table 12. Saturated one-dimensional consolidation test results

Site No	Site Name	Depth (ft)	*OCR*	σ'_p (tsf)	c_c	$c_r=c_s$	Initial w_n (%)
6	Wewoka	5.5	2.61	1.71	0.163	0.040	30.7
6	Wewoka	8.8	1.88	2.23	0.437	0.049	19.6
9	Fears Lab	2.2	4.50	1.52	0.054	0.124	23.1
9	Fears lab	4.5	3.34	1.41	0.238	0.085	23.9
9	Fears lab	7.7	1.63	1.64	0.116	0.042	16.9
7	Norman	6.6	1.87	1.76	0.100	0.029	7.3
7	Norman	8.2	1.46	1.66	0.081	0.035	19.1
7	Norman	10.2	1.84	1.78	0.219	0.038	15.1
5	Hobart	3.0	4.68	2.21	0.232	0.107	21.3
5	Hobart	4.7	4.02	2.61	0.220	0.021	23.2
5	Hobart	6.1	4.60	2.13	0.148	0.025	23.2
4	Wagoner	7.3	5.14	2.59	0.100	0.030	25.1
8	Fairview	7.2	6.00	1.88	0.110	0.020	31.4
3	Muskogee	3.8	8.40	2.19	0.090	0.050	22.1
4	Wagoner	5.5	5.60	1.76	0.080	0.020	27.9
2	Lake Hefner	0.3	80.00	1.62	0.080	0.020	17.1

Table 13. Unsaturated one-dimensional consolidation test results

Site No	Site Name	Depth (ft)	*OCR*	σ'_p (tsf)	c_c	c_r=c_s	Initial w_n (%)
6	Wewoka	5.5	2.09	2.3	0.108	0.006	30.7
6	Wewoka	8.8	1.57	2.8	0.127	0.046	19.6
9	Fears	2.2	2.92	1.8	0.026	0.009	23.1
9	Fears lab	4.5	3.43	1.5	0.178	0.106	23.9
9	Fears lab	7.7	1.21	1.4	0.106	0.194	16.9
7	Norman	6.6	2.05	1.5	0.141	0.087	7.3
7	Norman	8.2	1.52	1.6	0.078	0.051	19.1
7	Norman	10.2	1.36	1.5	0.287	0.050	15.1
5	Hobart	3.0	5.15	1.9	0.291	0.135	21.3
5	Hobart	4.7	3.84	3.0	0.223	0.055	23.2
5	Hobart	6.1	1.49	1.9	0.137	0.028	23.2
4	Wagoner	7.2	4.10	2.0	0.150	0.030	25.1
8	Fairview	7.3	6.50	1.9	0.120	0.020	31.4
3	Muskogee	4.0	9.20	2.3	0.070	0.050	22.1
4	Wagoner	5.6	7.00	2.1	0.090	0.030	27.9
2	Lake Hefmer	0.5	60.00	1.2	0.120	0.030	17.1

4.3.2.3 Triaxial test results

The triaxial test was conducted on Shelby tube samples collected from the field. This test was used to determine the soil's effective stress strength parameters represented in the cohesion c' and friction angle ϕ' and undrained shear strength s_u. A multi-stage CIUC test procedure was followed as described in Section 3.5.2. The forces applied on the sample for the first stage were based on the depth and estimated overburden pressure the soil experienced in the field. Larger confining stresses are applied for the second and third stages to see the effects of higher initial effective stresses on the sample.

Results from the tested soil samples are shown in Table 14. Site name, depth, effective stress cohesion and friction angle are shown. Also shown in Table 14 are the undrained shear strength and normalized undrained shear strength for the first stage, which corresponds to the estimated in situ average effective confining stress. Plots of deviator stress and excess pore water pressure versus vertical strain, and stress paths (p-q diagrams) for each triaxial test are shown in Appendix C. Tabulated results with undrained shear strength for every stage and the applied cell pressure during that stage are shown in Appendix D.

Table 14. Triaxial test results

Site Name	Depth (ft)	*c'* (psi)	*ϕ'* (°)	s_u (psi)	*Normalized* s_u
Wewoka	8.8	3.2	23.2	8.3	1.1
Norman	6.6	0.8	29.3	13.1	2.6
Norman	8.0	1.1	25.9	14.8	4.9
Fears	0.2	2.0	23.8	16.4	2.7
Fears	7.1	3.9	17.2	4.4	1.4
Hobart	4.0	5.8	11.8	11.6	1.9
Hobart	6.3	2.8	26.7	4.5	3.5
Fairview	1.2	1.6	40.3	15.9	3.2
Fairview	2.2	0.8	39.1	2.1	2.9
Fairview	6.5	0.2	14.2	4.1	2.8
Fairview	4.3	0.4	24.0	3.6	1.8
Wagoner	2.3	1.1	21.0	10.1	2.1
Wagoner	4.2	1.2	19.6	18.2	3.6
Wagoner	8.2	5.1	7.2	22.3	4.5
Lake Hefner	1.4	3.1	11.0	9.3	1.4
Fairview	7.8	0.1	28.5	11.0	3.1
Lake Hefner	1.2	0.4	37.0	30.7	4.6
Lake Hefner	2.0	3.5	12.2	10.1	10.1
Muskogee	6.3	4.1	16.5	11.0	3.7
Fairview	8.1	0.7	26.6	3.0	1.0
Wewoka	2.6	1.4	25.2	2.7	0.7
Wagoner	6.4	3.0	16.2	12.5	2.5
Muskogee	4.7	3.8	7.9	9.1	1.4
Muskogee	8.6	12.5	9.6	8.3	8.3

4.3 Field testing results

4.3.1 Seismic cone penetration test results

Results from the Cone Penetration testing are shown in Figures 8 through 16 for the upper portion of each test site where laboratory test samples were obtained. The data in these profiles represent the average from 4 soundings conducted in close proximity at each site. All of the soundings for each site are summarized in Appendix A, where it is seen that generally the soundings were quite repeatable at each site. For each site, the soil stratigraphy, natural water content (w_n), total suction (ψ_t), cone tip resistance (q_c), cone sleeve friction (f_s) and friction ratio (FR) are summarized with depth for each testing date in Figures 8 through 16. Testing dates are referred to as dry and wet dates, depending on whether antecedent weather conditions leading up to the visit represented a relatively drier or wetter period. The purpose was to highlight differences in the cone data obtained when soil conditions were in a drier or wetter state. In Figures 8 through 16, with few exceptions, it can be observed as the depth increases the differences in cone parameters, and suction between the site visits generally reduced due to the similarity in the moisture content at greater depths.

For each site, data presented in Figures 8 to 16 for the first visit are represented with a solid line and solid black circles, while the second visit corresponds to the dashed line and open circles. For some sites the first visit was during the wet period, so the water content was higher than the second visit (e.g. Wewoka, Norman MY and Fears Lab), while for other sites the first visit was during the dry season (e.g. Curtis, Fairview, Muskogee) corresponding to lower water contents. For some sites, the differences in water content were not so large during wet and dry periods.

4.3.1.1 Site 1 (Curtis)

Cone testing was conducted on June 18th, 2019 and January 29th, 2021. The water contents varied significantly for the first eight feet as shown in figure 8. For this soil, the tip resistance profile did not have a notable change between wet and dry states, while the sleeve friction showed higher values during the dry state compared to the wet state.

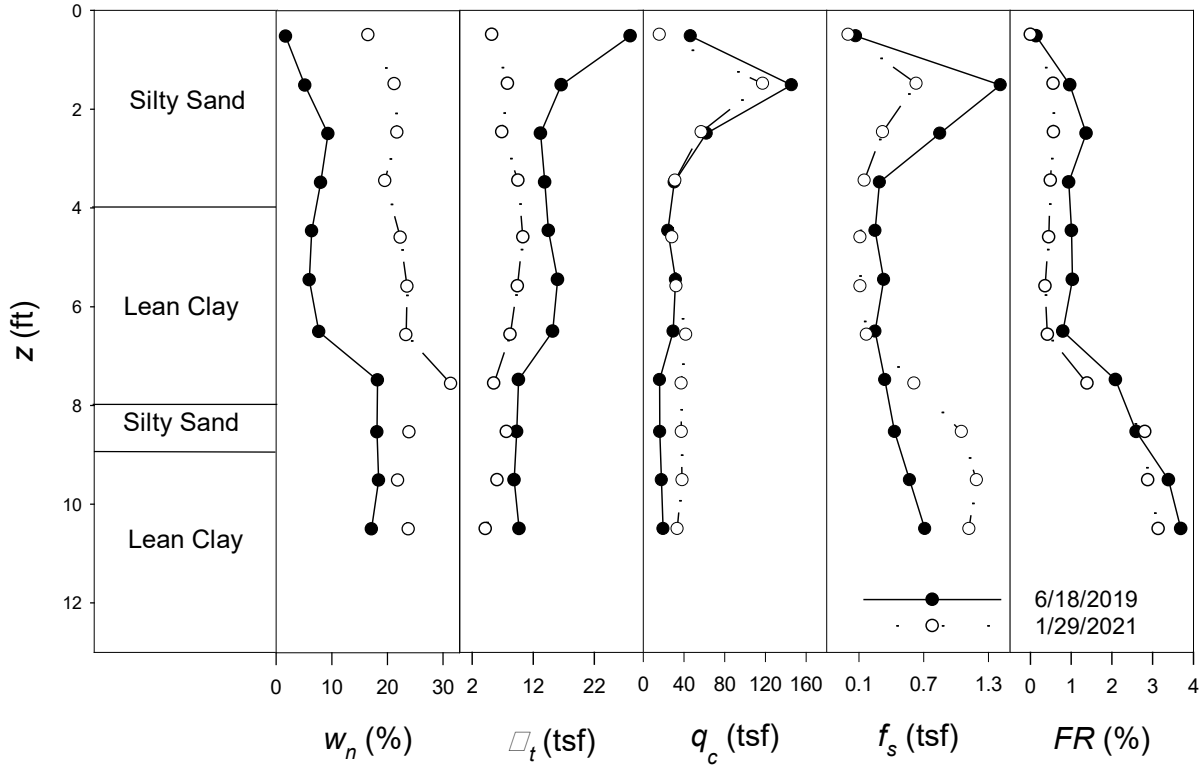

Figure 8. Data representing depth against soil stratigraphy, w_n, ψ_t, q_c, f_s, and FR during wet and dry periods in Site 1 (Curtis). Soil profiles are based on samples obtained from companion test borings

4.3.1.2 Site 2 (Lake Hefner)

This site consisted of a shallow profile, around six feet. Tip resistance and sleeve friction seemed to respond to changes in water content and suction as shown in Figure 9, particularly below 3.5 feet.

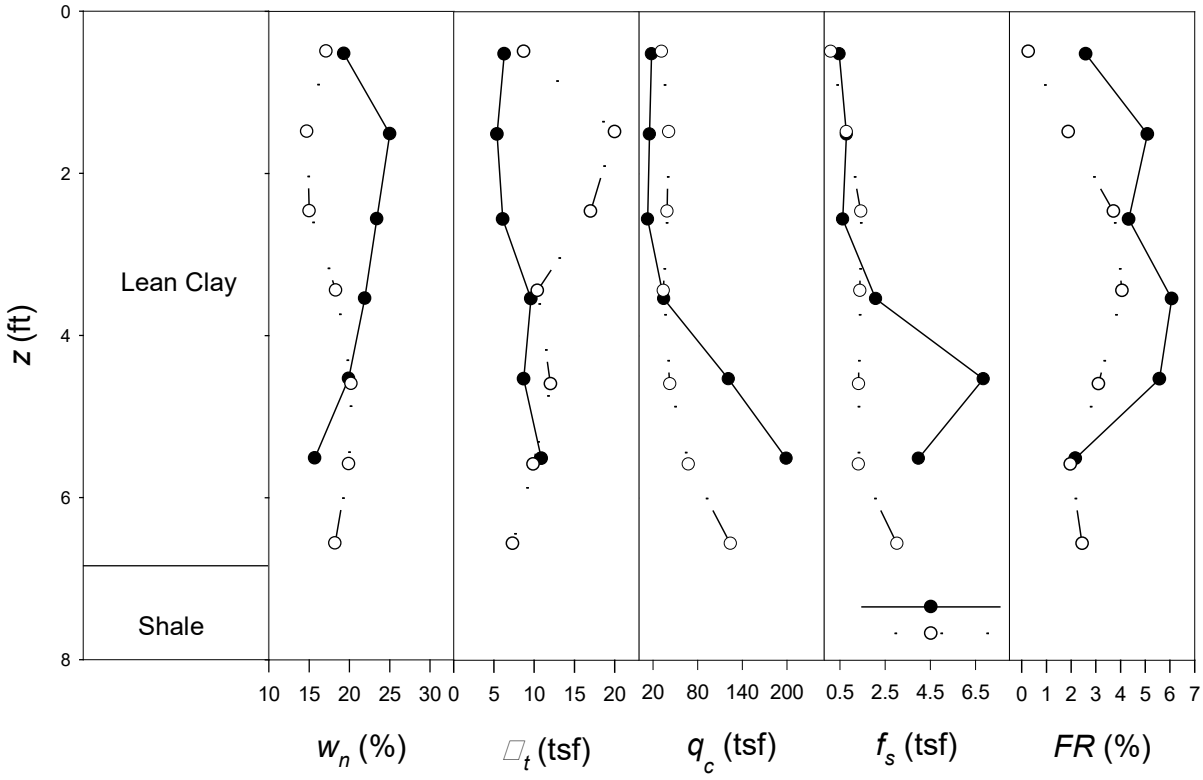

Figure 9. Data representing depth against soil stratigraphy, w_n, ψ_t, q_c, f_s, and FR during wet and dry periods in Site 2 (Lake Hefner). Soil profiles are based on samples obtained from companion test borings

4.3.1.3 Site 3 (Muskogee)

Site #3 was tested on July 17th, 2020 and April 14th, 2021. The water content was higher during the second visit through the first four feet of the soil profile, as shown in Figure 10. The effect of the water content differences is portrayed in the tip resistance and sleeve friction graphs, where the tip resistance and sleeve friction for the second visit are lower for the upper four feet.

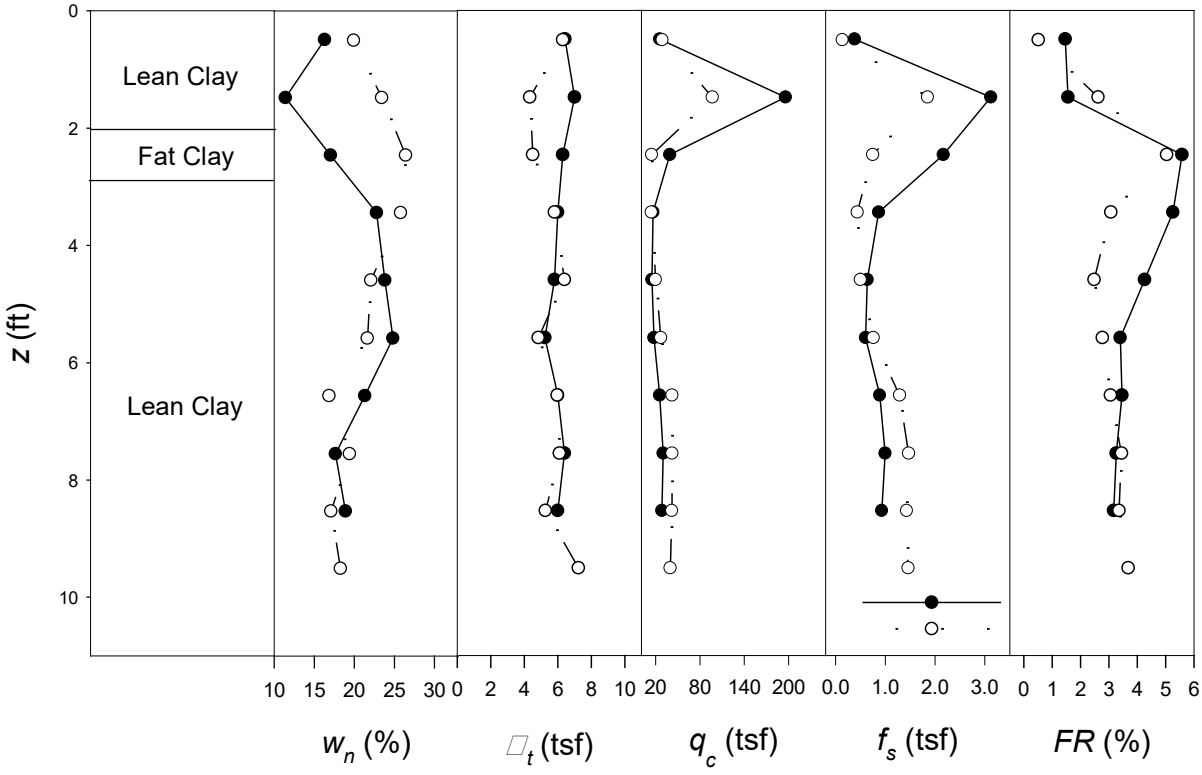

Figure 10. Data representing depth against soil stratigraphy, w_n, ψ_t, q_c, f_s, and *FR* during wet and dry periods in Site 3 (Muskogee). Soil profiles are based on samples obtained from companion test borings

4.3.1.4 Site 4 (Wagoner)

The profiles for this site showed some fluctuations in the water content values between site visits. However, as shown in Figure 11, the suction was generally greater throughout most of the profile on the second visit, as were the tip resistance and sleeve friction.

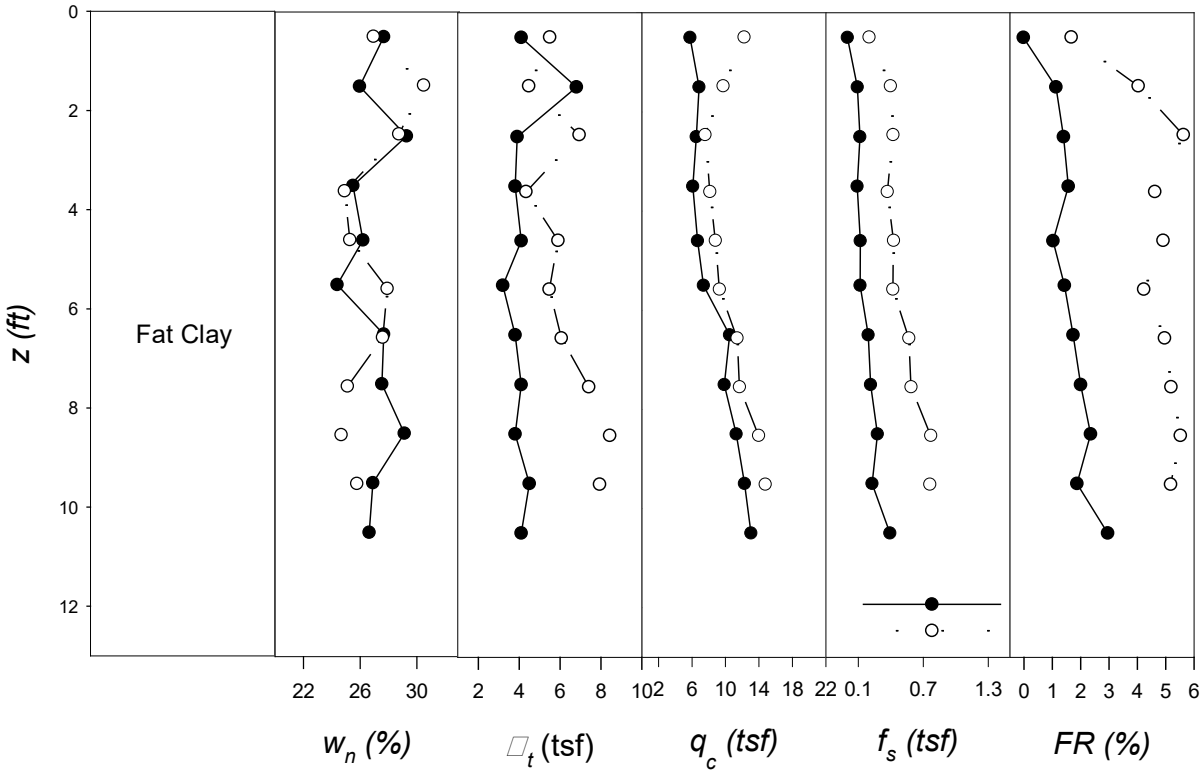

Figure 11. Data representing depth against soil stratigraphy, w_n, ψ_t, q_c, f_s, and *FR* during wet and dry periods in Site 4 (Wagoner). Soil profiles are based on samples obtained from companion test borings

4.3.1.5 Site 5 (Hobart)

For Site #5, there is a decrease in the water content for most test depths between the first and second visit. As seen in Figure 12, there is a corresponding increase in the tip resistance and sleeve friction for most depths. Interestingly, the suction did not change much in response to the changes in water content, which could be related to the hysteretic behavior exhibited in the water content-suction relationship. On a soil-water-characteristic curve, for the same suction, the water content will be lower upon wetting

as compared to drying. While the suction is the same; however, the mechanical properties such as shear strength and stiffness will also depend on the water content.

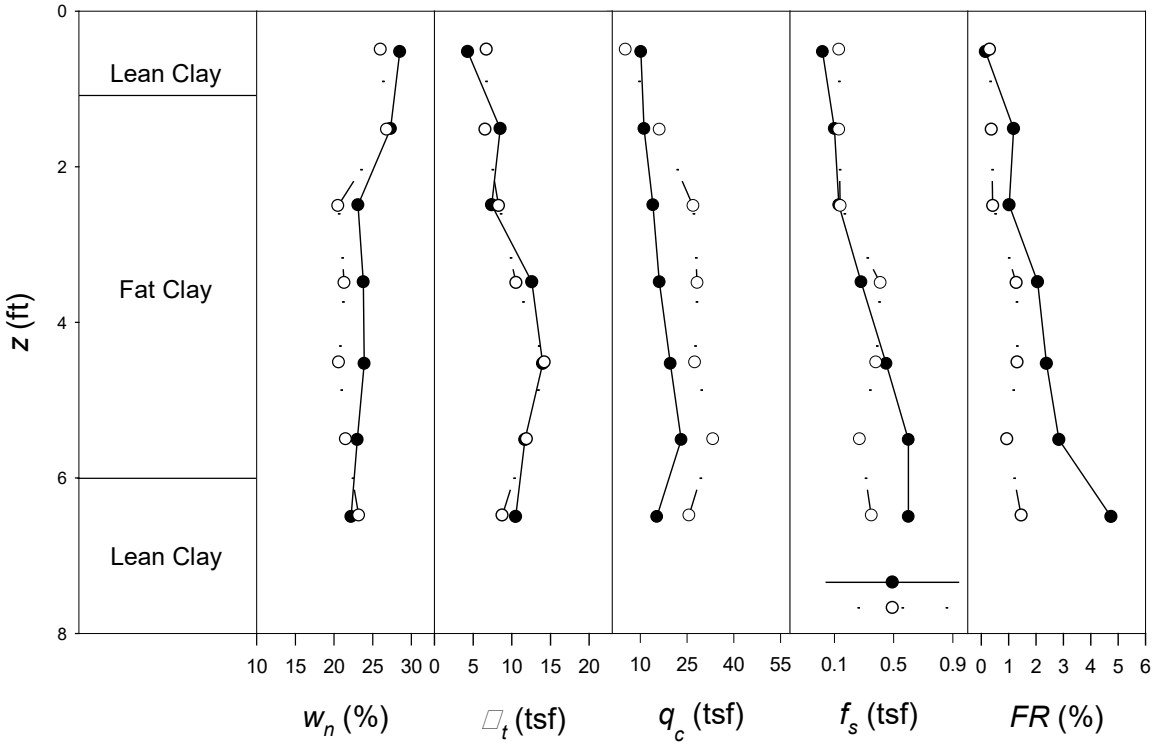

Figure 12. Data representing depth against soil stratigraphy, w_n, ψ_t, q_c, f_s, and FR during wet and dry periods in Site 5 (Hobart). Soil profiles are based on samples obtained from companion test borings

4.3.1.6 Site 6 (Wewoka)

The soil profile for Site #6 showed significant variation in the water content in the soil profile between the two site visits as shown in Figure 13. As with other sites, large changes in water content and suction had a corresponding significant influence on the tip resistance and sleeve friction, although the influence on tip resistance is more consistent.

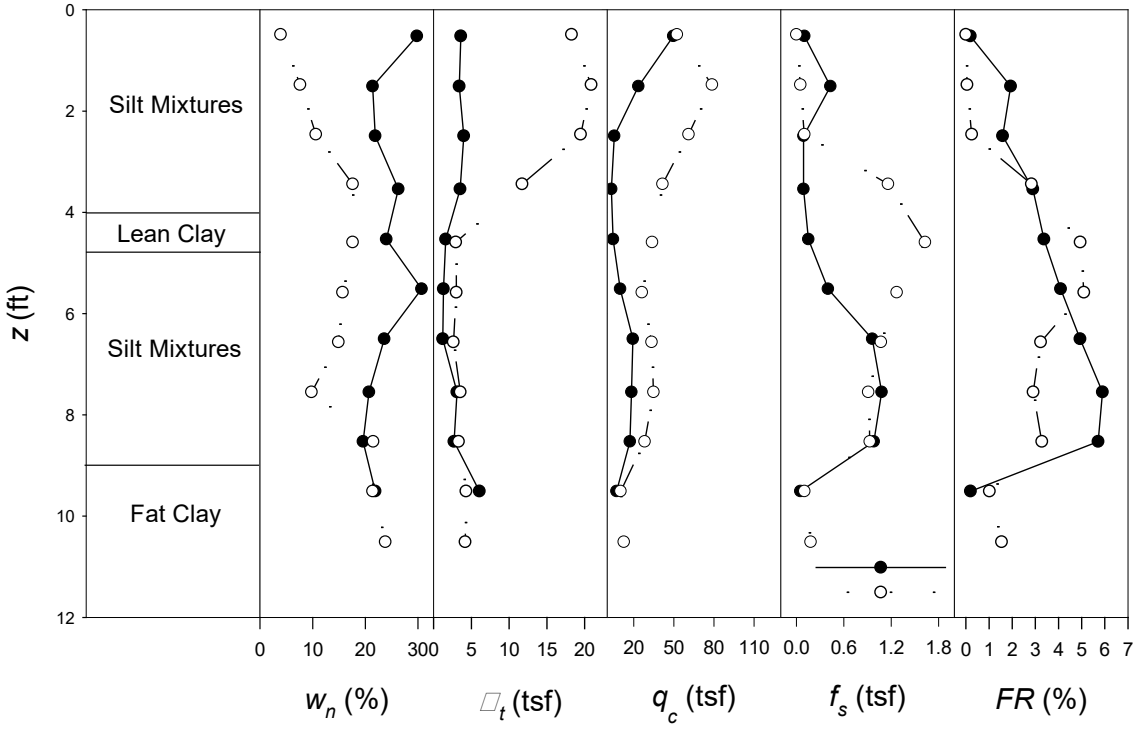

Figure 13. Data representing depth against soil stratigraphy, w_n, ψ_t, q_c, f_s, and *FR* during wet and dry periods in Site 6 (Wewoka). Soil profiles are based on samples obtained from companion test borings

4.3.1.7 Site 7 (Norman Maintenance Yard)

During the second visit the moisture content in the upper 3 feet in particular was lower than on the first visit. Tip resistance and sleeve were also noticeably higher in the upper 3 feet during the second visit. Interestingly, the total suction profile from 4 to 8 feet was considerably different between the first and second visits but seemingly had little influence on the cone parameters. This is likely due to the fact that total suction is affected by both osmotic and capillary pressure, but only the latter has a strong

influence on mechanical behavior, particularly in less plastic soils such as those found at the Norman MY. Possibly, during the initial visit the soils between 4 and 8 feet had a higher salt content which caused a higher total suction than on the second visit, even though moisture contents were lower on the second visit.

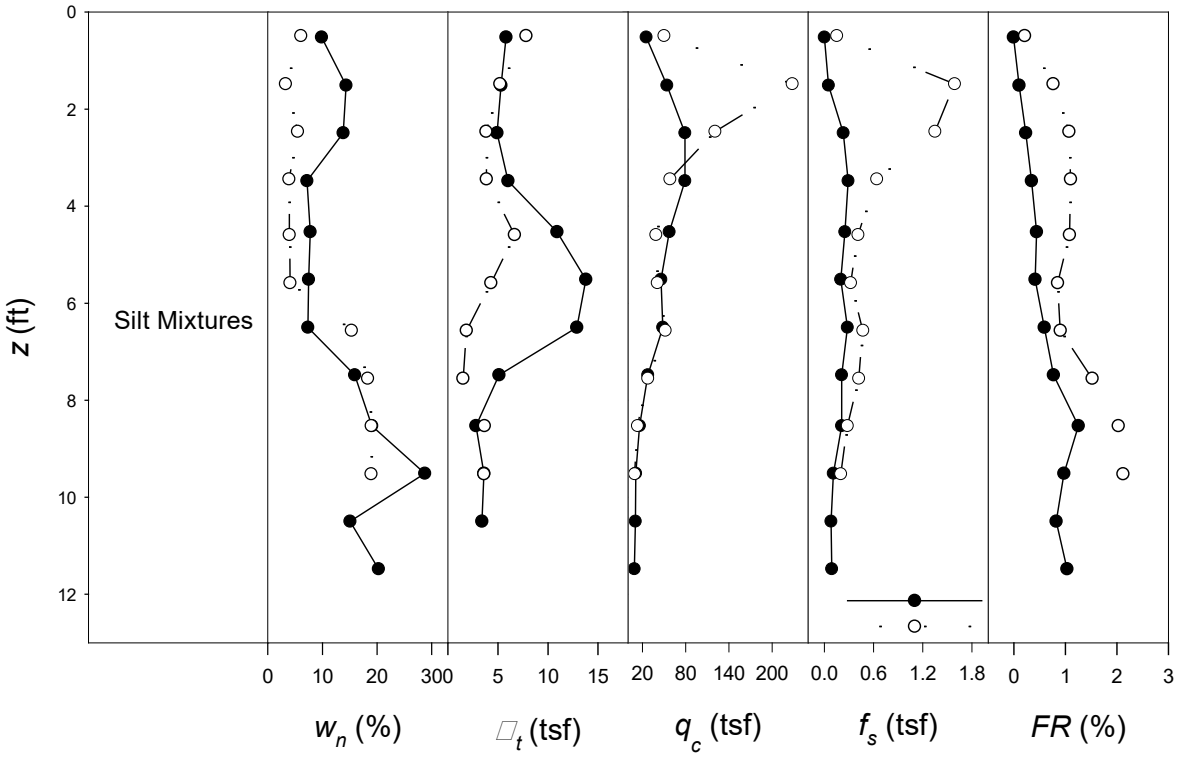

Figure 14. Data representing depth against soil stratigraphy, w_n, ψ_t, q_c, f_s, and *FR* during wet and dry periods in Site 7 (Norman Maintenance Yard). Soil profiles are based on samples obtained from companion test borings

4.3.1.8 Site 8 (Fairview)

As depth increased the water content of the soil increased for both visits. The water content varied from around 15% to around 25% with a maximum water content of 30%. On the second visit, water contents were lower and suction was higher which resulted in higher tip resistance and sleeve friction in the upper four feet as compared to the first visit.

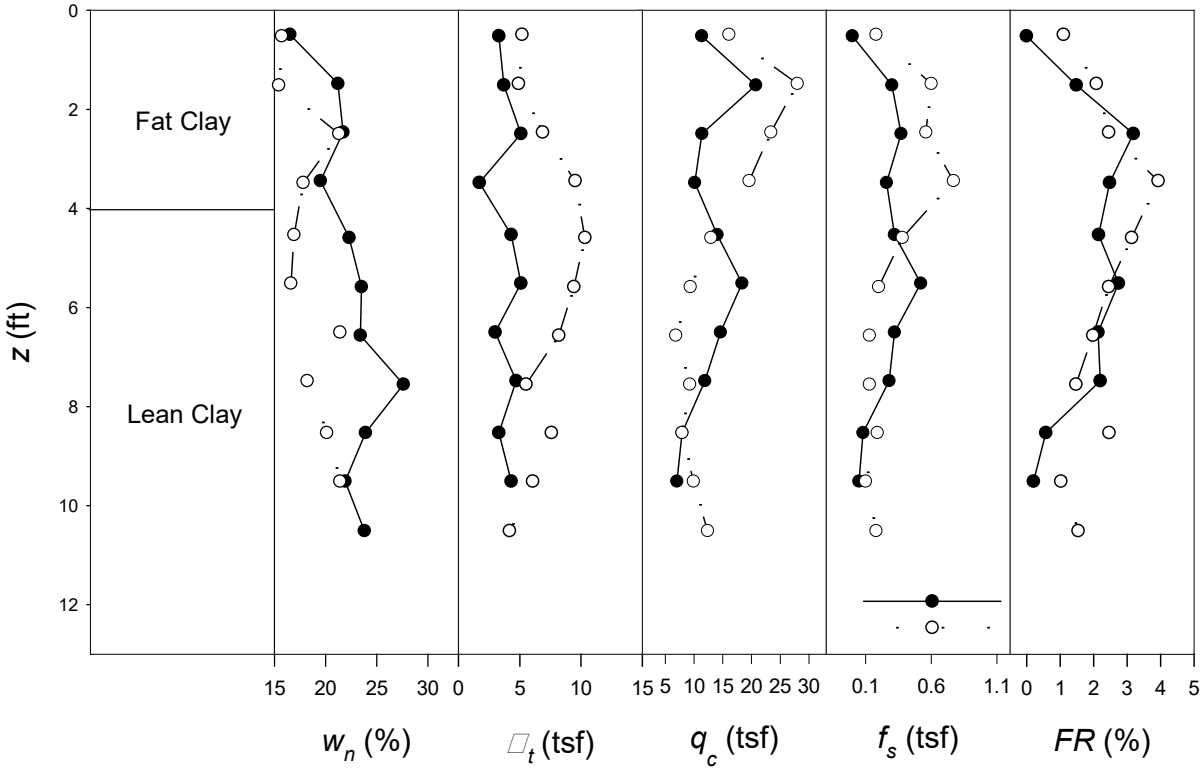

Figure 15. Data representing depth against soil stratigraphy, w_n, ψ_t, q_c, f_s, and *FR* during wet and dry periods in Site 8 (Fairview). Soil profiles are based on samples obtained from companion test borings

4.3.1.9 Site 9 (Fears Lab)

For Site #9 the water content decreased and suction increased in the upper seven feet between the first and second visit, as shown in Figure 16. Interestingly, the tip resistance seemed to respond very little to these changes, while on the other hand the sleeve friction noticeably increased in this zone during the second visit.

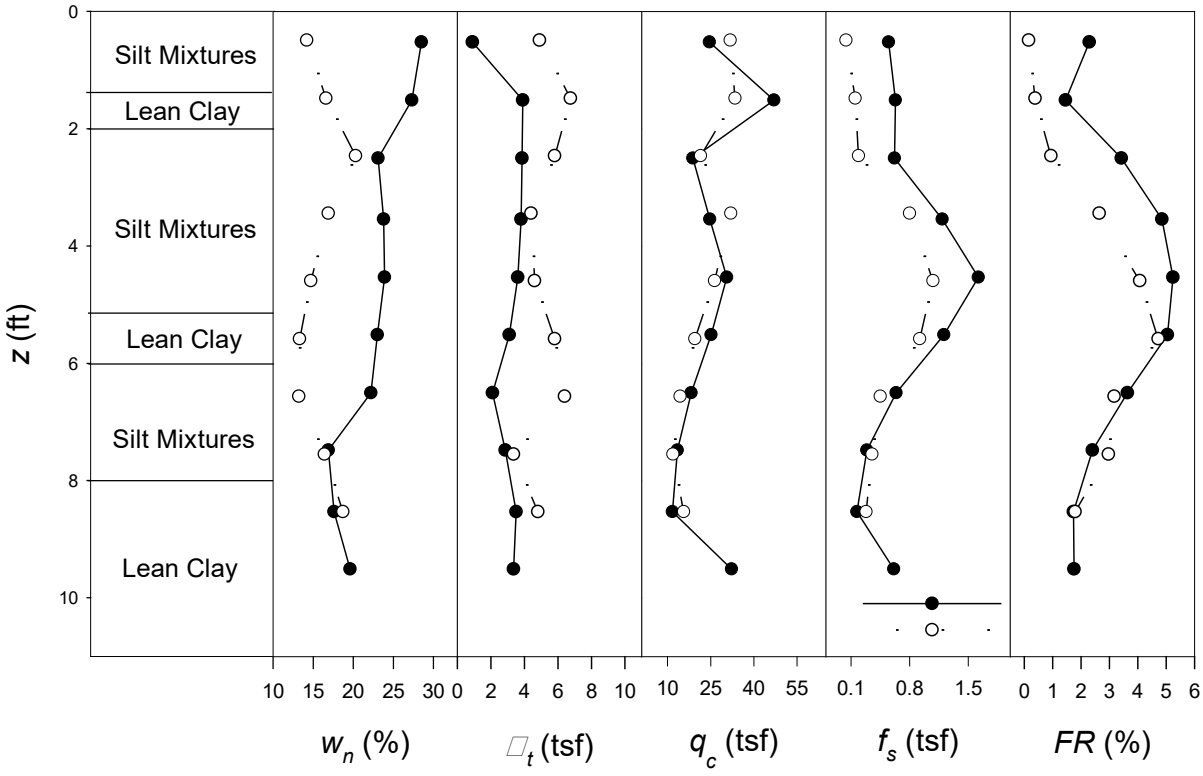

Figure 16. Data representing depth against soil stratigraphy, w_n, ψ_t, q_c, f_s, and *FR* during wet and dry periods in Site 9 (Fears Lab). Soil profiles are based on samples obtained from companion test borings

4.3.2 Seismic test results

Seismic cone tests were conducted at discrete depths during SCPTu testing. Geophones in the cone detect small strain movements in the soil caused by striking a plate with a hammer at the ground surface. Seismic tests were conducted every two to three feet throughout the depth of the soil profile. The shear wave arrival times are used to determine the average shear wave velocity through the tested layer. The first arrival method was used to determine the wave arrival time for the data collected in the field. Equation 12 which is referenced in ASTM D7400-19 “Standard Test Methods for Downhole Seismic Testing” (2019), was used to calculate the shear wave velocity.

$$V_s = \frac{L_{R2} - L_{R1}}{\Delta T_{R2-R1}} \tag{12}$$

Where L_{R2} is the distance from the source to the receiver at the greater depth, L_{R1} is the distance from the source to the receiver at the shallower depth, and $\Delta T_{R2\text{-}R1}$ is the difference between travel times from source to receivers at greater and shallower depths. Figure 17 shows an example of the raw shear wave data collected in the field and presented using the Vertek Coneplot program.

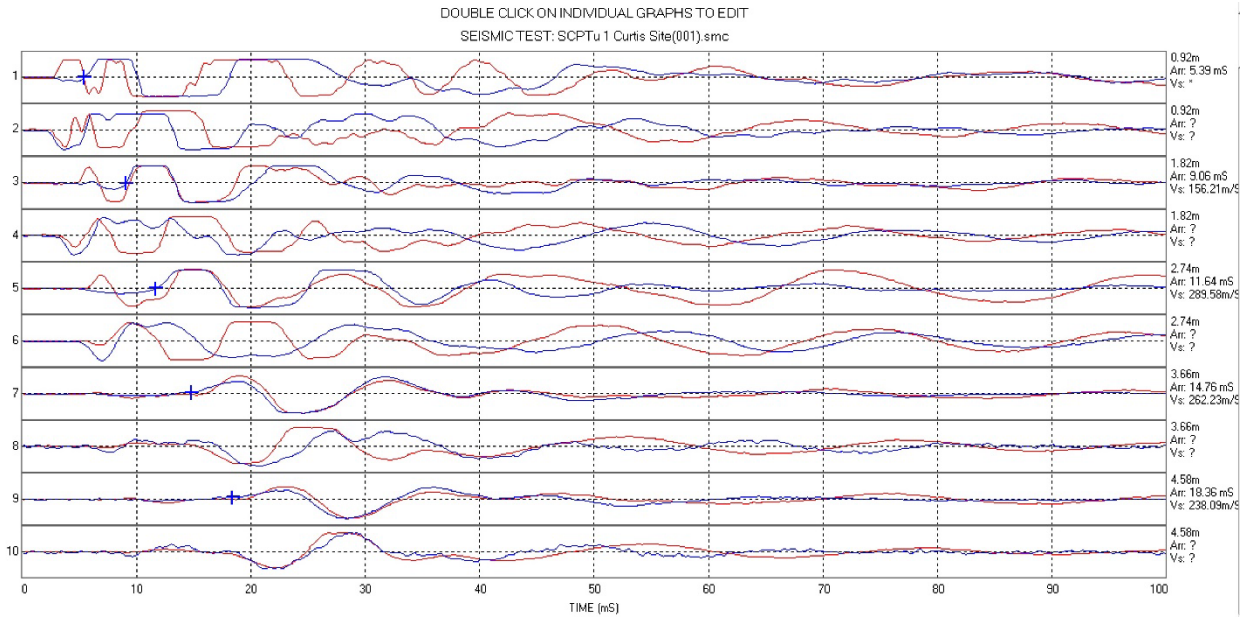

Figure 17. Cone plot shear wave velocity data for Site 1 (Curtis)

Shear wave velocity data analyzed at discrete depths are included in the average soundings plotted in Appendix A for wet and dry periods and tabulated for all sites in Appendix D.

5 Comparison of existing correlations to CPT and laboratory data

In this section existing correlations based on cone penetration testing parameters are presented. Comparisons of data collected from the lab and the field to correlations from the literature are shown. Also, some new correlations are shown for Oklahoma soils.

5.1 Correlation of SCPTu parameters to Soil Behavior Type (SBT)

Using the proposed correlation by Robertson (2010) the behavioral index I_c was calculated based on cone data from each site and the soil types were predicted based on Figure 18. The equations used to calculate Q_{tn}, *n, and* I_c are also shown in Figure 18.

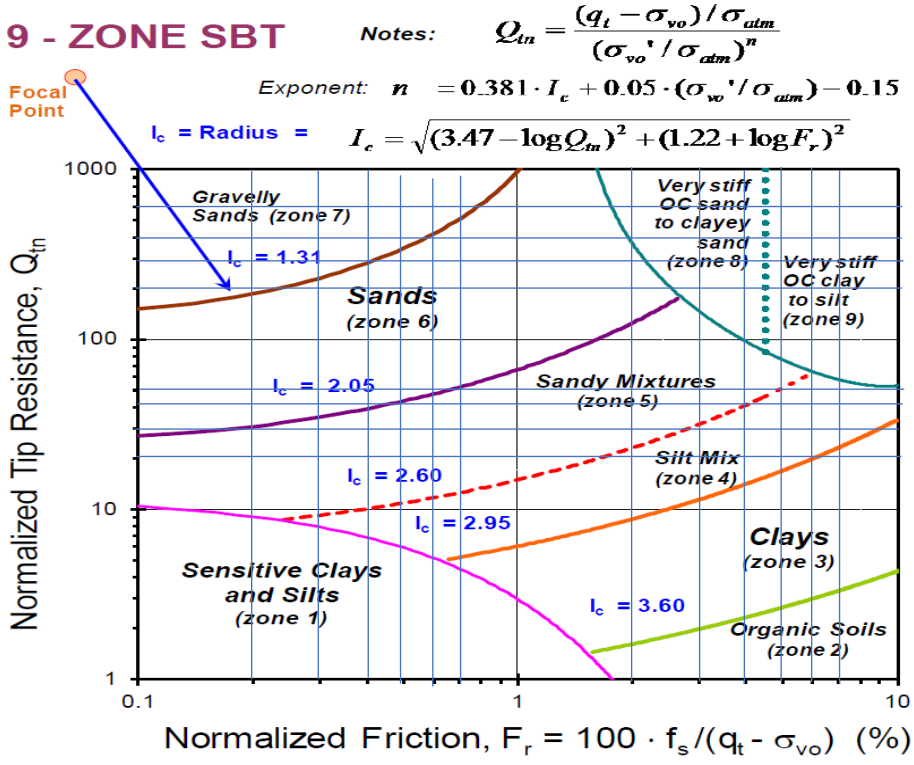

Figure 18. Soil Behavior Type normalized graph, Robertson (2010)

Data collected from the field were analyzed to predict the soil type throughout the soil profile. Soils were classified based on Figure 18 and Q_{tn} and F_r values for each site. For each site data were superimposed on the SBT graphs to visualize the differences in classifications between wet and dry periods as shown in Figures 19-27.

By observing the data in Figures 19 through 27, it can be seen in some cases the soil type predictions are sensitive to the moisture condition at the time of field testing. Tabulated SBT parameters including Q_{tn}, F_r, and I_c for all of the sites are listed in Appendix D.

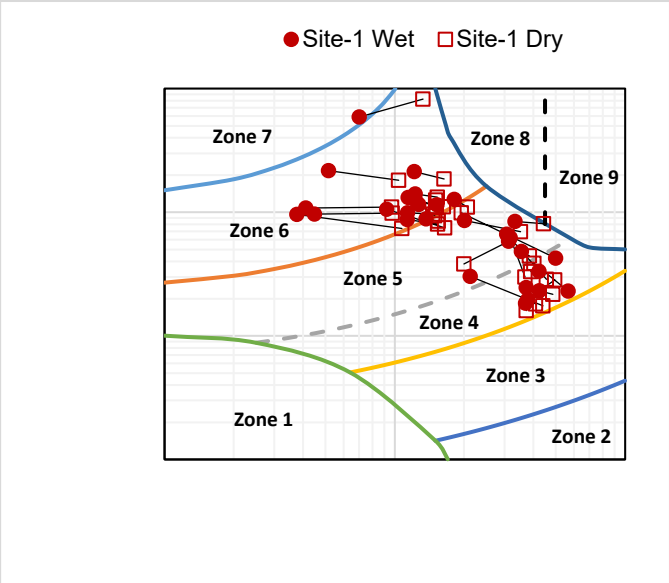

Figure 19. SBT graphs for Site-1 during wet and dry periods

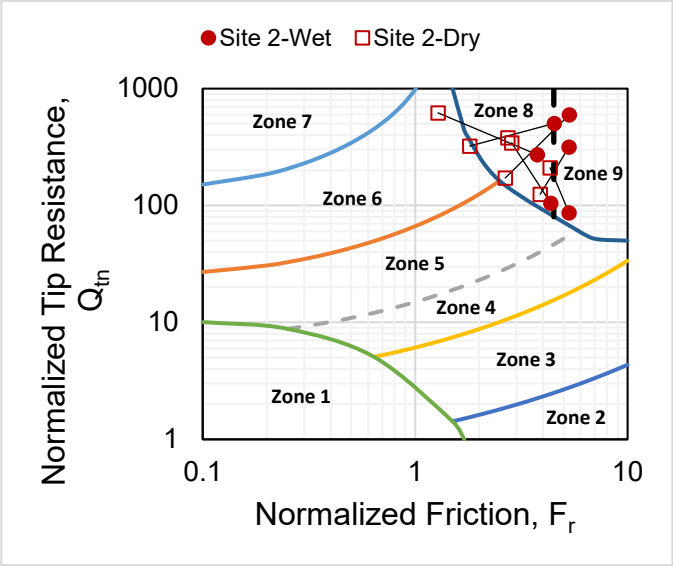

Figure 20. SBT graphs for Site-2 during wet and dry periods

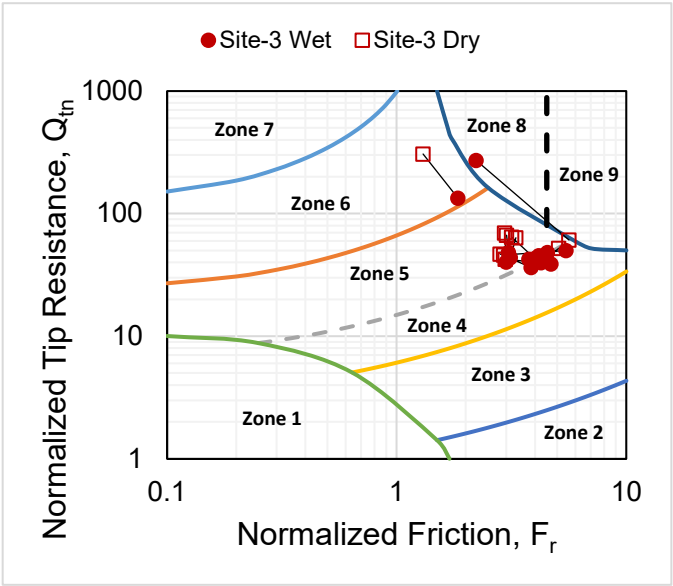

Figure 21. SBT graphs for Site-3 during wet and dry periods

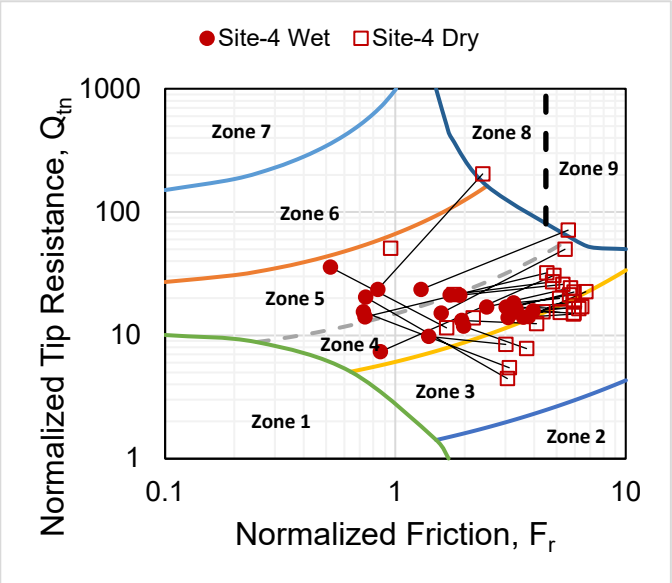

Figure 22. SBT graphs for Site-4 during wet and dry periods

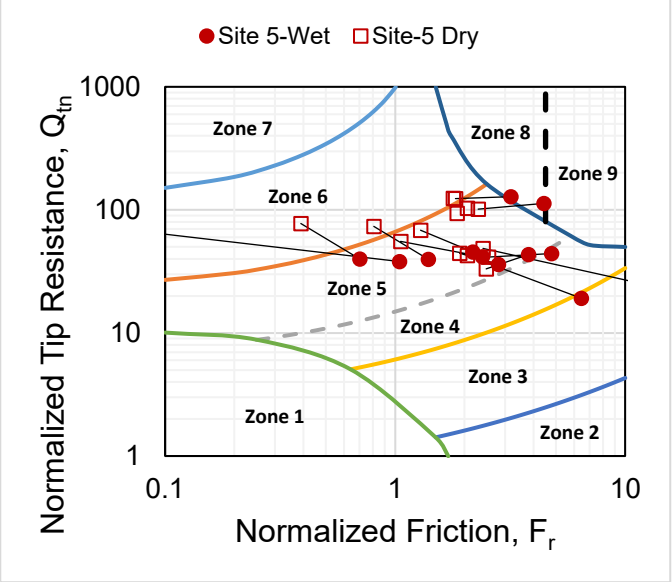

Figure 23. SBT graphs for Site-5 during wet and dry periods

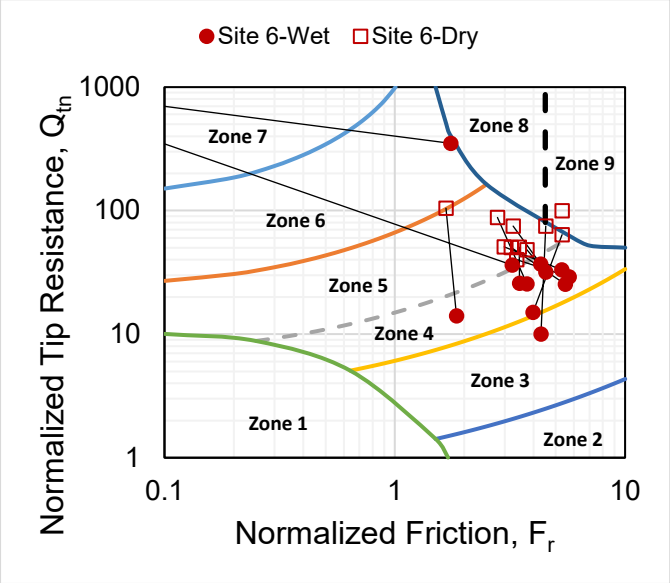

Figure 24. ***SBT graphs for Site-6 during wet and dry periods***

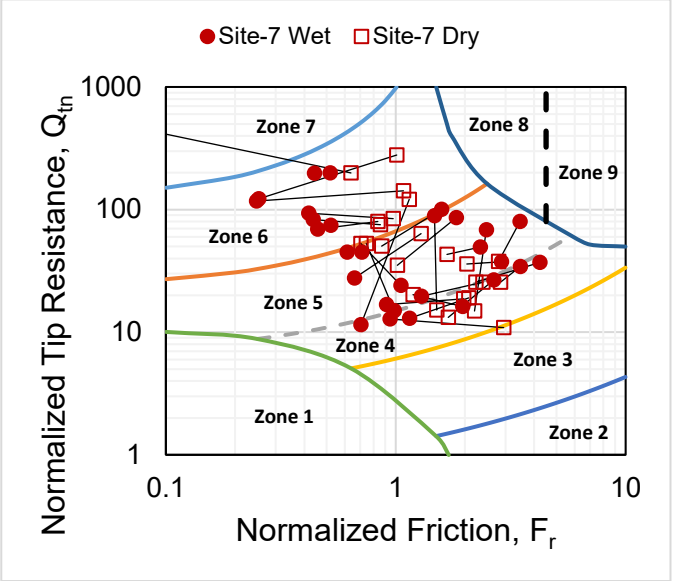

Figure 25. ***SBT graphs for Site-7 during wet and dry periods***

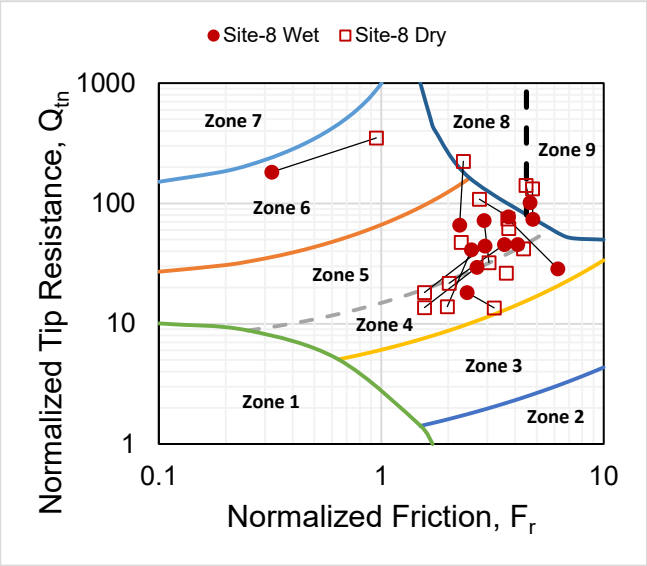

Figure 26. SBT graphs for Site-8 during wet and dry periods

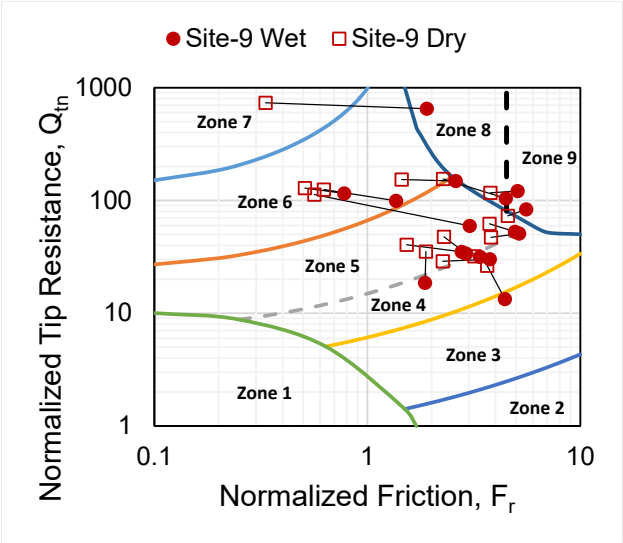

Figure 27. SBT graphs for Site-9 during wet and dry periods

5.2 Relationships between tip resistance, water content and total suction

Tip resistance data collected in the field were analyzed to understand the effect of changes in water content during wet and dry periods. Tip resistance q_c and normalized tip resistance q_c/σ_{vo} are plotted against natural water content (w_n) and total suction (ψ_t) in Figure 28. The data generally show that the tip resistance decreases as water content increases and suction decreases.

Regression equations for relating q_c and w_n and ψ_t are shown for plastic and non-plastic soils in Tables 15 and 16. Looking at the r^2 values it can be observed that the relationships between suction and both q_c and normalized q_c are stronger than the relationships between water content and q_c and normalized q_c. The r^2 values in some cases show reasonably strong trends while in others they are fairly weak. This is expected given the variability of soil properties at each site and across the nine test sites.

In spite of the lack of statistical strength in some of the trends shown, overall the data suggest that changes in water content have a significant effect on the SCPTu results with the tip resistance changing between wet and dry periods. This is an important consideration for analyzing cone penetration tests in unsaturated soil profiles that experience seasonal variations in water content.

Table 15. Regression equations for q_c and normalized q_c versus water content and suction in plastic and non-plastic soils during wet and dry periods

Type of soil	Regression wet	r^2 wet	Regression dry	r^2 dry
Plastic q_c versus w_n	q_c =-0.224* w_n +28.013	0.377	q_c =-0.167* w_n +23.633	0.377
Non Plastic q_c versus w_n	q_c =-0.351* w_n +33.690	0.056	q_c =-1.434* w_n +45.780	0.668
Plastic q_c versus ψ_t	q_c=0.047*ψ_t+2.526	0.183	q_c=0.046* ψ_t +3.304	0.625
Non Plastic q_c versus ψ_t	q_c =1.564* ψ_t +16.834	0.367	q_c =8.740* ψ_t -0.324	0.554
Plastic normalized q_c versus w_n	Normalized q_c=-0.385* w_n +53.851	0.002	Normalized q_c=-4.421*w_n +158.600	0.093
Non Plastic normalized q_c versus w_n	Normalized q_c=-1.114* w_n +98.892	0.051	Normalized q_c =-5.530*w_n +160.910	0.388
Plastic q_c normalized versus ψ_t	q_c=0.674*ψ_t+14.885	0.042	q_c=1.674* ψ_t +8.375	0.413
Non Plastic normalized q_c versus ψ_t	q_c =8.810 * ψ_t +21.600	0.309	q_c =5.896* ψ_t +32.010	0.580

Table 16. Regression equations for q_c and normalized q_c versus water content and suction in plastic and non-plastic soils

Type of soil	q_c	r^2	Normalized q_c	r^2
Plastic versus w_n	q_c =-1.090* w_n +41.401	0.227	q_c =-2.612* w_n +129.700	0.231
Non-Plastic versus w_n	q_c =-0.598* w_n +37.774	0.201	q_c =-3.210* w_n +126.210	0.076
Plastic versus ψ_t	q_c=1.055*ψ_t+13.186	0.159	q_c=9.00* ψ_t +6.210	0.427
Non-Plastic versus ψ_t	q_c =1.432* ψ_t +20.410	0.192	q_c =4.483* ψ_t +58.910	0.132

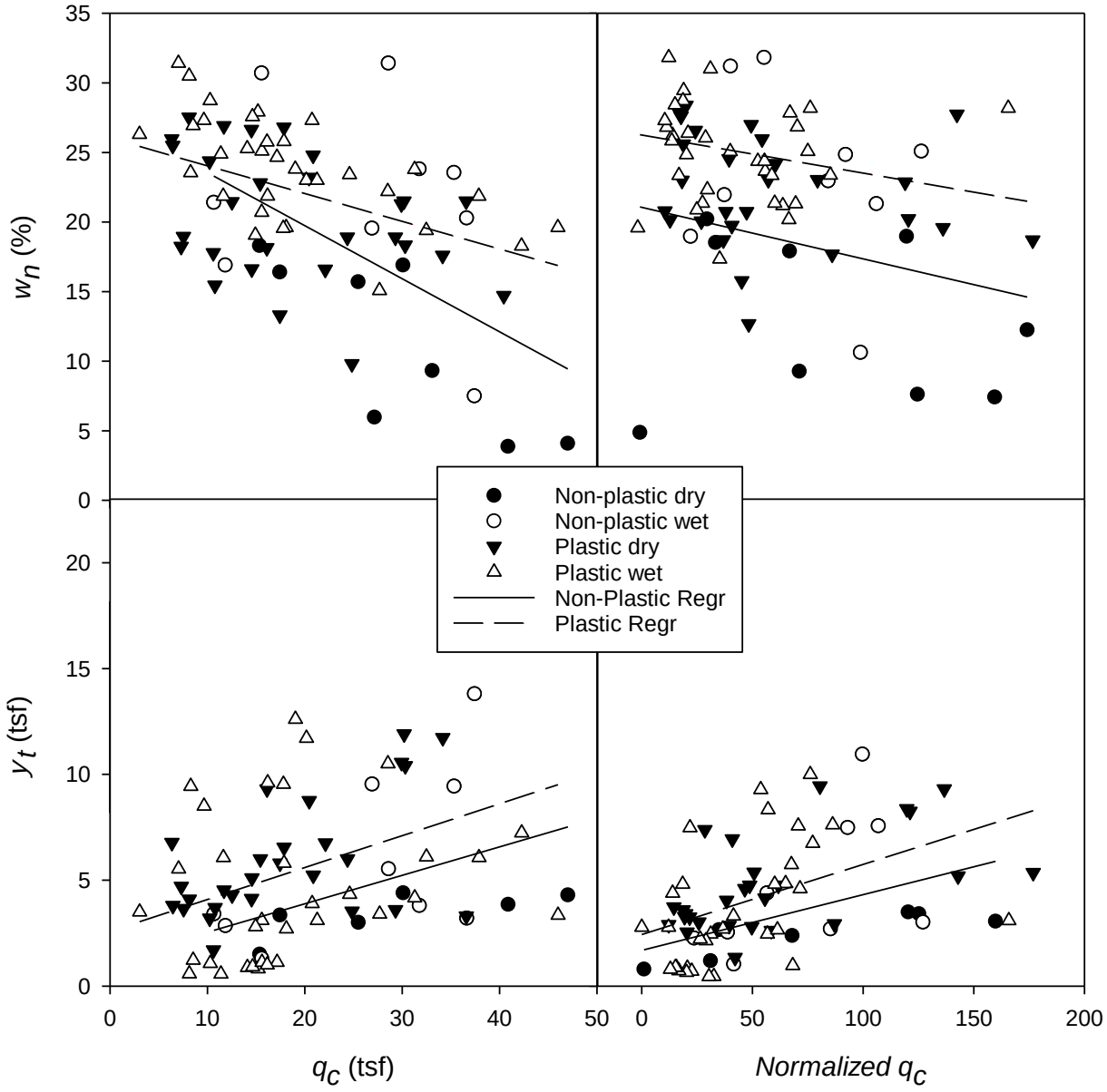

Figure 28. q_c and Normalized q_c versus water content and total suction for wet and dry periods in plastic and non-plastic soils

5.3 Correlation of tip resistance and sleeve friction to shear wave velocity

Proposed correlations by Rix and Mayne (1995) and Hegazy and Mayne (2006) for shear wave velocity prediction based on the CPT parameters were compared to the measured tip resistance, sleeve friction and shear wave velocity from SCPTu in the field. The Rix and Mayne (1995) Equation 8, uses the cone tip resistance measured in the field to predict the shear wave velocity and is based on testing in various clay soils. The Hegazy and Mayne (2006) Equation 9, uses the cone sleeve friction in a logarithmic relationship to predict the shear wave velocity; this correlation was proposed for cohesive and cohesionless soils. SI units were used for the proposed equations so data collected in the field in the current study were converted to the appropriate units and are plotted along with the curves representing the empirical equations in Figure 29. In Figure 29, the data points represent the average tip resistance and sleeve friction and measured shear wave velocity for a given layer determined from SCPTu testing in the current study.

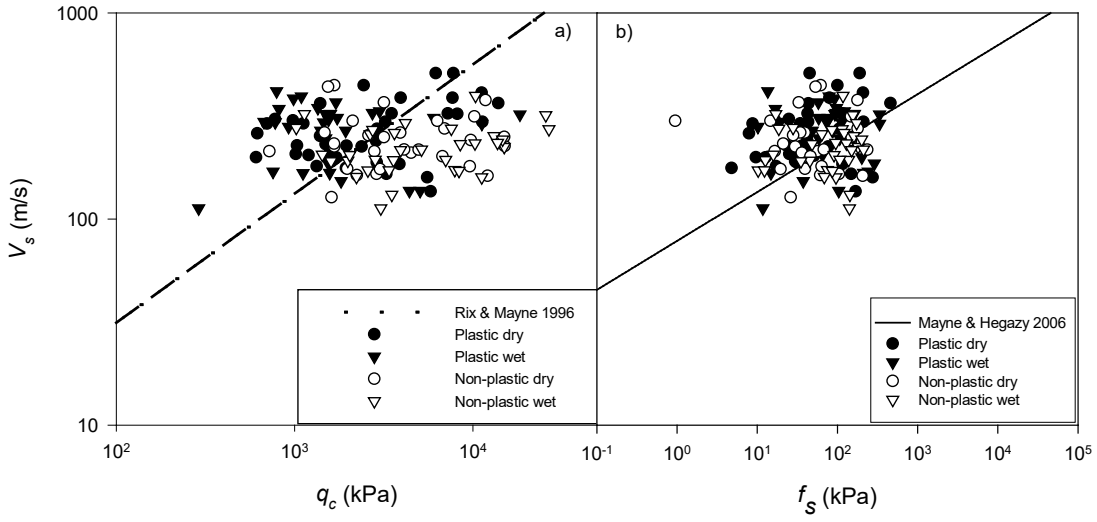

Figure 29. V_s and corresponding q_c and f_s data for plastic and non-plastic soils during wet and dry periods and correlations based on a) Rix & Mayne (1995) and b) Hegazy and Mayne (2006)

As shown in Figure 29 the data collected in the current study cluster around the Equations proposed by Rix and Mayne (1995) and Hegazy and Mayne (2006). While the scatter in these plots is significant, it is comparable to that observed in the Figures 5 and 6 from the original publications. Note the scales in Figure 29 are similar to those used in Figures 5 and 6 so a direct visual comparison can be made.

As shown in Figure 29, measured shear wave velocity during cone testing in the plastic soils tended to be higher than predicted using the empirical equations using tip resistance and sleeve friction. Measured shear wave velocities obtained in the non-plastic soils were on average less than predicted by the empirical equation based on tip resistance as shown in Figure 29a; however, they are roughly equally distributed above and below the line representing predicted velocities based on skin friction in Figure 29b. These observations suggest that shear wave velocity predictions based on tip

resistance and sleeve friction using the Rix and Mayne (1995) and Hegazy and Mayne (2006) equations are somewhat sensitive to the soil type.

The relationship between the shear wave velocity and water content is of interest in this research; hence, analyses were done to observe any noticeable trends between the natural water content and shear wave velocity measured with the SCPTu. Data were separated based on the soil's plasticity. Plastic soils were combined and plotted as shown in Figure 30a, and for non-plastic soils the data are shown in Figure 30b. As shown in Figures 30a and 30b there appears to be a trend of decreasing shear wave velocity with increasing water content, although the correlation is weak. Nevertheless, this observation aligns with what was found in the literature from studying the effect of changes in saturation and water content on shear wave velocity (Dong and Lu 2016, Leong et al. 2005). That there is scatter is not surprising considering there are many factors besides water content that influence the shear wave velocity including stress state, soil composition, and structure.

To investigate the relationship between water content and shear wave velocity further, for each site data representing plastic and non-plastic soils were plotted separately as shown in Figures 30 through 32 and for all of the sites together in Figure 33. Resulting linear equations and coefficients of determination (r^2) are shown on the individual graphs for each site. It is seen that for some sites the correlation is quite strong while for others it is weak. Again, even for individual sites, variations in stress state, soil composition, and structure are significant and will impact this relationship, depending on the uniformity of the individual site stratigraphy.

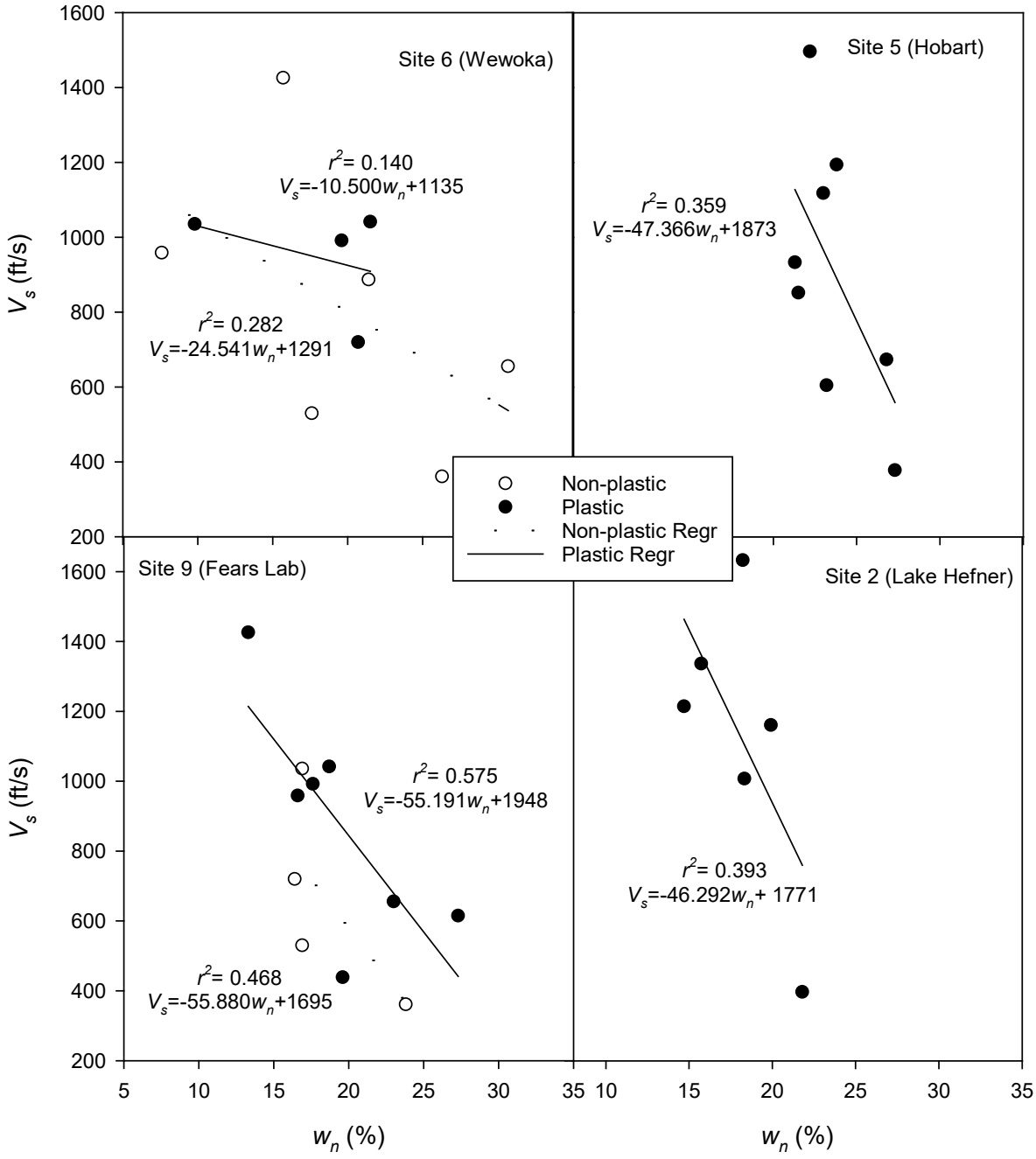

Figure 30. Shear wave velocity versus natural water content for Sites 2,5,6,9

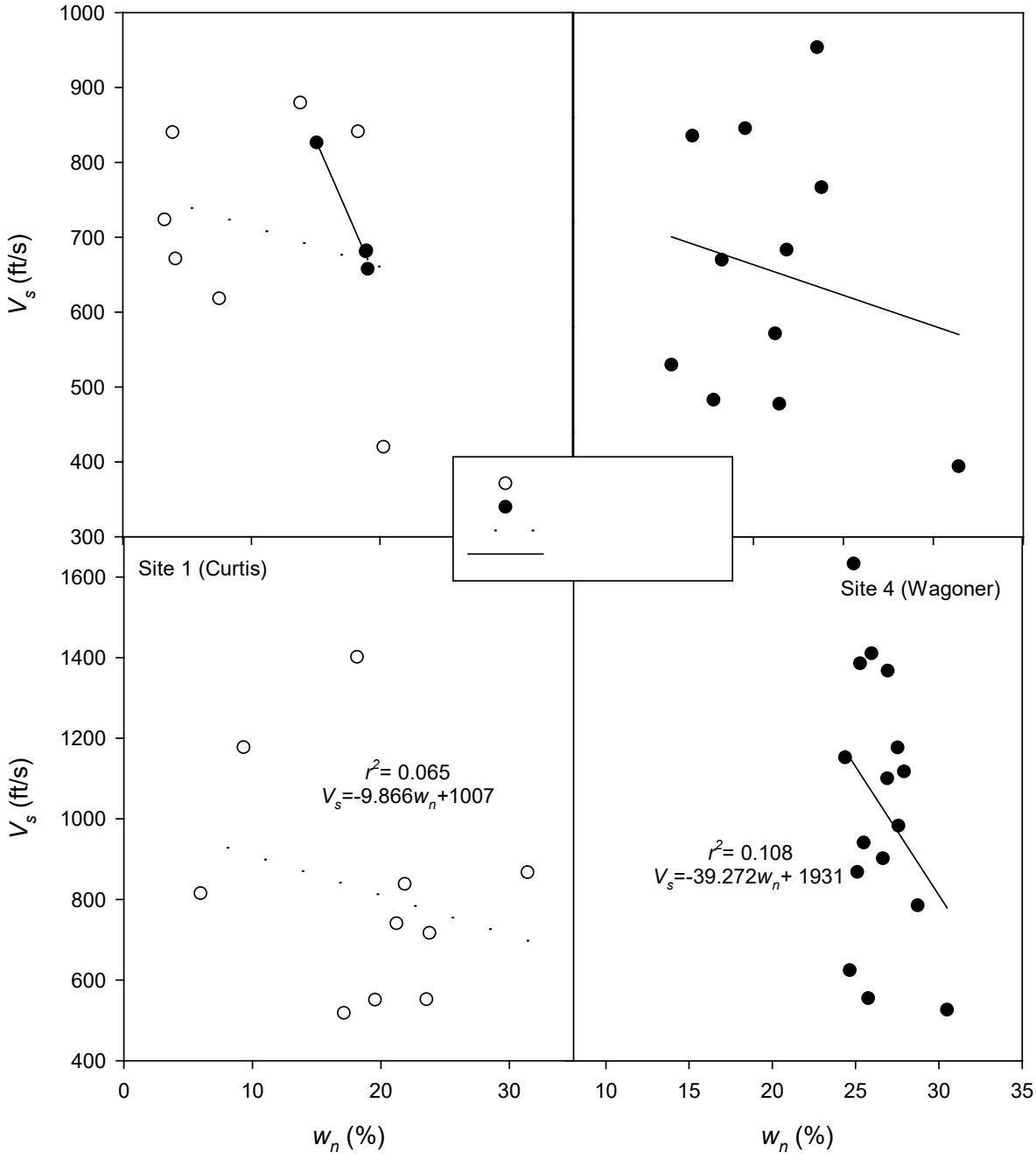

Figure 31. Shear wave velocity versus natural water content for Sites 1,4,7,8

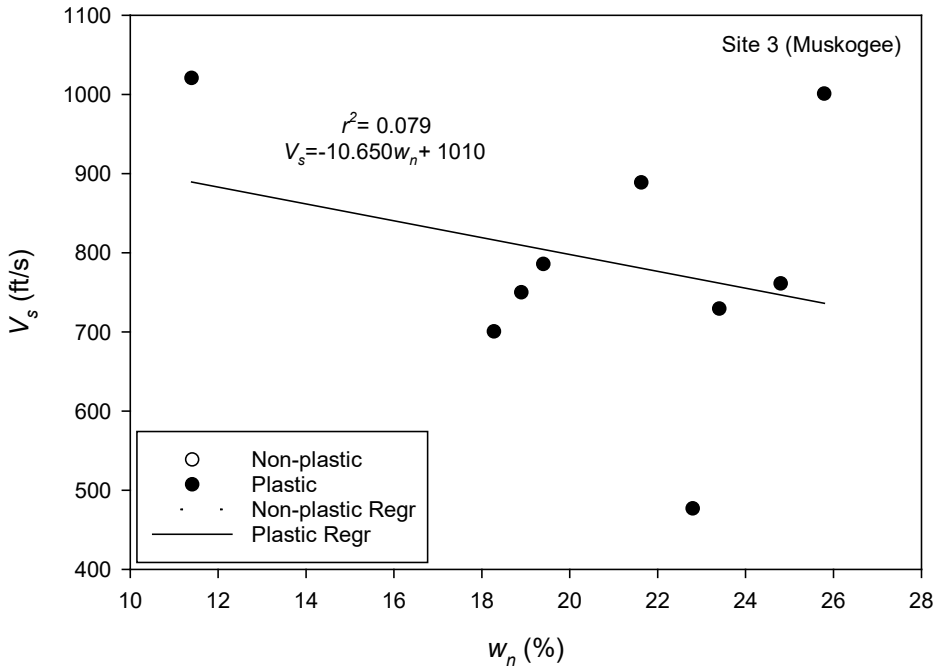

Figure 32. Shear wave velocity versus natural water content for Sites 3 (Muskogee)

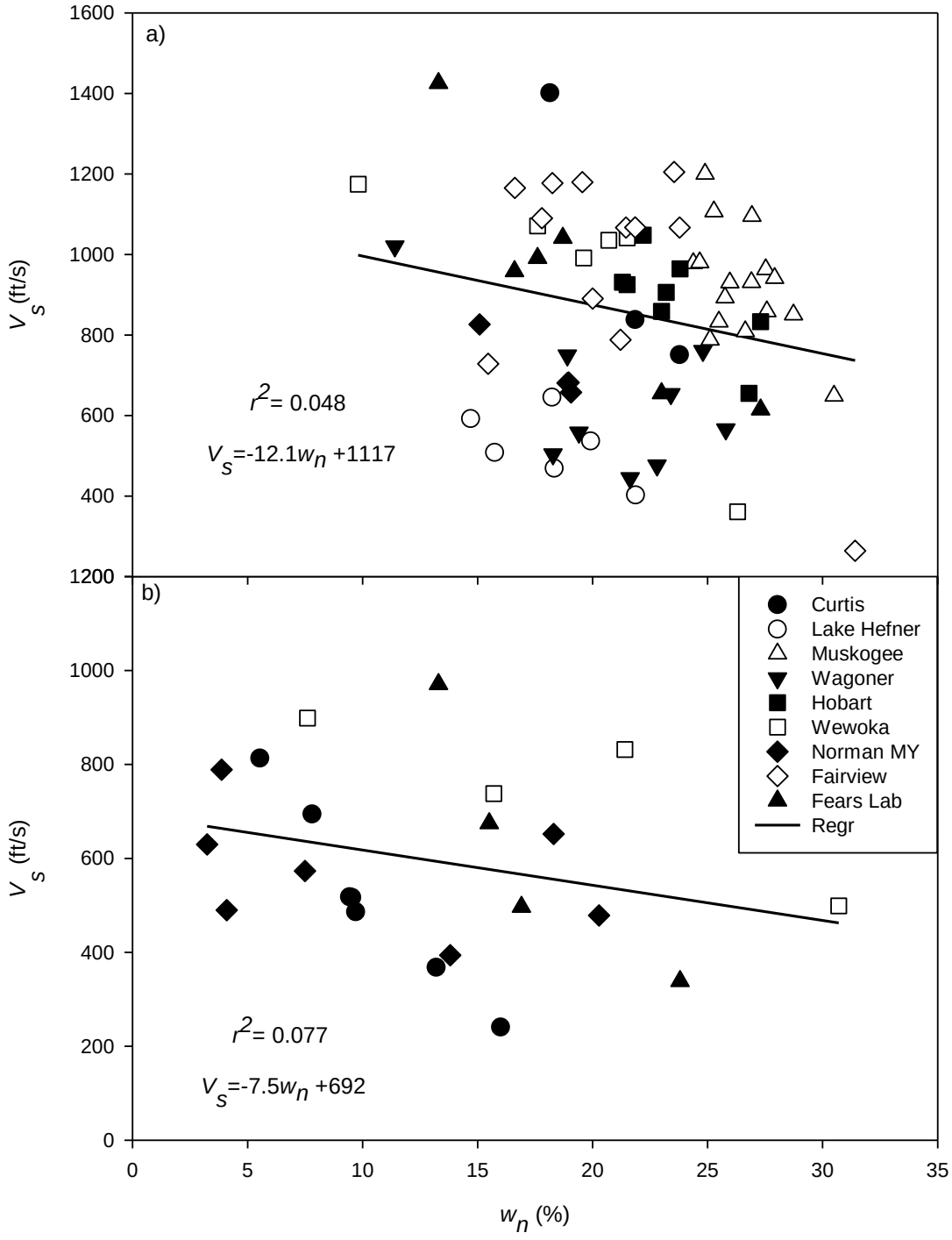

Figure 33. Shear wave velocity (V_s) versus natural water content (w_n) for all sites a) Plastic soils, b) non-plastic soils

5.4 Correlation of sleeve friction to total unit weight

Total unit weight (γ_t) measured in the lab was compared to predicted unit weights that are based on the cone sleeve friction and Equations 2 and 3 proposed by Mayne and Peuchen (2012). These equations are used with the specific units of kN/m^3 for γ_t and kPa for f_s, and were proposed for all soil types.

The measured unit weights based on Shelby tube sample measurements are plotted against the average cone sleeve friction obtained within the range of depths representing the Shelby tube sample taken on the same day. As shown in Figure 34, the data cluster around the curves representing the empirical equations. While there is scatter in the current data, it is similar to the scatter observed in the original data set shown in Figure 3. Note, the axis scales in Figure 34 are similar to those in Figure 3 so that a direct visual comparison can be made.

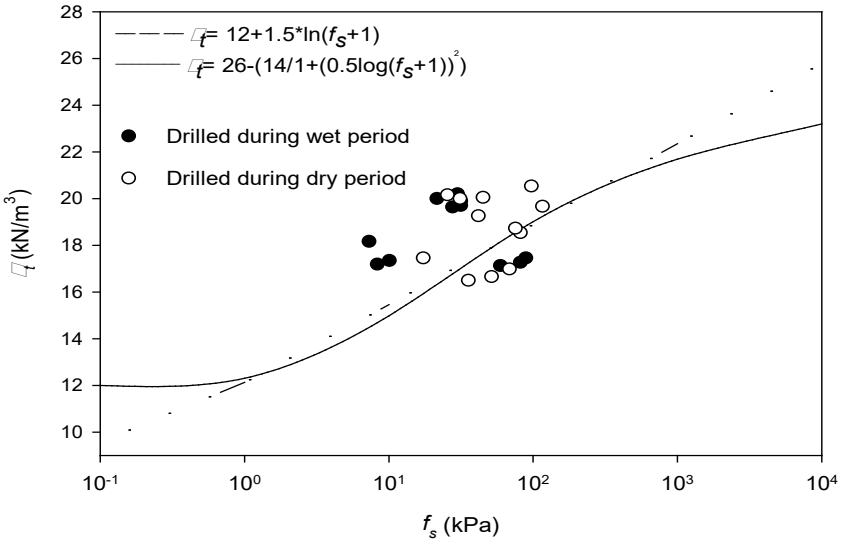

Figure 34. Soil unit weight correlations by Mayne and Puechen (2012) along with data points from SCPTu and lab testing from the current study

5.5 Correlation of cone tip resistance to 1-D compression parameters

5.5.1 Relationship between tip resistance and preconsolidation stress

The preconsolidation stress (σ'_p) is an indication of the stress history that the soil has experienced. It is essentially a yield stress that develops from past loading and physico-chemical changes in a soil profile. It is critical for the proper analysis of consolidation settlement of a soil profile. In order determine the preconsolidation stress, the Casagrande construction technique was used to analyze the one-dimensional compression curves obtained from oedometer tests. Tests were conducted at the natural water content in an unsaturated condition and in a saturated condition. The preconsolidation stresses obtained from the laboratory were compared to those predicted using cone tip resistance and Equation 6 (Mayne et al. 2009).

In Figure 35 the preconsolidation stresses from saturated and unsaturated oedometer tests are plotted against the average tip resistance in the depth vicinity where the oedometer samples were obtained. The cone profiles used correspond to the date when the tube samples were obtained. Also show in Figure 33 are curves corresponding to the empirical Equation 6 and Figure 4 (Mayne et al. 2009). As discussed previously, the exponent *m´* typically varies from 0.72 for sands to 1.0 for intact clays. Results from the current study plot within this range of *m´* values, with the clayey soils generally plotting toward the high end of this range. Interestingly, there was not much variation between the preconsolidation stress obtained for similar samples in a saturated and unsaturated condition.

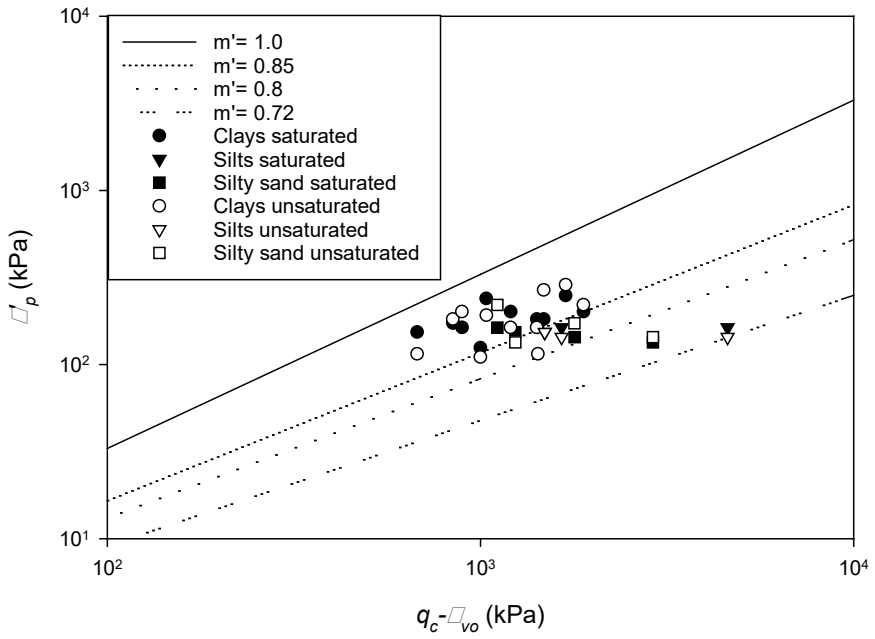

Figure 35. Preconsolidation stress vs net tip resistance plotted along with curves representing the correlation of Mayne et al. (2009)

5.5.2 Relationship between tip resistance and compression indices

The virgin compression index c_c, and recompression/swell index (c_r=c_s) are mechanical properties of the soil used to predict deformation of a soil profile during primary consolidation. The recompression index and swell index are assumed to be the same and are obtained from an unload-reload sequence during the oedometer test. Since correlations between these properties and the cone parameters were not found in the literature, the relationship between the compression indices and tip resistance were examined using the data collected in this study. A reasonable trend was observed between the compression indices and normalized cone tip resistance as shown in Figures 36 and 37.

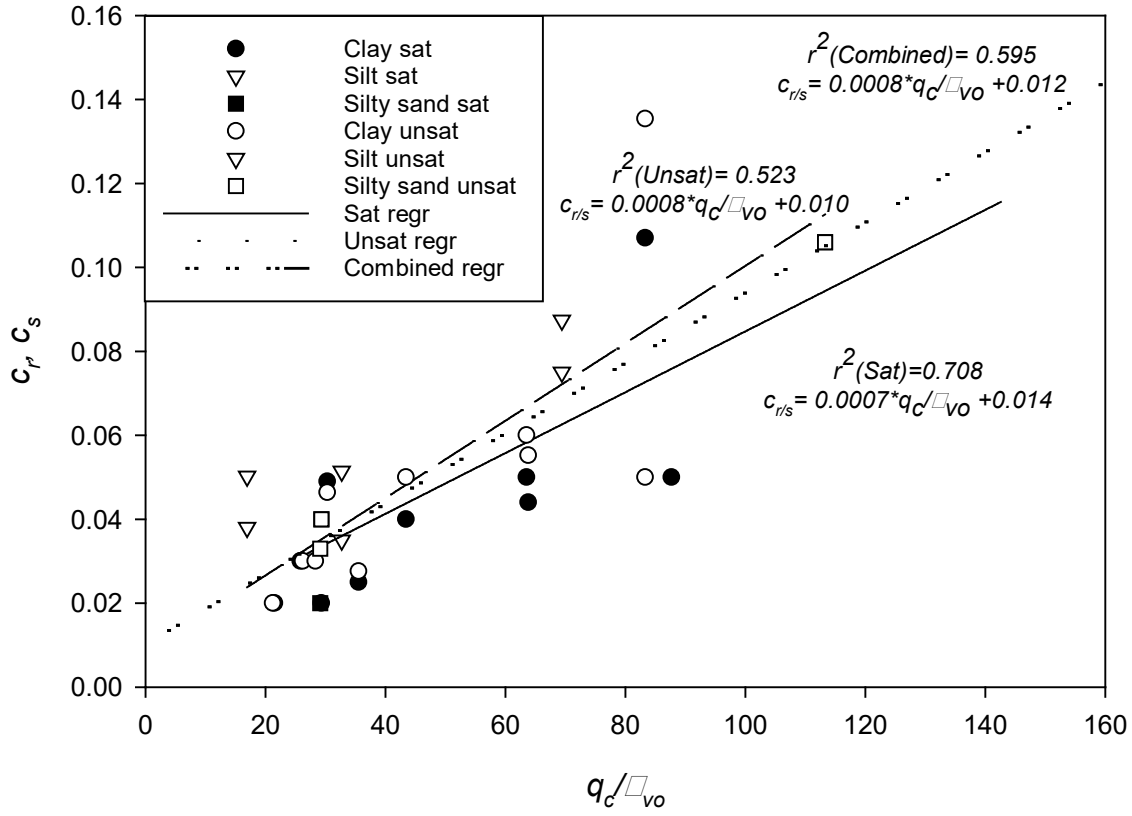

Figure 36. c_r, c_s versus q_c/σ_{vo} for saturated and unsaturated oedometer testing

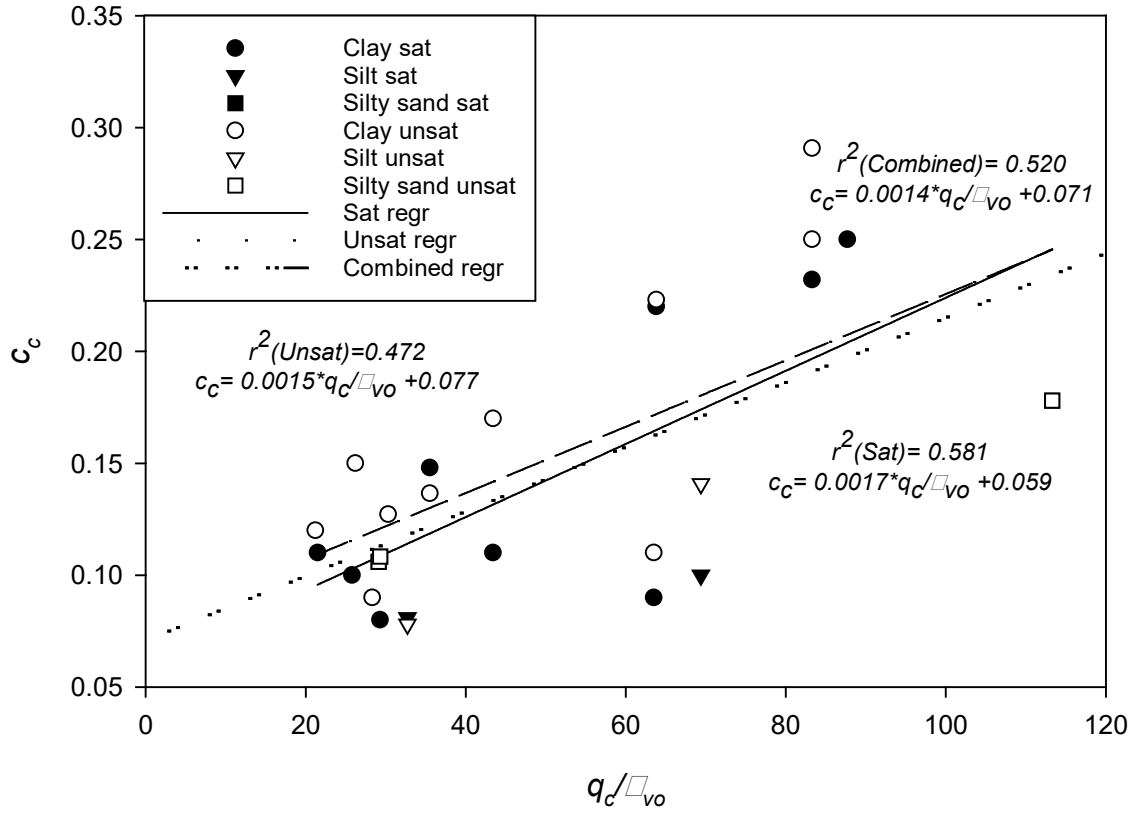

***Figure 37. c_c* versus q_c/σ_{vo} for saturated and unsaturated oedometer testing**

5.6 Correlation of cone tip resistance to undrained shear strength

The undrained shear strength (s_u) represents the shearing resistance of a soil when shear induced excess pore water pressures do not dissipate. It is important for estimating the bearing capacity of foundations and in assessing the stability of retaining walls, slopes, and embankments on saturated clay soils. In order to determine the undrained shear strength, isotropically consolidated undrained triaxial compression tests were conducted on tube samples collected from the field. The undrained shear strengths obtained from the laboratory were compared to those predicted using cone tip resistance and Equation 4 (Lunne et al. 1997).

In Figure 38 the undrained strength estimated from the first stage of triaxial tests is plotted against the average net tip resistance in the depth vicinity of the triaxial test sample. The first stage triaxial strengths were used since they were conducted using an initial effective confining stress equal to the estimated in situ effective confining stress at the sample depth. Also shown in Figure 38 are lines calculated using Equation 4 for the typical range of N_{kt} equal to 10 to 20 Lunne et al. (1997).

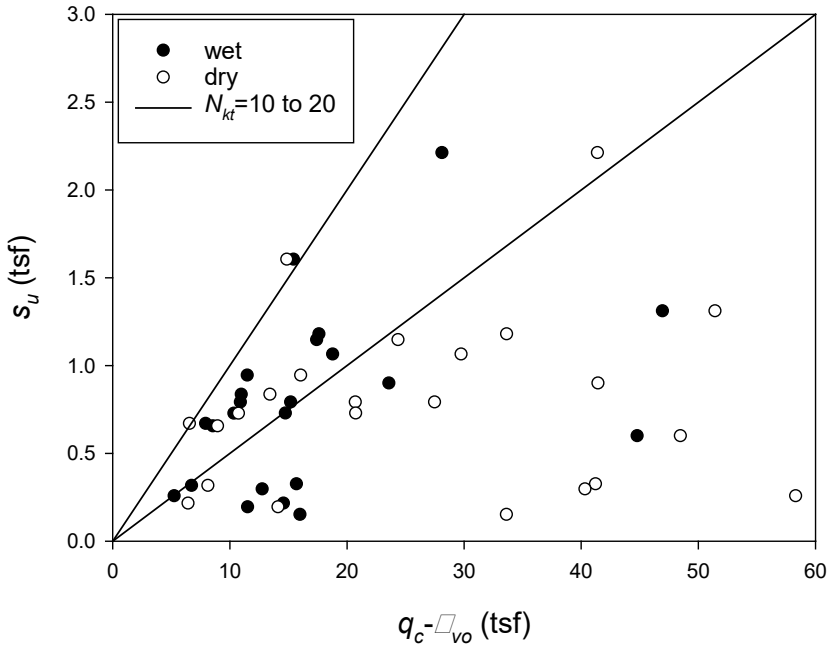

Figure 38. Comparison of undrained shear strength and net tip resistance from the current study and lines representing different cone factors based on Lunne et al. (1997)

Most of the data obtained in the current study falls outside and below the typical range of N_{kt} values in Figure 38, particularly for cone profiles obtained during drier periods. This makes sense, since the cone tests were conducted in partially saturated soils. In such soils the presence of matric suction will increase the tip resistance compared to the saturated condition; however, the undrained strength in the laboratory is measured under fully saturated conditions. Observations from Figure 38 suggests

that using the cone in an unsaturated profile is not a reasonable approach to estimating undrained shear strength for saturated conditions using Equation 4, since it would require knowledge of how N_{kt} varies with degree of saturation and matric suction.

Another approach is to normalize the variables involved by the stress conditions that influence those variables. In Figure 39, the net cone tip resistance normalized by the total suction is plotted against the undrained shear strength normalized by the initial effective confining stress. While the scatter is significant, there is a definite trend apparent in the data and the scatter is significantly reduced compared to Figure 38.

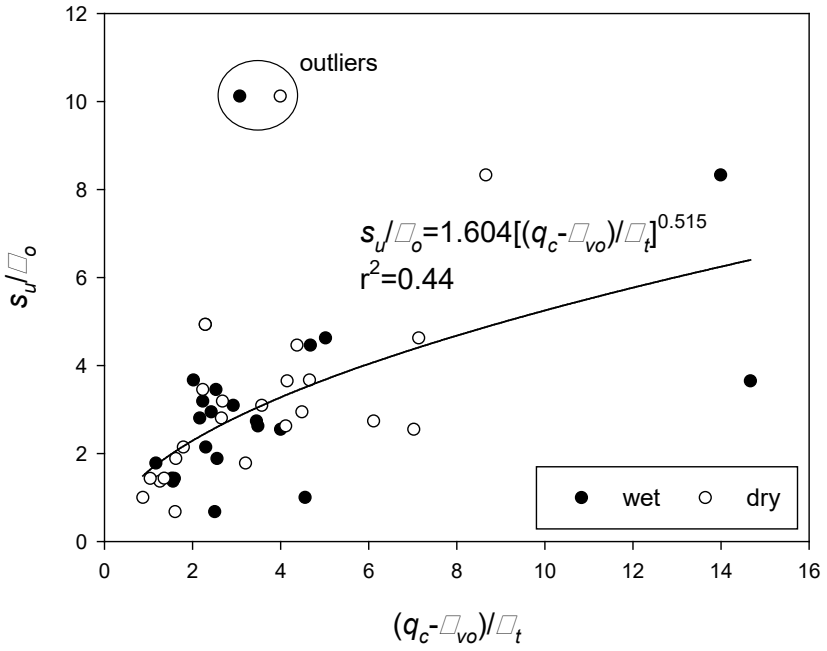

Figure 39. Normalized undrained shear strength versus suction normalized net tip resistance

5.7 Correlation of cone tip resistance to drained friction angle

The effective stress conditions at failure from the multistage triaxial tests were used to determine the effective stress friction angle (ϕ'). In Figure 40, these are plotted against the corresponding average cone tip resistance normalized by the overburden stress, along with the lines representing correlations proposed by Kulhawy and Mayne (1990) and Uzielli et al. (2013). Note, these correlations are based on sandy soils starting at ϕ'=25˚. As shown in Figure 40, there is a great deal of scatter, which is not surprising given that cone penetration in clays, even partially saturated clays, does not involve drained shearing of the soil. Rather, considerable excess pore water pressures can be seen in many of the cone plots (Appendix A). Given this fact, and the lack of trend in the data, it is not recommended that effective stress friction angle be estimated for fine grained soils on the basis of cone tip measurements.

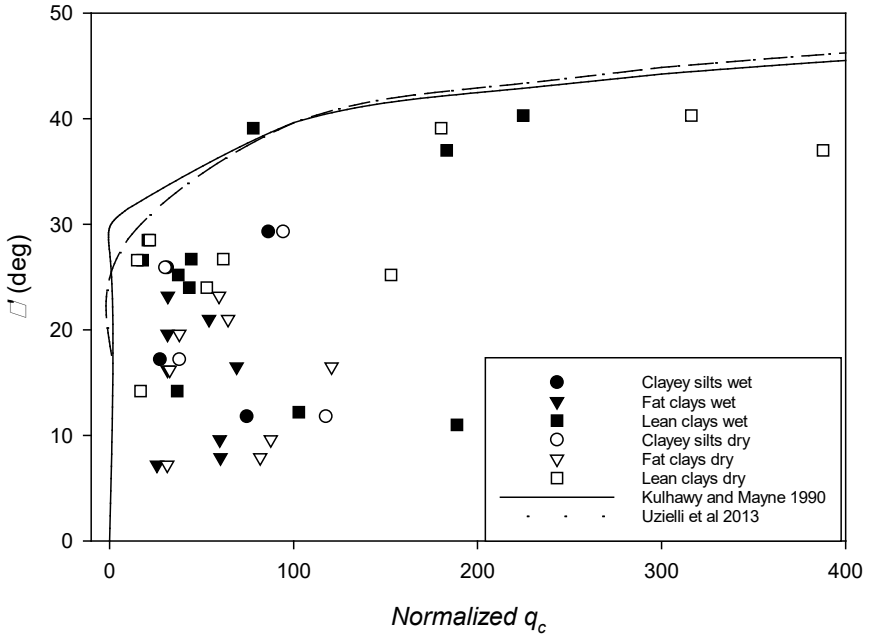

Figure 40. Effective friction angle versus normalize tip resistance and curves based on correlations from Kulhawy and Mayne (1990) and Uzielli et al. (2013)

6 Summary Conclusion and Recommendations

6.1 Introduction

Soil profiles were investigated at nine sites across the State of Oklahoma. Field testing was conducted at each site using the seismic cone penetration test (SCPTu) to determine cone parameter data (q_c, f_s, FR, u, and V_s). SCPTu testing was conducted twice at each site on different dates in an attempt to study how the degree of saturation in the unsaturated soil zone influences the estimation of soil parameters. Laboratory tests were also conducted on disturbed and undisturbed samples collected from the field to determine the soil's physical and mechanical properties. Measured soil properties from laboratory testing were compared to those estimated using empirical equations involving cone testing parameters. In some cases, new correlations were developed based on trends in the data. The analysis and comparison of results led to the following conclusions.

6.2 Summary and Conclusion

1. Using SCPTu parameters with some empirical equations provides a reasonable means for making a first approximation of mechanical properties of soil. In this study empirical correlations relating cone test parameters, primarily tip resistance and in some cases sleeve friction, were examined as a means of estimating shear wave velocity in soil, soil total unit weight, preconsolidation stress, compression index, recompression/swell index, undrained shear strength and effective stress friction angle.
2. For each site the SCPTu parameters, q_c, f_s, u, FR, and V_s were plotted versus depth along with the natural water content and total suction of samples obtained on each of the two visits. The comparison of multiple SCPTu profiles at each site showed

that the soundings were generally repeatable, with a few exceptions. For analysis, average profiles of cone parameters with depth were determined for each site. For some of the sites there were clear differences in the moisture content and suction profiles measured on the two testing dates, which appeared to influence the SCPTu parameters obtained on those dates. Generally, it was observed that the SCPTu parameters obtained during wetter and drier testing dates roughly correlated to the water content or suction measured in the profile on the testing dates. For the data obtained from nine sites in this study, results showed that as the soil water content decreases the suction generally increased, as expected. Further analysis also showed that differences in water content between SCPTu testing on wet and dry dates, led to differences in q_c, f_s, *FR*, *u*, and V_s.

The main observation was that as water content decreased or suction increased, the tip resistance (q_c), sleeve friction (f_s) and shear wave velocity (V_s) generally tended to increase. The friction ratio (FR) did tend to change somewhat from wet to dry periods; however, it was less predictable. The excess pore water pressure measured during penetration was generally quite erratic with depth, which is attributed to penetration through a substantial unsaturated, in many cases, variable profile at test sites.

The pore water pressure measuring system on the cone will not function properly if not maintained in a saturated condition. It is unclear whether saturated conditions could be maintained for penetration through strongly dilative unsaturated soils. However, at some sites on a given day the pore pressure profiles were quite similar from sounding to sounding, while at other sites they were not as repeatable. Another point to consider is that excess pore pressure generation in unsaturated soils involves

both the air phase and water phase, the air phase being compressible. Thus, it is not possible to know whether the pore pressure response measured by the cone is due to air pressure, water pressure, or both. This will depend on the degree of saturation of the soil and the measuring system, the compressibility of the soil skeleton, and the transmissibility of the air and water through the pore pressure measuring system and surrounding soil. For these reasons, there is uncertainty regarding the meaning or use of pore pressure measurements in unsaturated soils. This is an area where more research would be beneficial.

3. The Soil Behavior Type (SBT) was used to classify the soil profiles tested in the field using the normalized tip resistance and sleeve friction. Results showed that as the CPT data changed between the wet and dry periods, the classification of the soils based on the SBT changed somewhat for some of the test sites. The SBT depends on the tip resistance and sleeve friction, which are sensitive to the moisture content and suction.

4. As noted, tip resistance was sensitive to water content and total suction of the soil tested. Generally, results showed that as the water content increased, suction decreased, and tip resistance decreased. Plots of tip resistance and normalized tip resistance for all of the sites together revealed expected trends but coefficients of determination for first order trends were relatively weak. When the soils were grouped according to whether they were predominantly plastic or non-plastic, the strength of the trends improved in some cases and it was found that the whether the soils were tested during a wetter or drier period had some effect on these trends. It is not surprising that

there is significant scatter in these trends given the substantial spatial variations in soil properties at individual sites and differences in soil types across the nines sites.

5. For shear wave velocity, the correlations proposed by Rix and Mayne (1995) using tip resistance, and Hegazy and Mayne (2006) using sleeve friction, were examined. Predicted shear wave velocities based on tip resistance and sleeve friction were plotted against measured shear wave velocities from the SCPTu and superimposed on the curves suggested by Rix and Mayne (1995) and Hegazy and Mayne (2006), respectively. While the results were scattered, the predictions were generally clustered around the empirical trend lines. It is noted that the degree of scatter observed in the current data was similar to that observed in the data presented by Rix and Mayne (1995) and Hegazy and Mayne (2006). It was also observed that the soil plasticity had some influence on the predictions, particularly for those based on tip resistance.

6. Consolidation test parameters including preconsolidation stress (σ'_p), compression (c_c) and recompression/swell indices (c_r=c_s) obtained from odeometer tests under saturated and unsaturated conditions were compared to the tip resistance. The correlation proposed by Mayne et al. (2009) that relates preconsolidation stress to the tip resistance compared favorably to the measured preconsolidation stress and corresponding tip resistance found in the current study. Results also showed that the differences between saturated and unsaturated testing were minor with respect to the preconsolidation stress.

Compression indices (c_c *and* c_r=c_s) were compared to the corresponding tip resistance normalized by the vertical overburden pressure (q_c/σ_{vo}) and fitted with first

order trend lines. While some scatter was observed, the trends were relatively good especially considering the significant spatial variations in soil properties in the data set. The results also showed minor differences between results based on saturated and unsaturated oedometer tests.

7. The commonly used correlation (e.g. Lunne 1997) that relates undrained strength to net tip resistance ($s_u=(q_c-\sigma_{vo})/N_{kt}$) was compared to s_u values obtained from the multi-stage CIUC triaxial tests and corresponding net tip resistance ($q_c-\sigma_{vo}$) values. For saturated soils, cone factors used in this correlation typically range between 10 and 20; however, most results from the current study showed that N_{kt} falls outside of this range and is considerably higher. This is not surprising given that cone testing was performed in an unsaturated soil profile and compared to a saturated undrained strength. However, when the net tip resistance is normalized by suction and compared to the laboratory undrained strength normalized by the effective confining stress, a stronger trend is observed when this relationship is represented with a power model.

8. The comparison of effective stress friction angles determined from triaxial testing to corresponding tip resistance revealed no obvious trends. This is attributed to the fact that cone penetration, even in unsaturated fine-grained soils is not likely to occur under drained conditions.

6.3 Recommendations for implementation

Correlations between SCPTu parameters and soil mechanical properties provide a reasonable means for making first approximations of soil properties needed for analysis of geotechnical problems. Most existing correlations are based on laboratory testing of saturated soils or dry sands and corresponding cone penetration testing in saturated

soils or dry sands. In Oklahoma, it is common to encounter unsaturated conditions over a significant depth in the upper soil profile during field testing. This is also the portion of the profile which is often subjected to the greatest increases in stress due to surface loading from structures. Thus, it is important to properly characterize the upper profile for geotechnical analyses.

Depending on seasonal weather variations and climate cycles it is possible for moisture conditions at many sites to vary between relatively low to relatively high degrees of saturation over time scales that range from months to years. Therefore, it is typical and conservative to base geotechnical analyses on the worst-case soil conditions, which generally correspond to the saturated condition with regard to soil strength and stiffness. Herein lies the dilemma, in that while a site may become nearly saturated at some point in its design life, it may be at a lower degree of saturation at the time of subsurface exploration. So the question is, how do engineers use results of in situ tests, such as the cone penetration test to determine soil properties corresponding to saturated conditions? The research in this report was an attempt to partly address this question. The research examined how existing correlations between cone parameters and soil properties performed when cone testing was conducted at sites with variable moisture conditions. Further, new correlations were developed for some soil properties where existing correlations were limited.

Regarding implementation, as discussed in this report, some existing correlations performed reasonably well given the unsaturated nature of the deposits in which the cone tests were performed. However, as is the case with nearly all empirical correlations in the literature, estimations of soil properties using these correlations

should be considered a first approximation. This is true regardless of whether the sites are in a saturated or unsaturated condition. It is recommended that these correlations could be used for first approximations of saturated soil properties based on SCPTu results; however, companion laboratory testing should always be conducted for validation and to develop site specific correlations as needed. The SCPTu is a very effective profiling tool and can provide extremely valuable information regarding the spatial variation of soil types across a site. However, the determination of soil properties is largely based on empirical relationships between the cone parameters and the soil properties. By conducting some companion testing, such as saturated triaxial and oedometer testing at selected locations, the usefulness of the cone data is greatly extended. It is also recommended that when cone penetration testing is conducted in unsaturated soils, companion measurements of moisture content and suction (if possible) be obtained at regular intervals through the unsaturated profile.

6.4 Recommendations for research

The following are recommendations for future research based on the finding of this study:

1. Collecting field and laboratory data takes a great deal of time and effort. While the 9 test sites investigated in this research is significant, it is desirable to continuing building on this database given the broad range of soil types in Oklahoma and extensive variations found in natural soils. This doesn't necessarily have to be accomplished with another research project, rather the ODOT Materials Division could make the required testing protocol part of their investigation strategy when cone penetration testing is conducted. That is, it is recommended that when cone testing is conducted, companion

test borings and thin-walled tube sampling should also be conducted along with laboratory testing to determine mechanical properties, natural water content and total suction measurements. In this way, the database can be expanded and correlations can be refined. Possibly, some additional funding could be set aside to support the additional work if it falls beyond the scope or budget of the work proposed, and some funding could also be set aside to support outside researchers for some of the extra work. Possibly this could involve a research task order or other funding procedure on an as needed basis.

2. Shear wave velocity measurements are the basis for determining seismic site class for civil engineering structures. However, the shear wave velocity measurements are dependent on the moisture condition and suction, among other factors, present at the time of testing. It is possible that for some soil profiles the seismic site class could change depending on when the seismic velocity measurements are obtained with the SCPTu for example. Thus, it is important to consider the influence of environmental factors affecting the determination of seismic velocity in unsaturated soil profiles.

Some recent work by OU investigators involving laboratory measurements of shear wave velocity on unsaturated samples under controlled suction during wetting and drying has revealed strong relationships between shear wave velocity, suction and water content for a given soil. Results in this report from the current study show that shear wave velocity does correlate to water content and suction, but the trends are relatively weak from a statistical perspective. This is attributed partly to the significant variability in the natural soils that were tested and since shear wave velocity depends on several factors including soil composition, structure, and overall stress state, which

includes the suction. To better understand the relationships between shear wave velocity and the various factors that influence it, it is proposed to broaden the initial laboratory study to examine these relationships systematically. In addition to testing on laboratory prepared samples, the proposed study will examine the relationship between laboratory measurements of shear wave velocity and those obtained by the SCPTu at different test sites. This will include field testing with the SCPTu and collection of companion thin-walled tube samples that will be subjected to shear wave velocity testing in the laboratory under controlled stress conditions. This will allow for direct comparison of shear wave velocity obtained in the field and lab. The field samples will first be tested at a water content and stress conditions simulating the field conditions, and will then be subjected to controlled changes in suction with additional shear wave velocity measurements. This will provide great insight into how the shear wave velocity varies with changes in moisture content and suction under wetting and drying cycles.

Knowing how the water content and suction affects the shear wave velocity of lab samples, and knowing the relationship between laboratory and field determined shear wave velocities, it will be possible to estimate how the field determined shear wave velocities will change due to changes in the in situ moisture content and suction. Thus, when shear wave velocities are obtained using SCPTu profiles, engineers will have a method for estimating how these will change due to estimated changes in moisture conditions considering the initial moisture state and expected seasonal variations. Ultimately, this will lead to better estimates of seismic site class for engineering design.

Another outcome of this work is that it may be possible to exploit these findings to develop a method for estimating suction in situ using SCPTu measurements of shear

wave velocity and knowledge of the soil type and initial moisture state. This study will be substantial in scope and probably best suited to a multi-year investigation.

3. As discussed, there is much uncertainty associated with pore pressure measurements during cone penetration through unsaturated soil. Research is needed to study the meaning of these measurements for different soils under different degrees of saturation. Research envisioned would include: cone testing under laboratory bench scale conditions where initial degrees of saturation and stress conditions could be controlled for different soil types, field testing with the CPTu along with companion sampling to study pore pressure development in the samples under laboratory controlled tests with pore air and pore water measurements, studying CPTu pore pressure dissipation tests in unsaturated soil profiles, and development of new cone pore pressure measurement systems to separate pore air from pore water pressures. The latter will be incorporated into the lab and field testing aspects of the study.

References

1. ASTM (2012). D5778-12 Standard test method for electronic friction cone and piezocone penetration testing of soils. Annual Book of ASTM Standards, 4, 1587-1605.

2. ASTM (2014). D6282/D6282M-14 Standard Guide for Direct Push Soil Sampling for Environmental Site Characterizations.

3. ASTM (2015). D1587/D1587M-15 Standard Practice for Thin-Walled Tube Sampling of Fine-Grained Soils for Geotechnical Purposes

4. ASTM (2017). D6913/D6913M-17 Standard Test Methods for Particle-Size Distribution (Gradation) of Soils Using Sieve Analysis

5. ASTM (2017). D4318-17e1 Standard Test Methods for Liquid Limit, Plastic Limit, and Plasticity Index of Soils

6. ASTM (2021). D7263-21 Standard Test Methods for Laboratory Determination of Density and Unit Weight of Soil Specimens

7. ASTM (2011). D2435/D2435M-11 Standard Test Methods for One-Dimensional Consolidation Properties of Soils Using Incremental Loading

8. ASTM (2011). D4767-11 Standard Test Method for Consolidated Undrained Triaxial Compression Test for Cohesive Soils

9. Collins, R.W. (2016). In situ testing and its application to foundation analysis for fine-grained unsaturated soils. Ph.D. Dissertation, University of Oklahoma, 217 p.

10. Collins, R., & Miller, G. A. (2014). Cone penetration testing in unsaturated soils at two Instrumented test sites. In Proceedings of the 6th International Conference on Unsaturated Soils, UNSAT, Sydney, Australia, 2-4.

11. Durgunoglu, H. T., & Mitchell, J. K. (1973). Static penetration resistance of soils. For NASA Grant NGR 05-003-406: Lunar Soil Properties and Soil Mechanics, Space Sciences Laboratory Series 14, Issue 24, UC Berkeley, 223 p.

12. Freitag, D. R., Green, A. J., & Melzer, K. J. (1970). Performance evaluation of wheels for lunar vehicles (No. AEWES-TR-M-70-2). Army Engineer Waterways Experiment Station, Vicksburg, MS.

13. Hegazy, Y. A., & Mayne, P. W. (2006). A global statistical correlation between shear wave velocity and cone penetration data. In Site and Geomaterial Characterization (pp. 243-248).

14. Houston, S. L., Houston, W. N., & Anderson, T. W. (1995). Moisture and strength variability in some Arizona subgrades. Transportation Research Record, (1481), 35-43.

15. Hryciw, R. D., & Dowding, C. H. (1987). Cone penetration of partially saturated sands. Geotechnical Testing Journal, 10(3), 135-141.

16. Jarast, S. P., & Ghayoomi, M. (2016). Simple numerical model to simulate penetration testing in unsaturated soils. In E3S Web of Conferences (Vol. 9). EDP Sciences.

17. Lehane, B. M., Ismail, M. A., & Fahey, M. (2004). Seasonal dependence of in situ test parameters in sand above the water table. Géotechnique, 54(3), 215-218.

18. Lo Presti, D., Stacul, S., Meisina, C., Bordoni, M., & Bittelli, M. (2018). Preliminary Validation of a Novel Method for the Assessment of Effective Stress State in Partially Saturated Soils by Cone Penetration Tests. Geosciences, 8(1), 30.

19. Lunne, T., Robertson, P. K., & Powell, J. J. M. (1997). Cone penetration testing in geotechnical engineering. Spon Press an Imprint of Taylor and Francis Group, 312 p.

20. Mayne, P. W. (2006a). In-situ test calibrations for evaluating soil parameters. In Characterisation and Engineering Properties of Natural Soils–Proceedings of the Second International Workshop on Characterisation and Engineering Properties of Natural Soils: Taylor & Francis, 1601-1652.

21. Mayne, P. W. (2006b). The Second James K. Mitchell Lecture Undisturbed sand strength from seismic cone tests. Geomechanics and Geoengineering: An International Journal, 1(4), 239-257.

22. Mayne, P. W. (2014). Interpretation of geotechnical parameters from seismic piezocone tests. In Proceedings of 3rd International Symposium on Cone Penetration Testing, CPT14, Las Vegas, Nevada, Gregg Drilling & Testing, Inc. www. cpt14. com.

23. Hegazy, Yasser & Mayne, Paul. (2006). A Global Statistical Correlation between Shear Wave Velocity and Cone Penetration Data. Geotechnical Special Publication. 243-248. 10.1061/40861(193)31.

24. Mayne, P. W., & Kemper, J. B. (1988). Profiling OCR in stiff clays by CPT and SPT. Geotechnical testing journal, 11(2), 139-147.

25. Mayne, P. W., & Rix, G. J. (1995). Correlations between shear wave velocity and cone tip resistance in natural clays. Soils and foundations, 35(2), 107-110.

26. Marsland, A., & Quarterman, R. S. T. (1982). Factors affecting the measurements and interpretation of quasi static penetration tests in clays. In Proc. 2nd European Symposium on Penetration Testing ESOPT II (2), AA Balkema, Amsterdam (The Netherlands) (pp. 697-702).

27. Massarsch, K. R. (2014, May). Cone penetration testing—a historic perspective. In Proceedings 3rd international symposium on cone penetration testing. Las Vegas, Nevada, USA, 97-134.

28. Miller, G.A., Hatami, K., Cerato, A.B. and Osborne, C. (2013). Applied Approach Slab Settlement Research, Design/Construction. Final Report FHWA-OK-13-09, ODOT SPR 2227, 162 p.

29. Miller, G.A., Collins, R.W., Muraleetharan, K.K., Cerato, A.B., Doumet, R. (2015). Interpretation of In Situ Tests as Affected by Soil Suction. Final Report FHWA-OK-15-09, ODOT SPR 2160, 181 p.

30. Miller, G.A, Tan, N.K, Collins, R.W, Muraleetharan, K.K. (2018). Cone penetration testing in unsaturated soils. Transportation Geotechnics, Volume 17, Part B, Pages 85-99, ISSN 2214-3912,

31. Miller, G. A, Collins, R.W, Muraleetharan, K.K, Abuawad, T.Z. (2021). Application of in situ tests in unsaturated soils to analysis of spread footings. Soils and Rocks, v. 44.

32. Mohamed, F. M., & Vanapalli, S. K. (2015). Bearing capacity of shallow foundations in saturated and unsaturated sands from SPT–CPT correlations. International Journal of Geotechnical Engineering, 9(1), 2-12.

33. Nevels, Jr, J. B. (2006). Spatial distribution of electric cone tip resistance measurements with depth for a Burleson clay site. In GeoCongress 2006: Geotechnical Engineering in the Information Technology Age.

34. Oklahoma Department of Transportation boring logs for Curtis, Oklahoma site. July, 2000.

35. Oklahoma Department of Transportation boring logs for Fairview, Oklahoma site. May, 1995.

36. Oklahoma Department of Transportation boring logs for Hobart, Oklahoma site. January, 2017.

37. Oklahoma Department of Transportation boring logs for Lake Hefner, Oklahoma site. 2004.

38. Oklahoma Department of Transportation boring logs for Muskogee, Oklahoma site. January, 2003.

39. Oklahoma Department of Transportation boring logs for Wagoner, Oklahoma site.

40. Oklahoma Department of Transportation boring logs for Wewoka, Oklahoma site. December, 2002.

41. Pournaghiazar, M., Russell, A. R., & Khalili, N. (2013). The cone penetration test in unsaturated sands. Geotechnique, 63(14), 1209-1220.

42. Robertson, P.K., 2010a. Soil behaviour type from the CPT: an update. 2nd International Symposium on Cone Penetration Testing, CPT'10, Huntington Beach, CA, USA.

43. Robertson, P. K. (2009). Interpretation of cone penetration tests—a unified approach. Canadian geotechnical journal, 46(11), 1337-1355.

44. Robertson, P. K. (2016). Cone penetration test (CPT)-based soil behaviour type (SBT) classification system—an update. Canadian Geotechnical Journal, 53(12), 1910-1927.

45. Robertson, P. K., Campanella, R. G., Gillespie, D., & Rice, A. (1986). Seismic CPT to measure in situ shear wave velocity. Journal of Geotechnical Engineering, 112(8), 791-803.

46. Robertson, P.K. and Cabal, K.L. (2015), Guide to Cone Penetration Testing for Geotechnical Engineering, 6th Edition, Gregg Drilling & Testing, Inc., 133 p.

47. Robertson, P. K., & Campanella, R. G. (1983a). Interpretation of cone penetration tests. Part I: Sand. Canadian geotechnical journal, 20(4), 718-733.

48. Robertson, P. K., & Campanella, R. G. (1983b). Interpretation of cone penetration tests. Part II: Clay. Canadian Geotechnical Journal, 20(4), 734-745.

49. Rocha, B. P., dos Santos, R. A., Bezerra, R. C., Rodrigues, R. A., & Giacheti, H. L. (2016). Characterization of unsaturated tropical soil site by in situ tests. Geotechnical and Geophysical Site Characterisation 5 – Lehane, Acosta-Martínez & Kelly (Eds), © 2016 Australian Geomechanics Society, Sydney, Australia, ISBN 978-0-9946261-2-7 ISC-5, 1129-1136.

50. Saye, S. R., Lutenegger, A. J., Santos, J., & Kumm, B. P. (2013). Assessing overconsolidation ratios in soil with piezocone: Referencing soil index properties. Journal of Geotechnical and Geoenvironmental engineering, 139(7), 1075-108

51. Schmertmann, J. H. (1978). Guidelines for cone penetration test: performance and design (No. FHWATS-78-209). United States. Federal Highway Administration.

52. Tan, N.K. (2005). Pressuremeter and cone penetrometer testing in a calibration chamber with unsaturated Minco Silt. Ph.D. Dissertation, University of Oklahoma, 198 p.

53. Tan, N. K., Miller, G. A., & Muraleetharan, K. K. (2003). Preliminary laboratory calibration of cone penetration in unsaturated silt. In Proceedings of the 12th Pan

American Conference on Soil Mechanics and Geotechnical Engineering, Cambridge, Mass, Vol. 1, 391-396.

54. Tang, C. T., Borden, R. H., & Gabr, M. A. (2017). Approach for Estimating Effective Friction Angle from Cone Penetration Test in Unsaturated Residual Soils. Journal of Geotechnical and Geoenvironmental Engineering, 143(11), 04017087.

55. Wair, B. R., DeJong, J. T., & Shantz, T. (2012). Guidelines for estimation of shear wave velocity profiles. Pacific Earthquake Engineering Research Center, PEER Report 2012/08, 95 p.

56. Yang, H., & Russell, A. R. (2013). Preparing unsaturated samples of decomposed granite for laboratory controlled CPTs. In Proc. 1st Pan-Am Conf. on Unsaturated Soils, Cartagena, 191-197.

57. Yang, H., & Russell, A. R. (2015). Cone penetration tests in unsaturated silty sands. Canadian Geotechnical Journal, 53(3), 431-444.

Appendix A: Cone data

Average results:

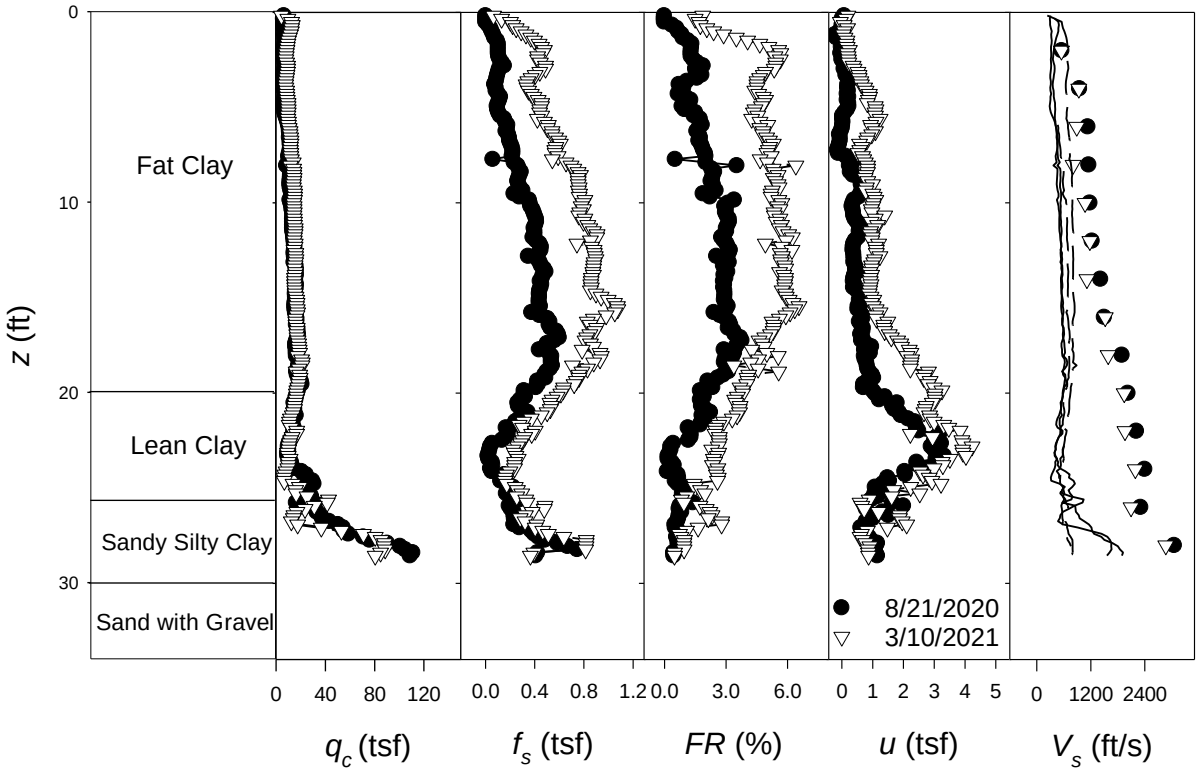

Figure A 1. Average data representing depth against soil stratigraphy, q_c, f_s, *u*, *FR*, and V_s from four soundings conducted at the Wagoner site during wet and dry periods. Soil profiles are based on samples obtained from companion test borings. Note: symbols in the V_s plot represent shear wave velocity measurements using the seismic cone, solid lines in the V_s plot represent the predictions of V_s for wet and dry periods based on tip resistance using the Rix and Mayne (1995) equation, and dashed lines similarly correspond to V_s predictions based on the Hegazy and Mayne (2006) equation based on cone sleeve friction.

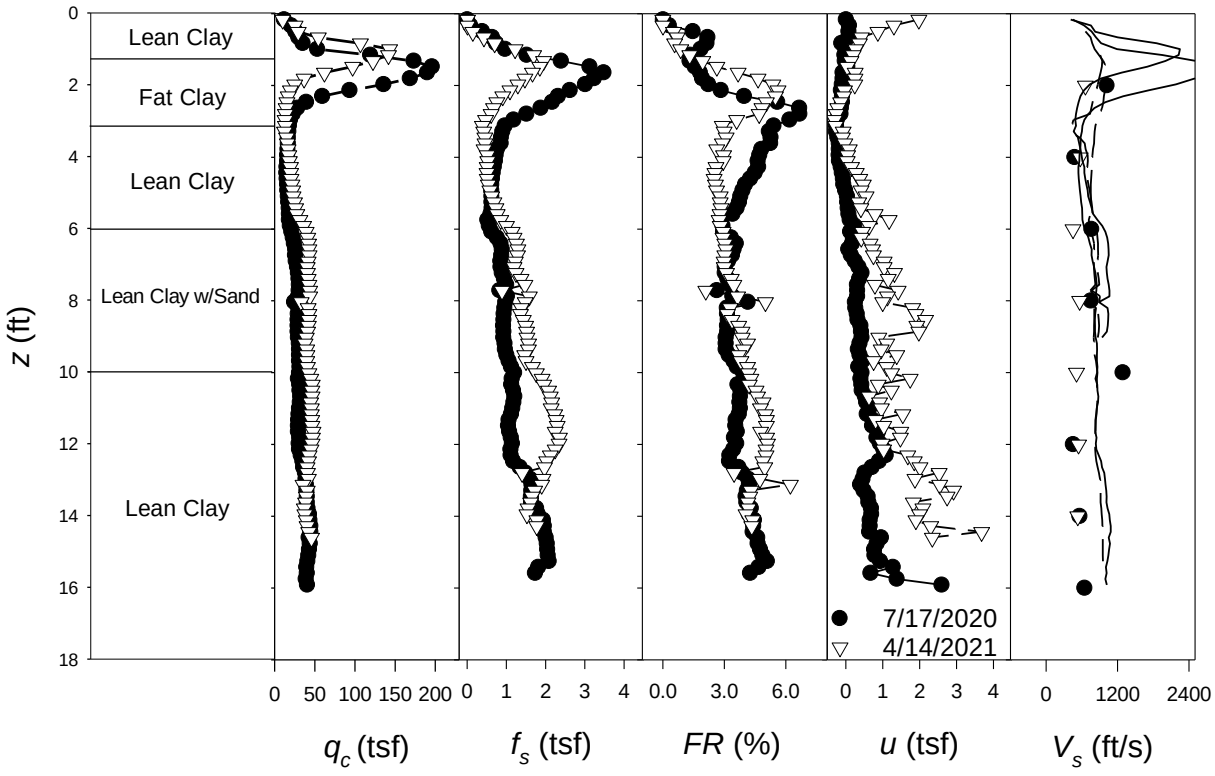

Figure A 2. Average data representing depth against soil stratigraphy, q_c, f_s, *u*, *FR*, and V_s from four soundings conducted at the Muskogee site during wet and dry periods. Soil profiles are based on samples obtained from companion test borings. Note: symbols in the V_s plot represent shear wave velocity measurements using the seismic cone, solid lines in the V_s plot represent the predictions of V_s for wet and dry periods based on tip resistance using the Rix and Mayne (1995) equation, and dashed lines similarly correspond to V_s predictions based on the Hegazy and Mayne (2006) equation based on cone sleeve friction.

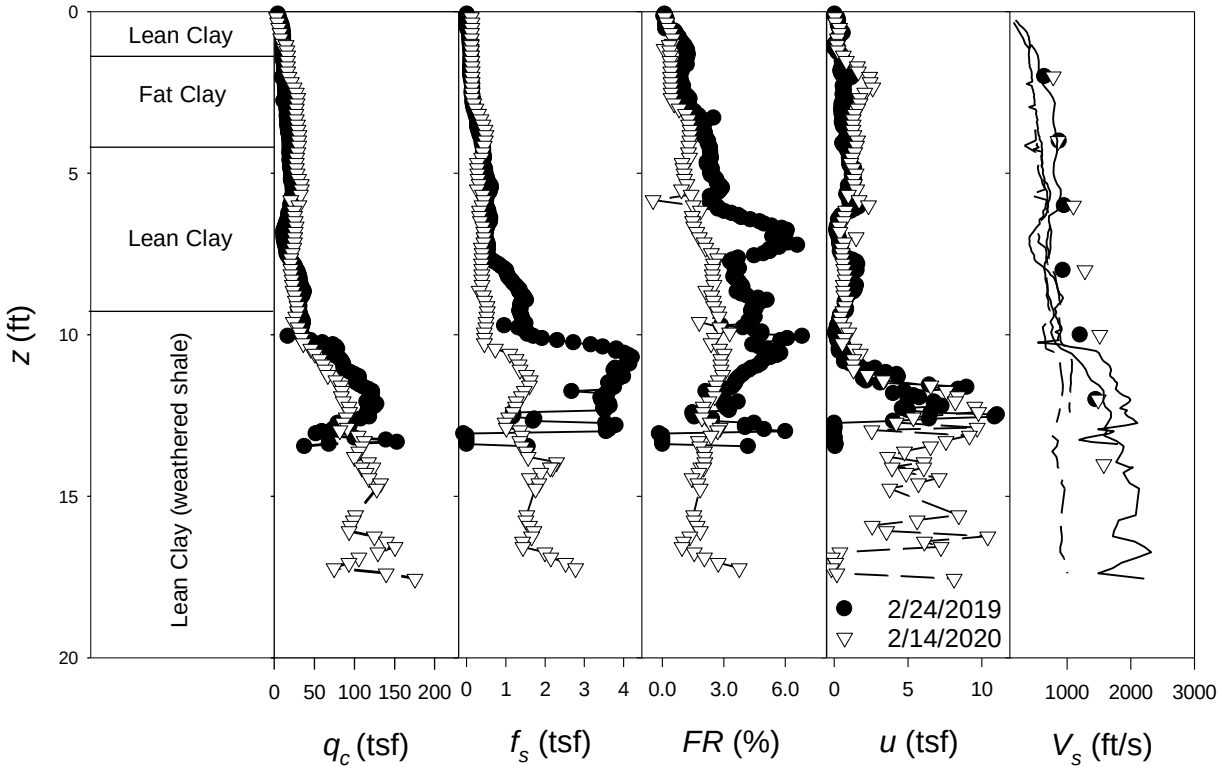

Figure A 3. Average data representing depth against soil stratigraphy, q_c, f_s, *u*, *FR*, and V_s from four soundings conducted at the Hobart site during wet and dry periods. Soil profiles are based on samples obtained from companion test borings. Note: symbols in the V_s plot represent shear wave velocity measurements using the seismic cone, solid lines in the V_s plot represent the predictions of V_s for wet and dry periods based on tip resistance using the Rix and Mayne (1995) equation, and dashed lines similarly correspond to V_s predictions based on the Hegazy and Mayne (2006) equation based on cone sleeve friction.

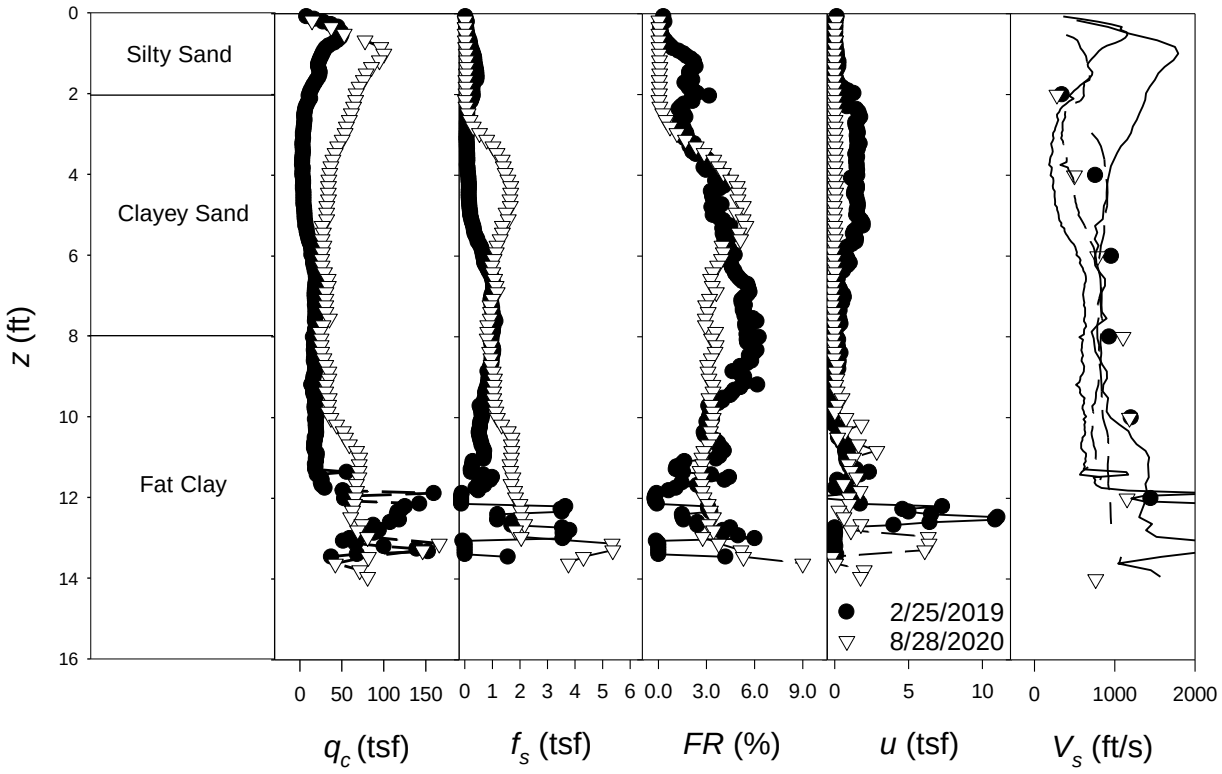

Figure A 4. Average data representing depth against soil stratigraphy, q_c, f_s, *u*, *FR*, and V_s from four soundings conducted at the Wewoka site during wet and dry periods. Soil profiles are based on samples obtained from companion test borings. Note: symbols in the V_s plot represent shear wave velocity measurements using the seismic cone, solid lines in the V_s plot represent the predictions of V_s for wet and dry periods based on tip resistance using the Rix and Mayne (1995) equation, and dashed lines similarly correspond to V_s predictions based on the Hegazy and Mayne (2006) equation based on cone sleeve friction.

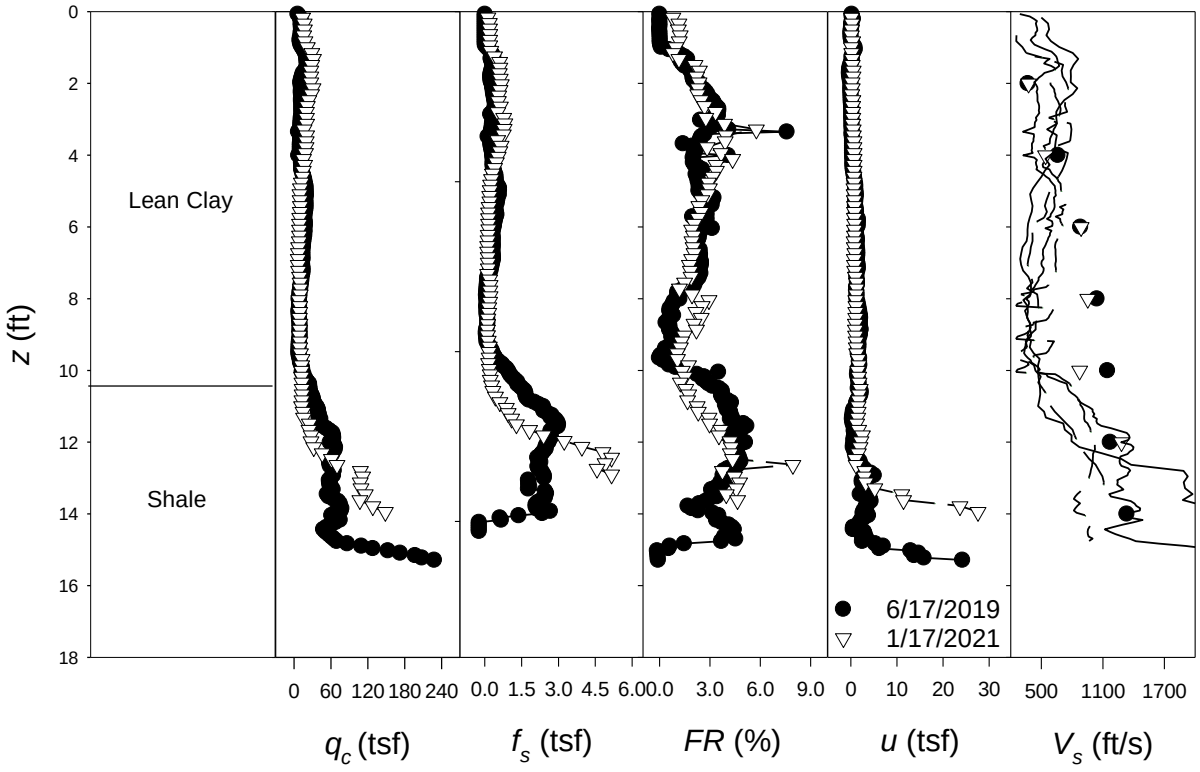

Figure A 5. Average data representing depth against soil stratigraphy, q_c, f_s, u, FR, and V_s from four soundings conducted at the Fairview site during wet and dry periods. Soil profiles are based on samples obtained from companion test borings. Note: symbols in the V_s plot represent shear wave velocity measurements using the seismic cone, solid lines in the V_s plot represent the predictions of V_s for wet and dry periods based on tip resistance using the Rix and Mayne (1995) equation, and dashed lines similarly correspond to V_s predictions based on the Hegazy and Mayne (2006) equation based on cone sleeve friction.

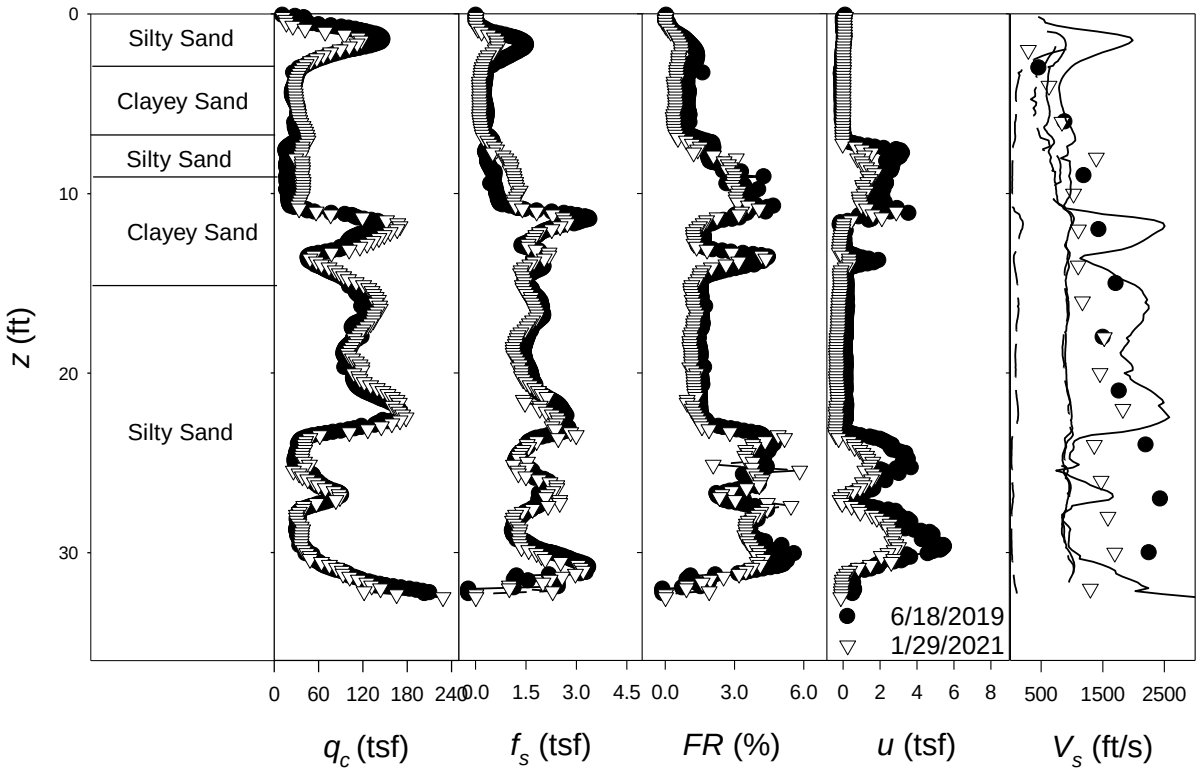

Figure A 6. Average data representing depth against soil stratigraphy, q_c, f_s, *u*, *FR*, and V_s from four soundings conducted at the Curtis site during wet and dry periods. Soil profiles are based on samples obtained from companion test borings. Note: symbols in the V_s plot represent shear wave velocity measurements using the seismic cone, solid lines in the V_s plot represent the predictions of V_s for wet and dry periods based on tip resistance using the Rix and Mayne (1995) equation, and dashed lines similarly correspond to V_s predictions based on the Hegazy and Mayne (2006) equation based on cone sleeve friction.

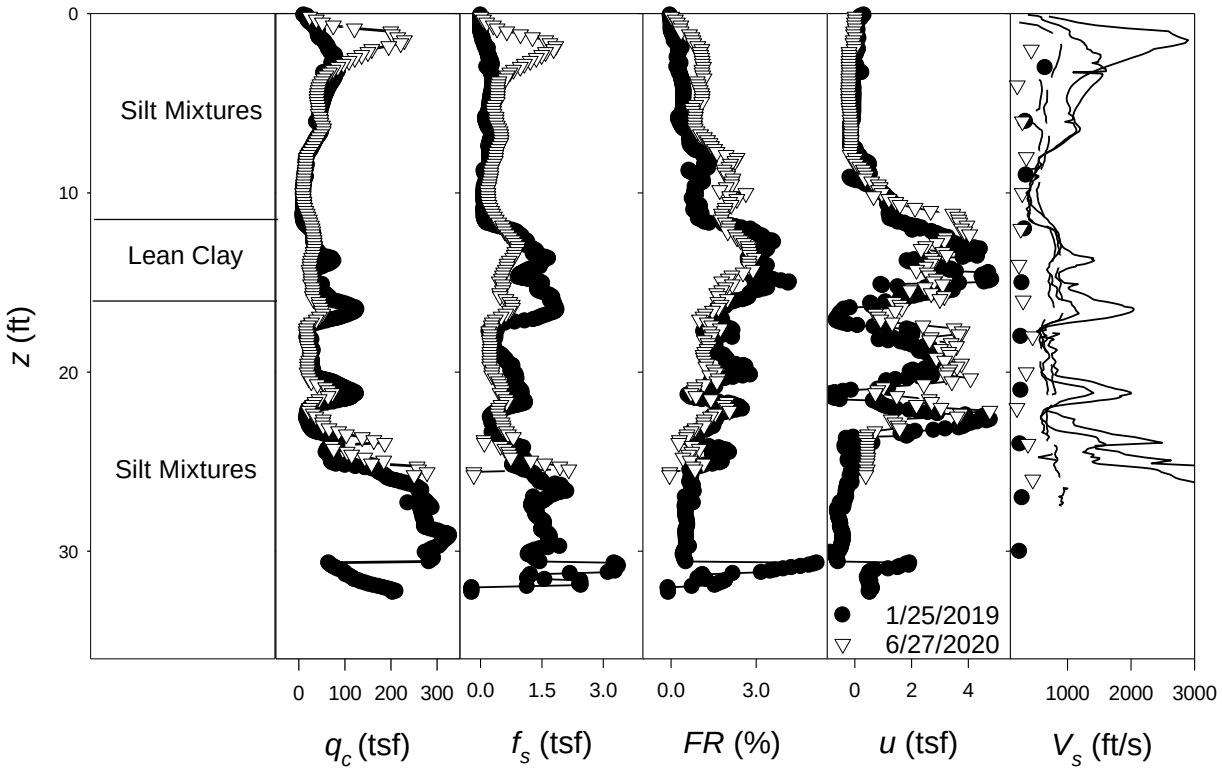

Figure A 7. Average data representing depth against soil stratigraphy, q_c, f_s, u, FR, and V_s from four soundings conducted at the Norman Maintenance Yard site during wet and dry periods. Soil profiles are based on samples obtained from companion test borings. Note: symbols in the V_s plot represent shear wave velocity measurements using the seismic cone, solid lines in the V_s plot represent the predictions of V_s for wet and dry periods based on tip resistance using the Rix and Mayne (1995) equation, and dashed lines similarly correspond to V_s predictions based on the Hegazy and Mayne (2006) equation based on cone sleeve friction.

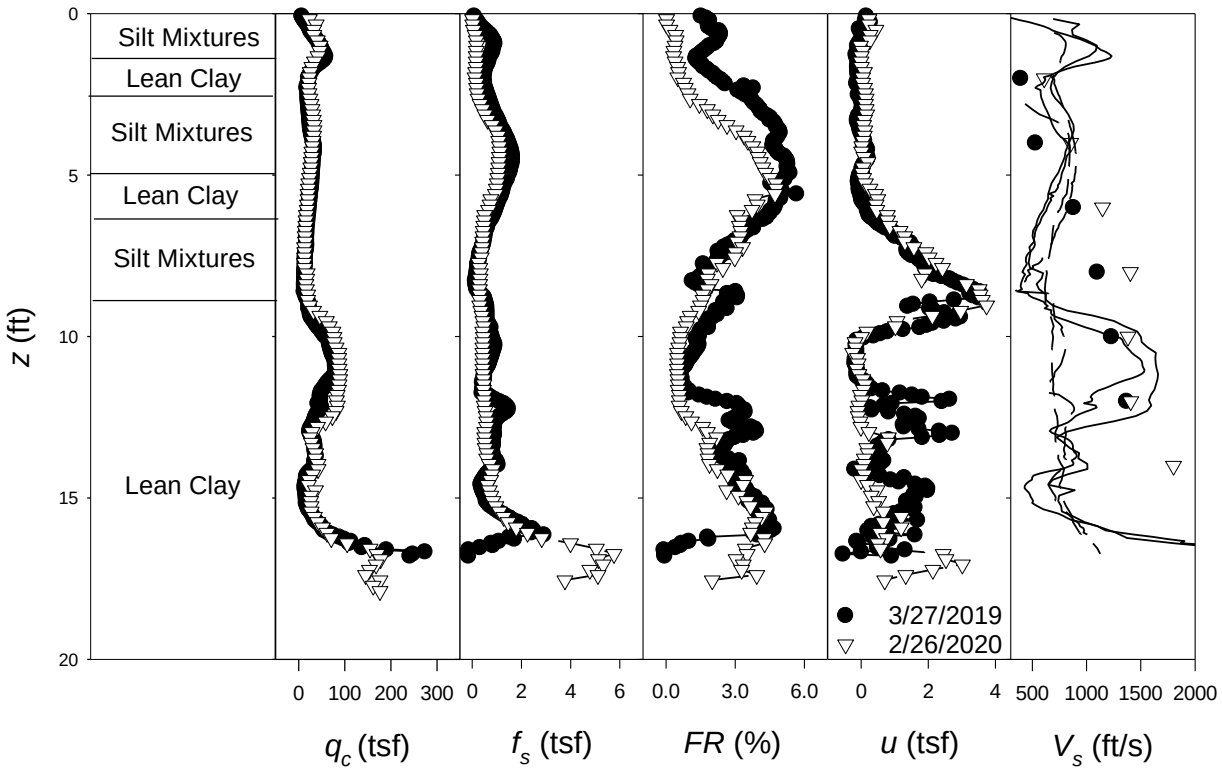

Figure A 8. Average data representing depth against soil stratigraphy, q_c, f_s, *u*, *FR*, and V_s from four soundings conducted at the Fears Lab site during wet and dry periods. Soil profiles are based on samples obtained from companion test borings. Note: symbols in the V_s plot represent shear wave velocity measurements using the seismic cone, solid lines in the V_s plot represent the predictions of V_s for wet and dry periods based on tip resistance using the Rix and Mayne (1995) equation, and dashed lines similarly correspond to V_s predictions based on the Hegazy and Mayne (2006) equation based on cone sleeve friction.

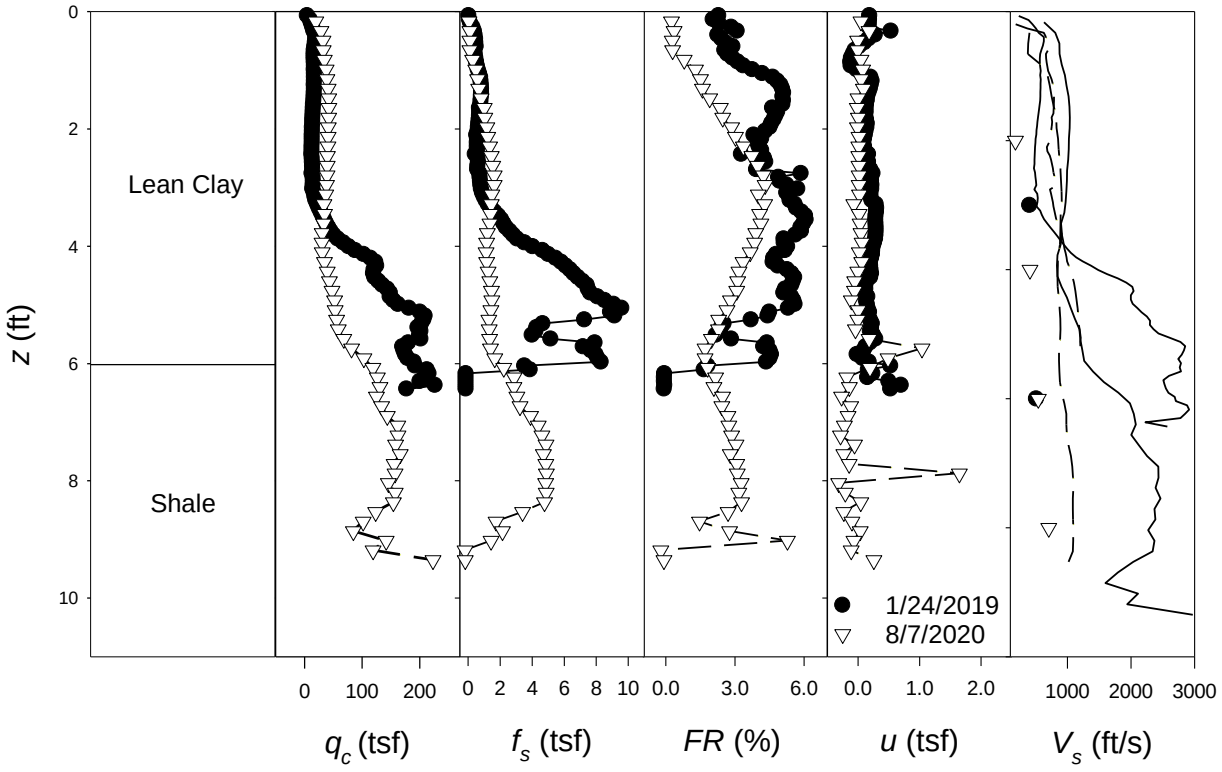

Figure A 9. Average data representing depth against soil stratigraphy, q_c, f_s, *u*, *FR*, and V_s from four soundings conducted at the Lake Hefner site during wet and dry periods. Soil profiles are based on samples obtained from companion test borings. Note: symbols in the V_s plot represent shear wave velocity measurements using the seismic cone, solid lines in the V_s plot represent the predictions of V_s for wet and dry periods based on tip resistance using the Rix and Mayne (1995) equation, and dashed lines similarly correspond to V_s predictions based on the Hegazy and Mayne (2006) equation based on cone sleeve friction.

Full Soundings:

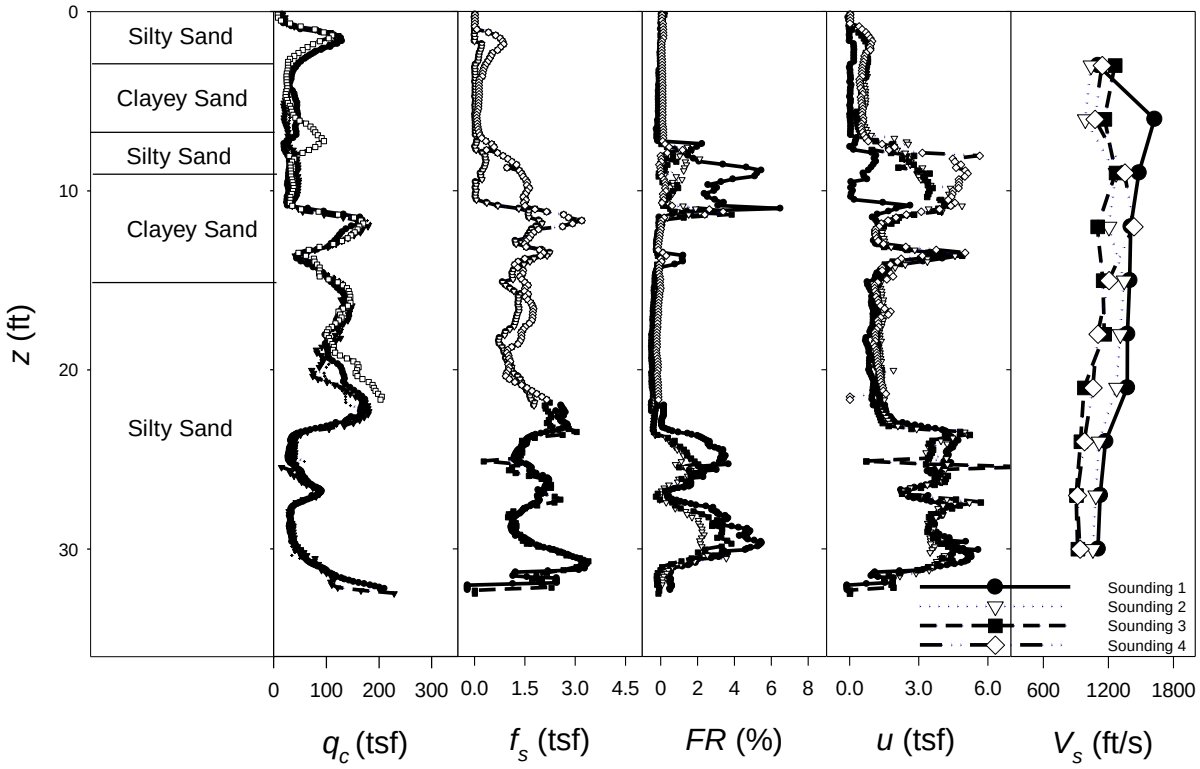

Figure A 10. Full data for q_c, f_s, u, FR, and V_s from four soundings conducted on 1/29/2021 for Site 1 (Curtis). Note: Soil profiles are based on samples obtained from companion test borings

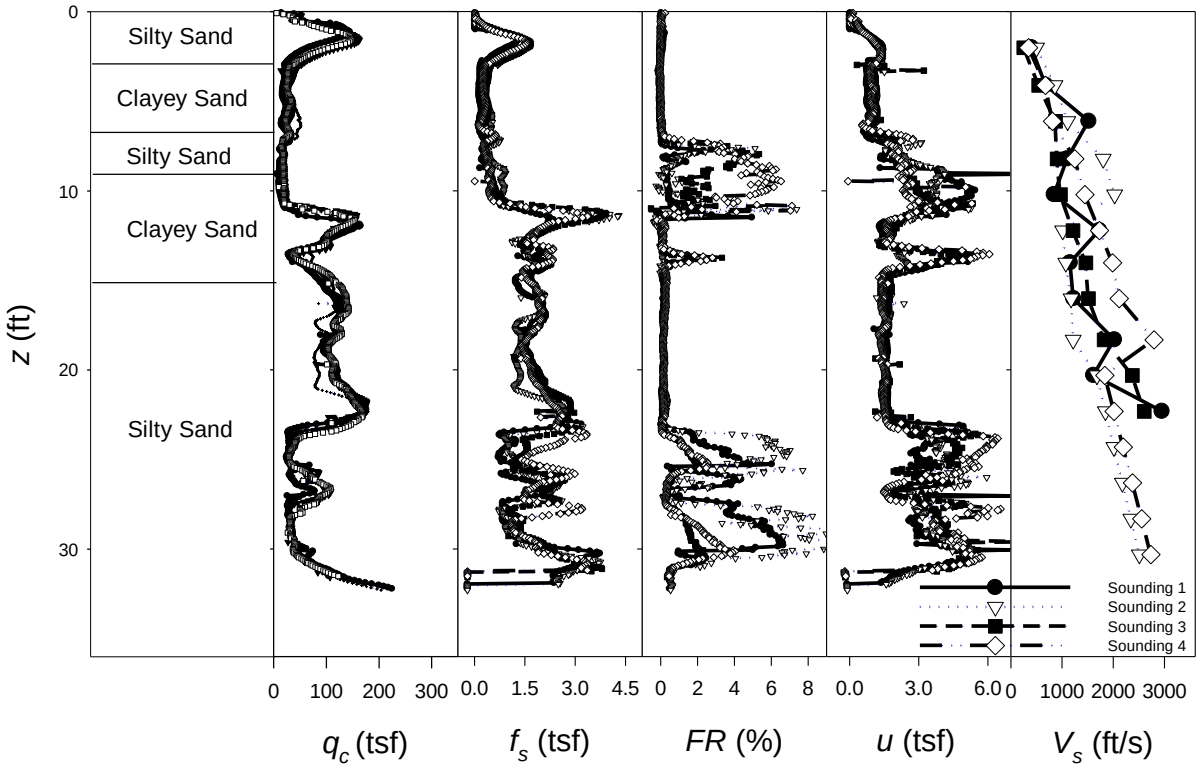

Figure A 11. Full data for q_c, f_s, u, FR, and V_s from four soundings conducted on 6/8/2019 for Site 1 (Curtis). Note: Soil profiles are based on samples obtained from companion test borings

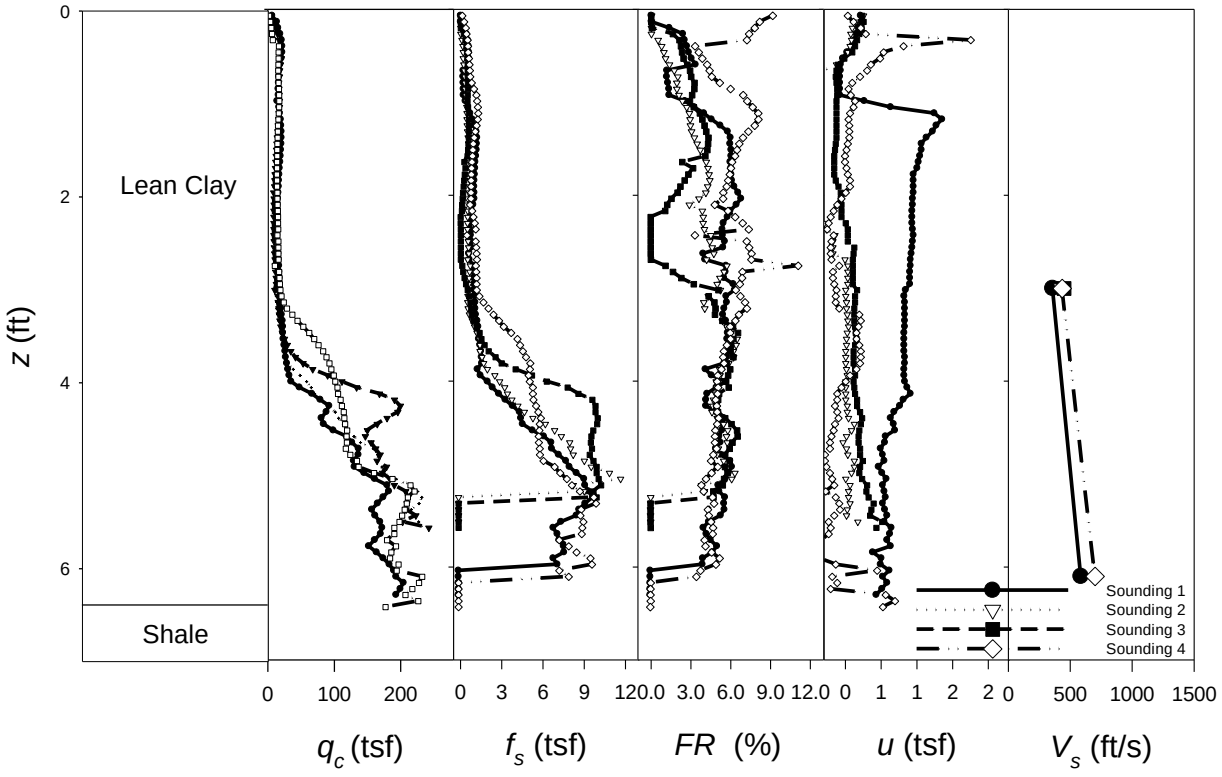

Figure A 12. Full data for q_c, f_s, u, FR, and V_s from four soundings conducted on 1/24/2019 for Site 2 (Lake Hefner). Note: Soil profiles are based on samples obtained from companion test borings

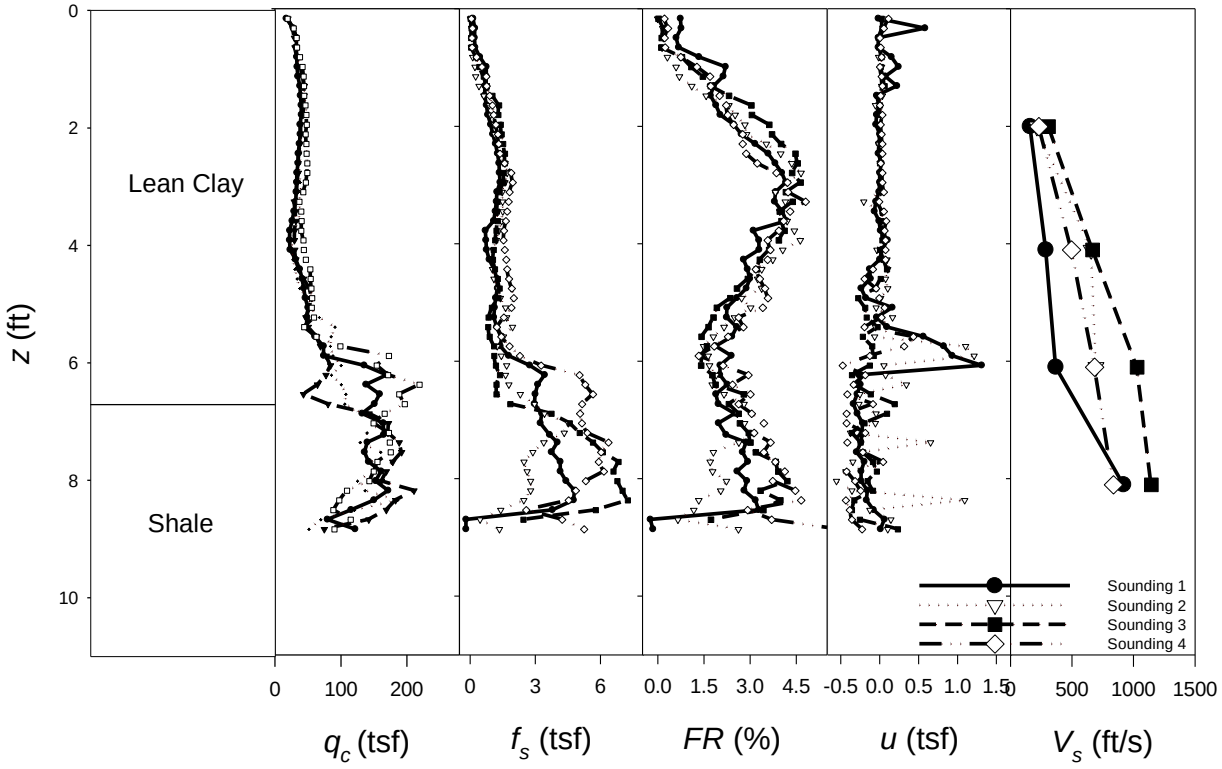

Figure A 13. Full data for q_c, f_s, u, FR, and V_s from four soundings conducted on 8/7/2020 for Site 2 (Lake Hefner). Note: Soil profiles are based on samples obtained from companion test borings

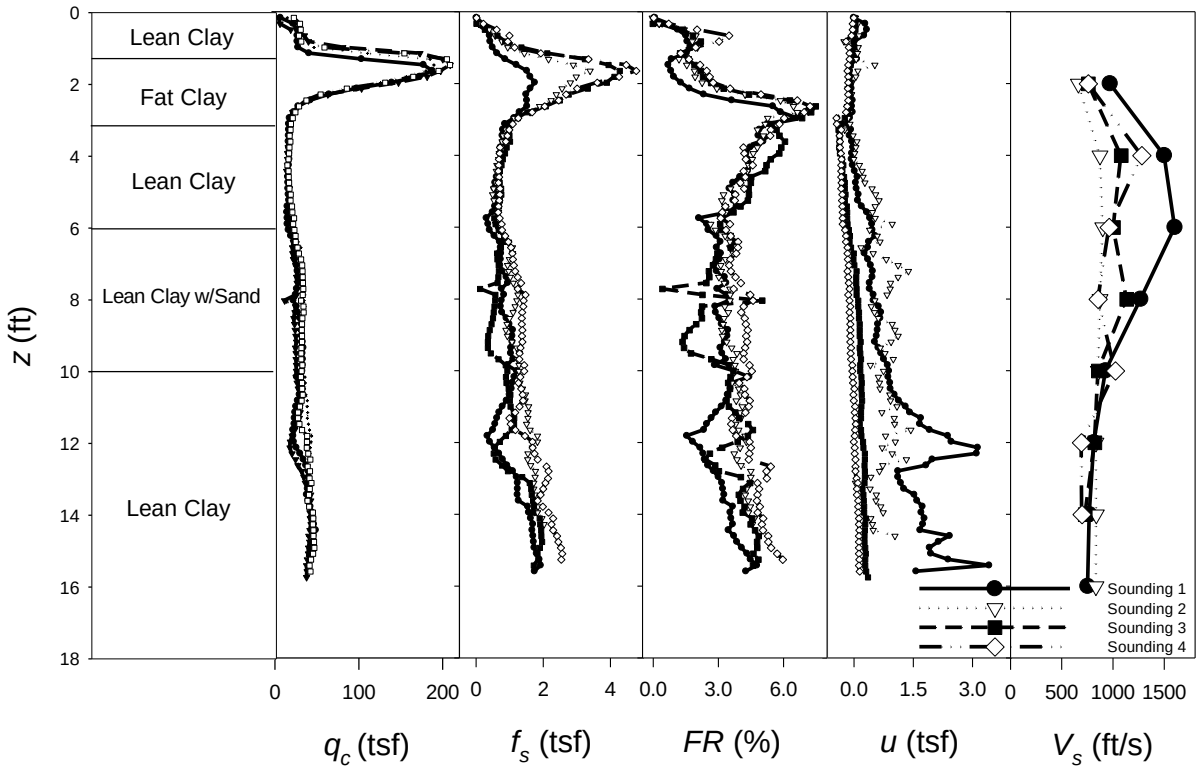

Figure A 14. Full data for q_c, f_s, u, FR, and V_s from four soundings conducted on 7/17/2020 for Site 3 (Muskogee). Note: Soil profiles are based on samples obtained from companion test borings

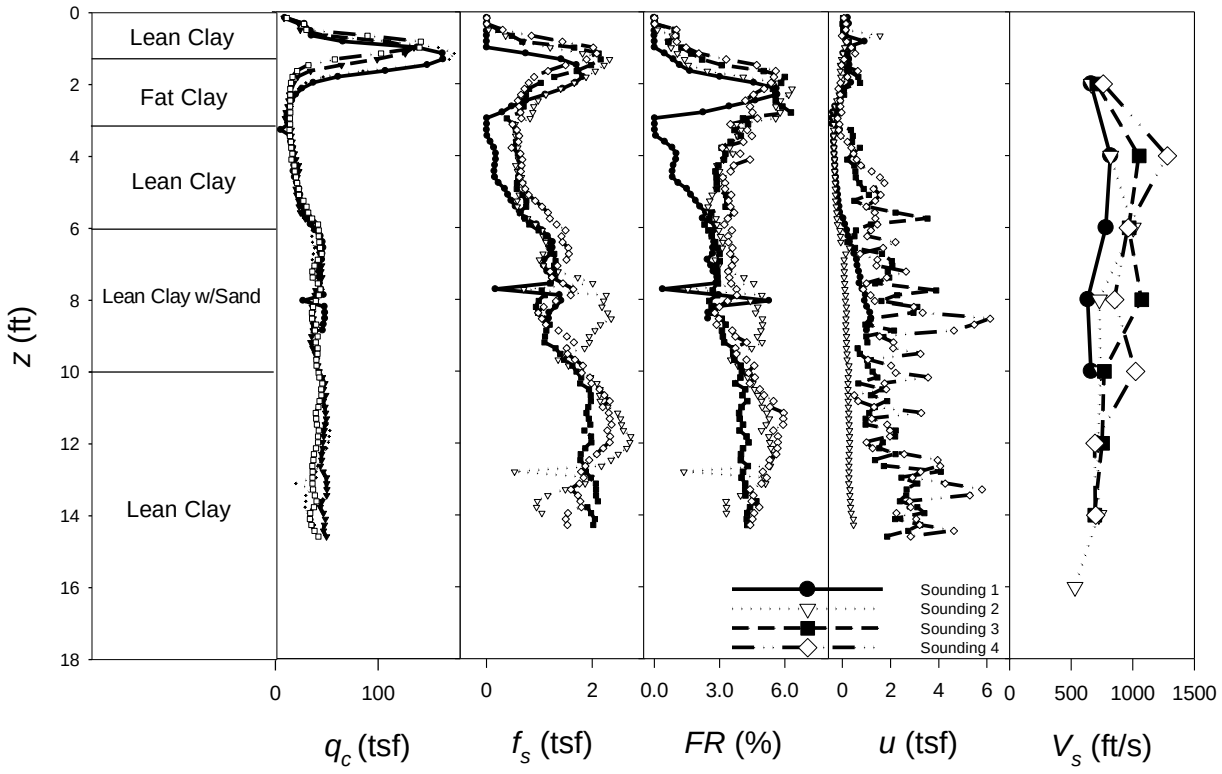

Figure A 15. Full data for q_c, f_s, *u*, *FR*, and V_s from four soundings conducted on 4/14/2021 for Site 3 (Muskogee). Note: Soil profiles are based on samples obtained from companion test borings

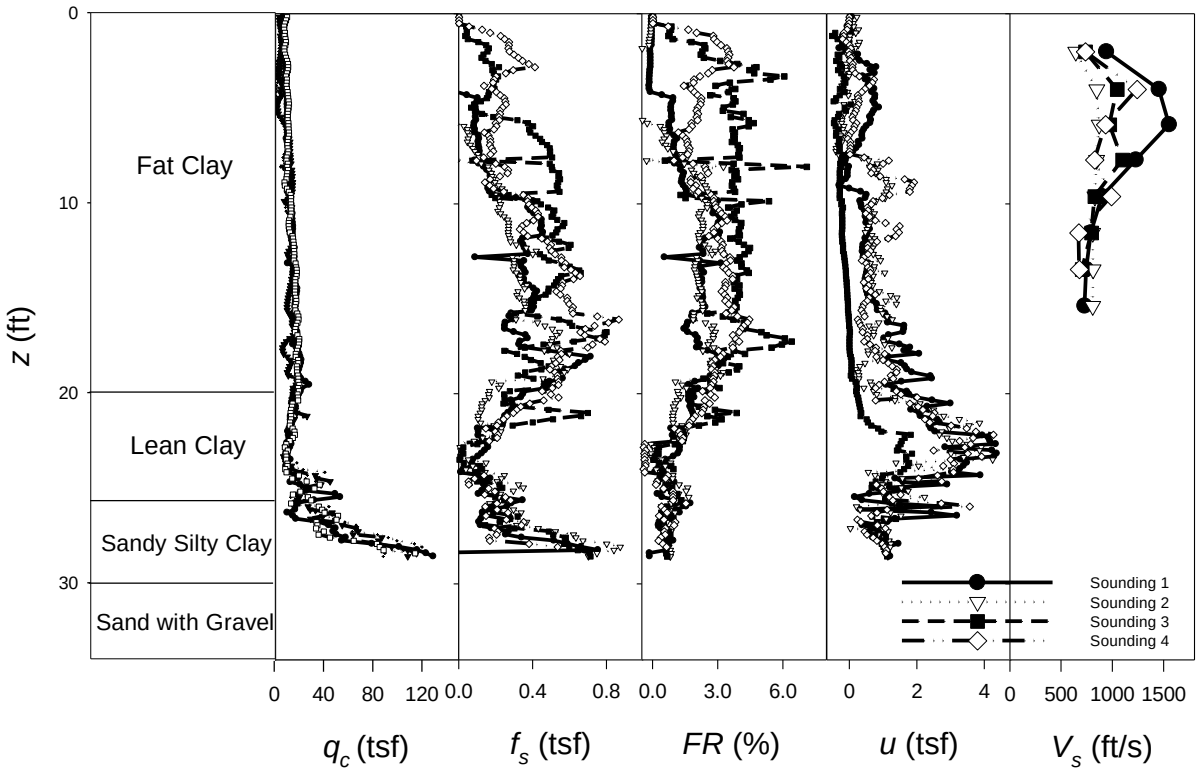

Figure A 16. Full data for q_c, f_s, *u*, *FR*, and V_s from four soundings conducted on 8/21/2020 for Site 4 (Wagoner). Note: Soil profiles are based on samples obtained from companion test borings

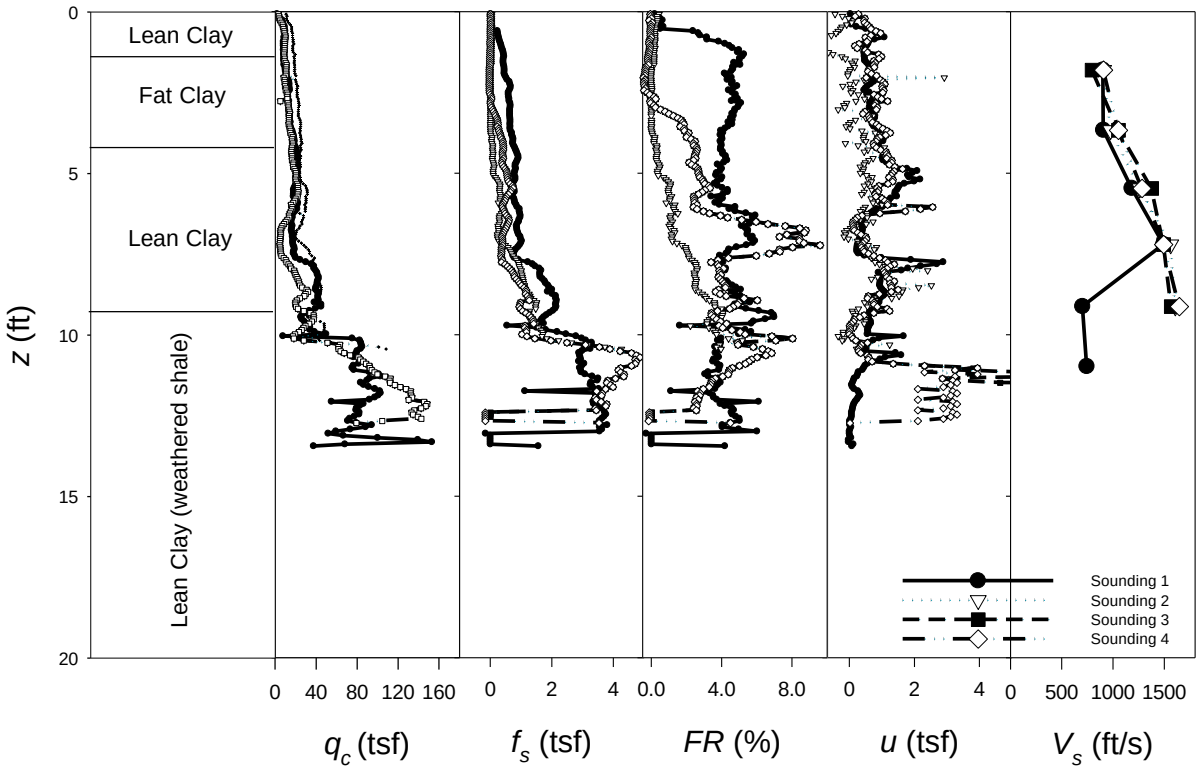

Figure A 17. Full data *for q_c, f_s, u, FR, and V_s* from four soundings conducted on 2/24/2019 for Site 5 (Hobart). Note: Soil profiles are based on samples obtained from companion test borings

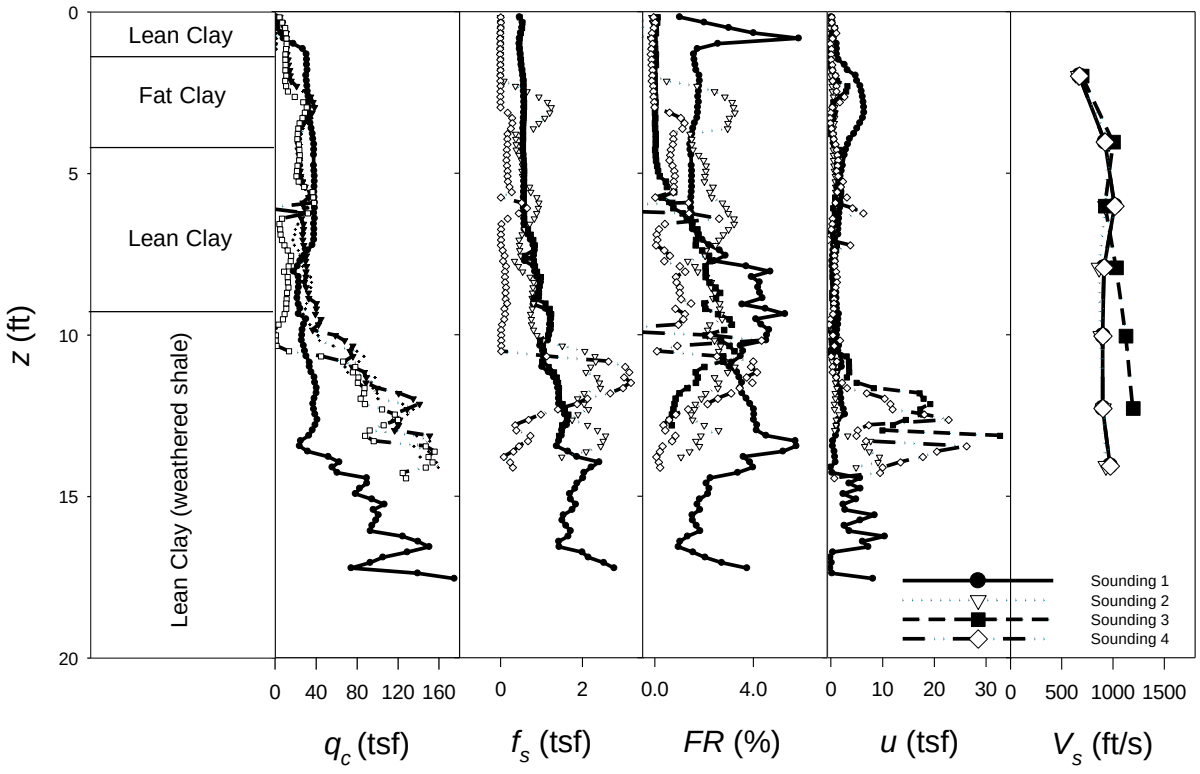

Figure A 18. Full data *for q_c, f_s, u, FR, and V_s* from four soundings conducted on 2/14/2020 for Site 5 (Hobart). Note: Soil profiles are based on samples obtained from companion test borings

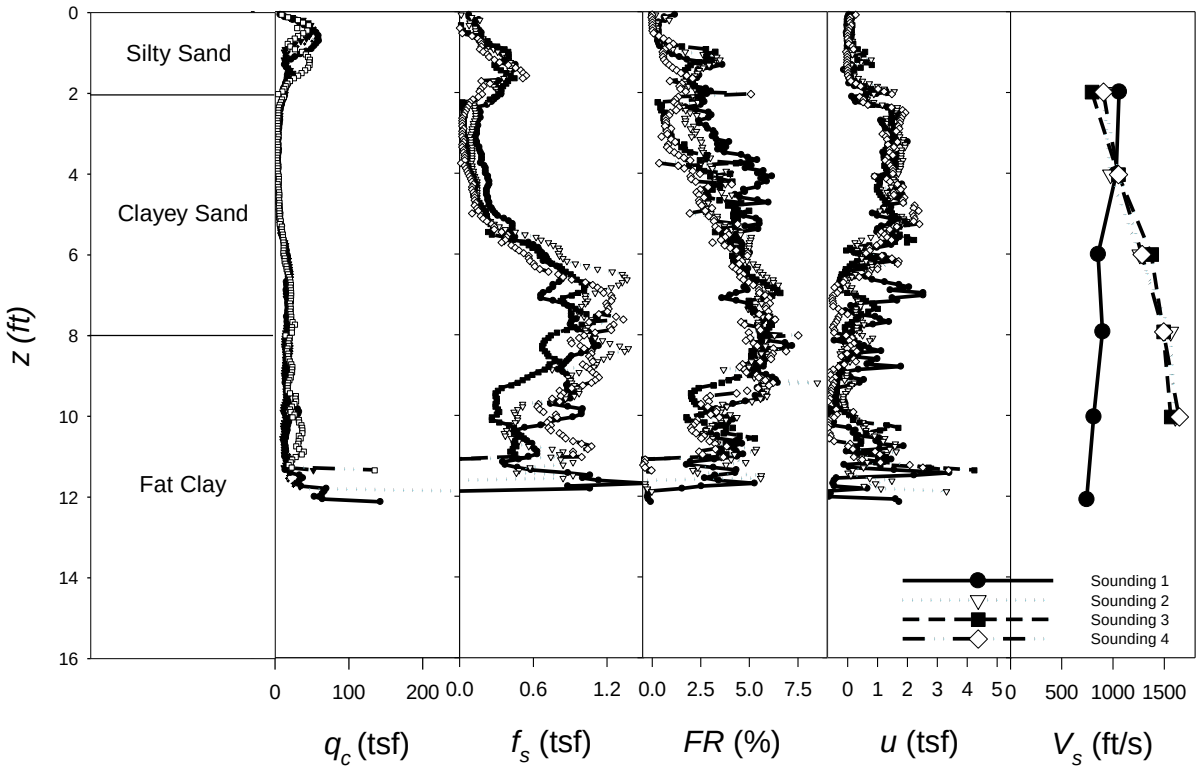

Figure A 19. Full data *for q_c, f_s, u, FR, and V_s* from four soundings conducted on 2/25/2019 for Site 6 (Wewoka). Note: Soil profiles are based on samples obtained from companion test borings

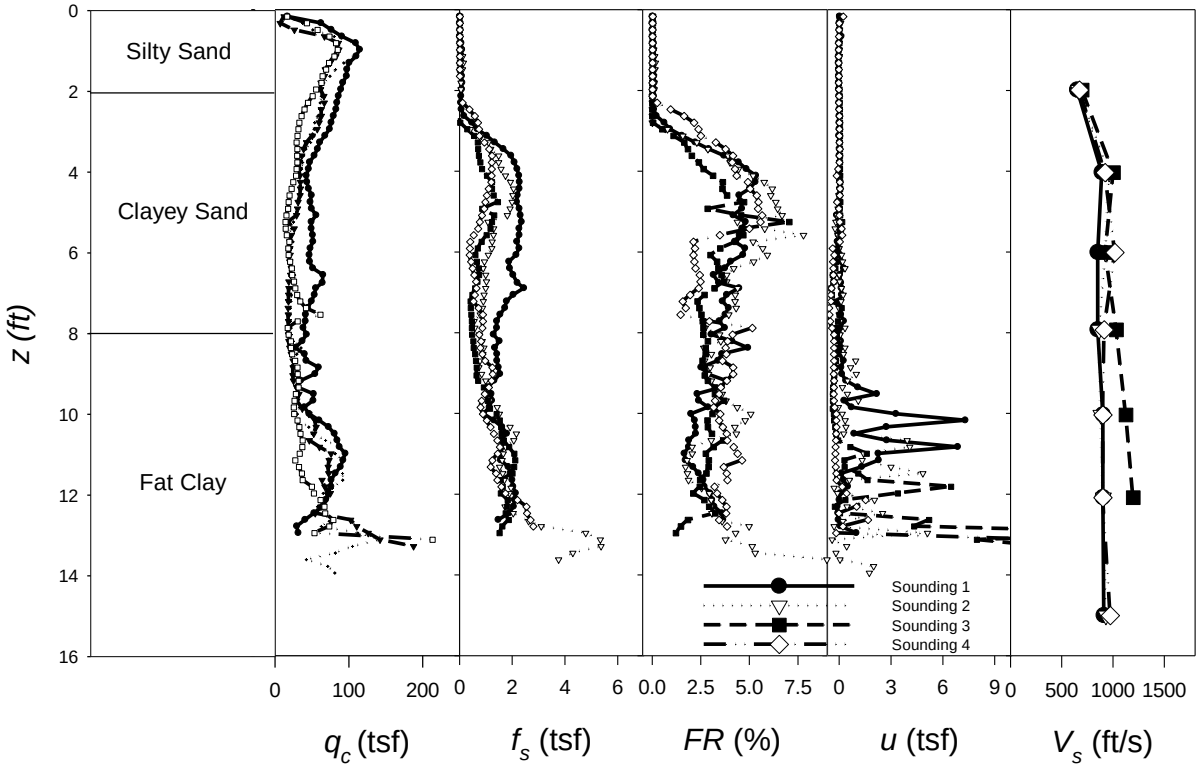

Figure A 20. Full data *for q_c, f_s, u, FR, and V_s* from four soundings conducted on 8/28/2020 for Site 6 (Wewoka). Note: Soil profiles are based on samples obtained from companion test borings

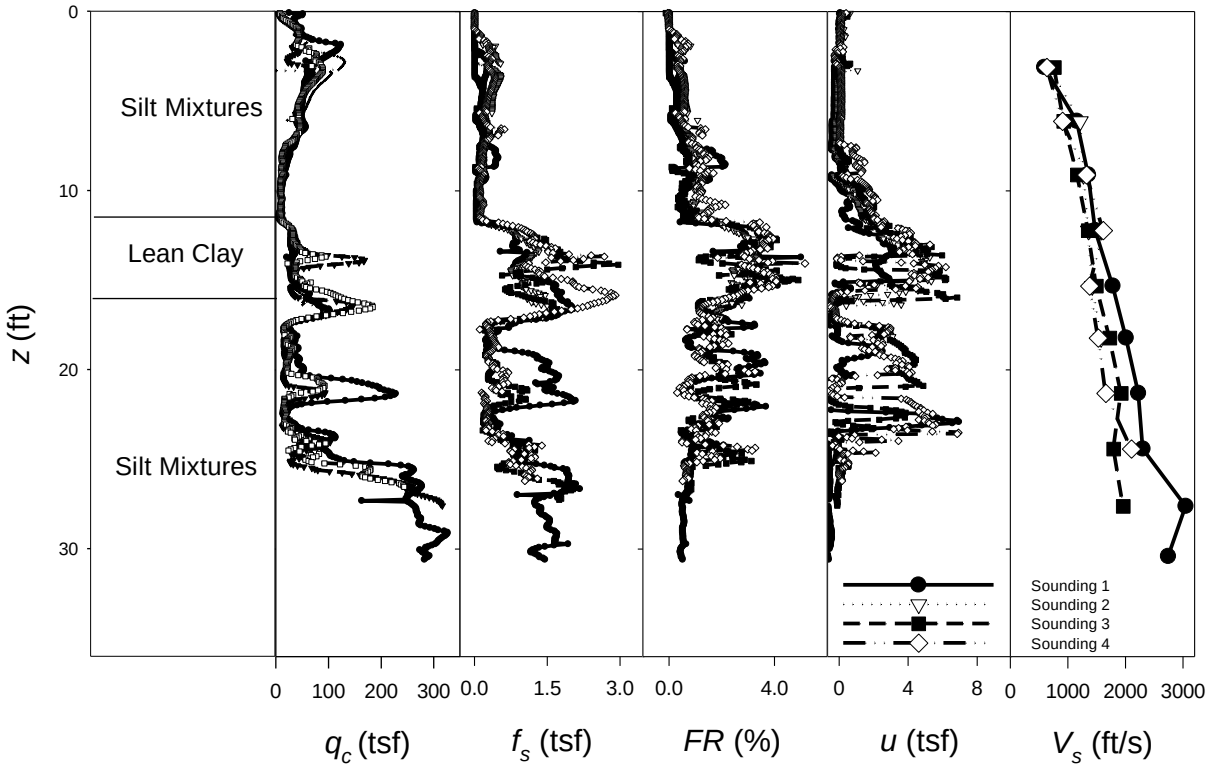

Figure A 21. Full data *for q_c, f_s, u, FR, and V_s* from four soundings conducted on 1/25/2019 for Site 7 (Norman MY). Note: Soil profiles are based on samples obtained from companion test borings

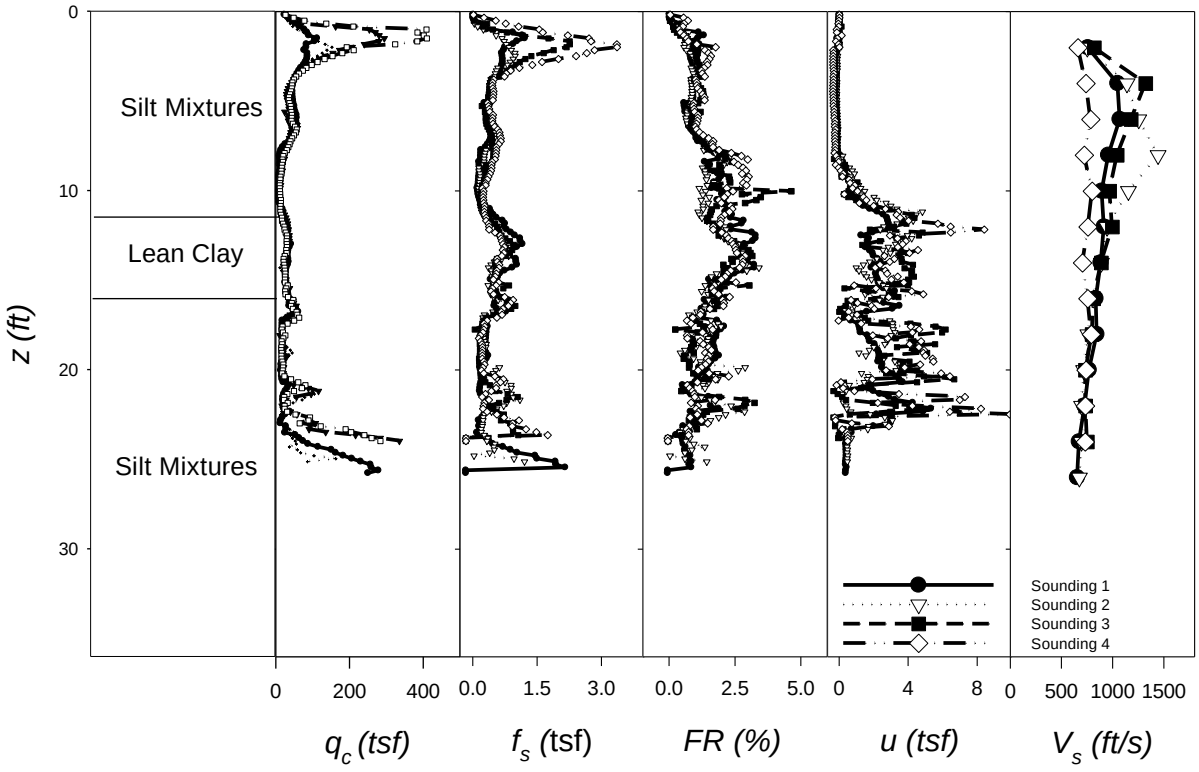

Figure A 22. Full data *for q_c, f_s, u, FR, and V_s* from four soundings conducted on 6/27/2020 for Site 7 (Norman MY). Note: Soil profiles are based on samples obtained from companion test borings

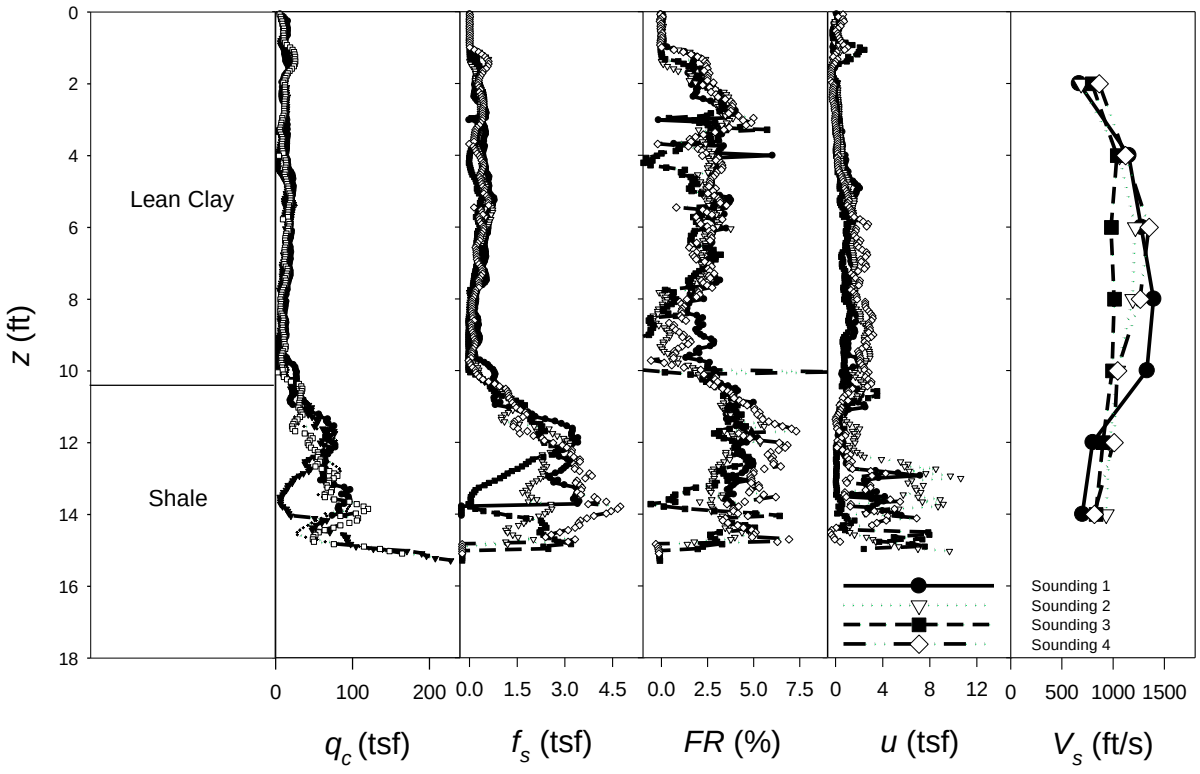

Figure A 23. Full data *for q_c, f_s, u, FR, and V_s* from four soundings conducted on 6/17/2019 for Site 8 (Fairview). Note: Soil profiles are based on samples obtained from companion test borings

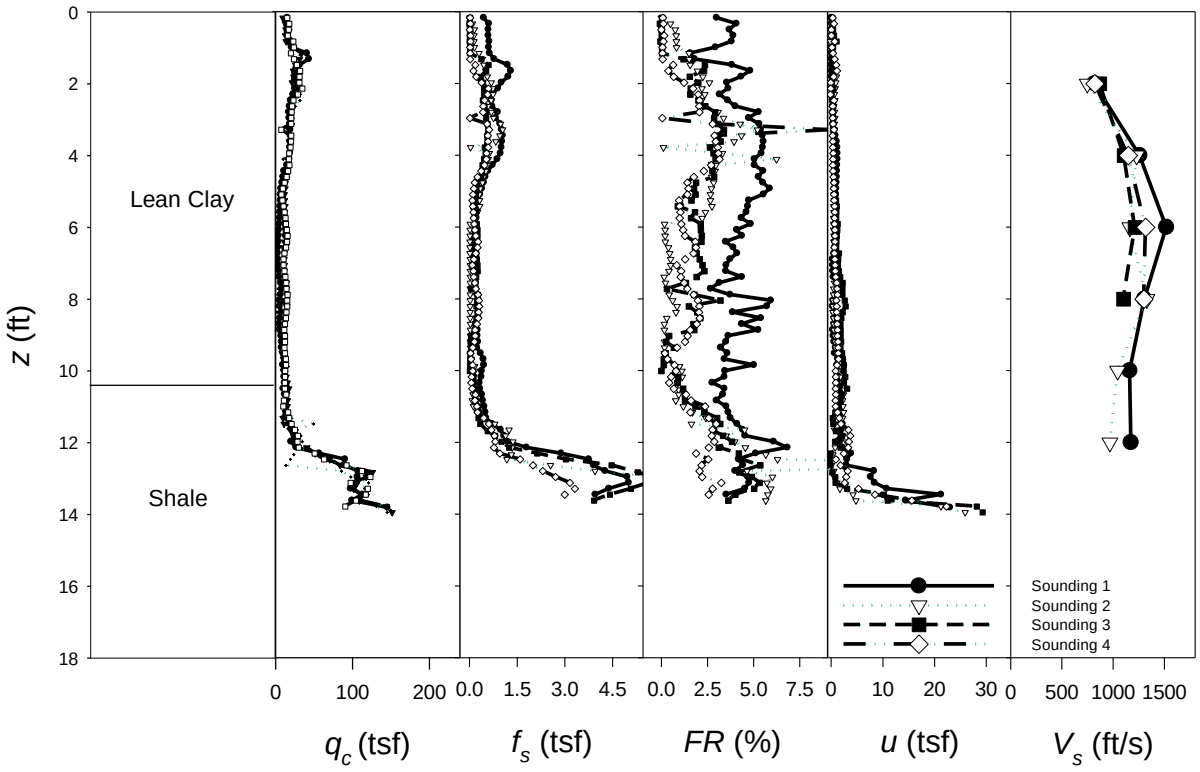

Figure A 24. Full data *for q_c, f_s, u, FR, and V_s* from four soundings conducted on 1/17/2021 for Site 8 (Fairview). Note: Soil profiles are based on samples obtained from companion test borings

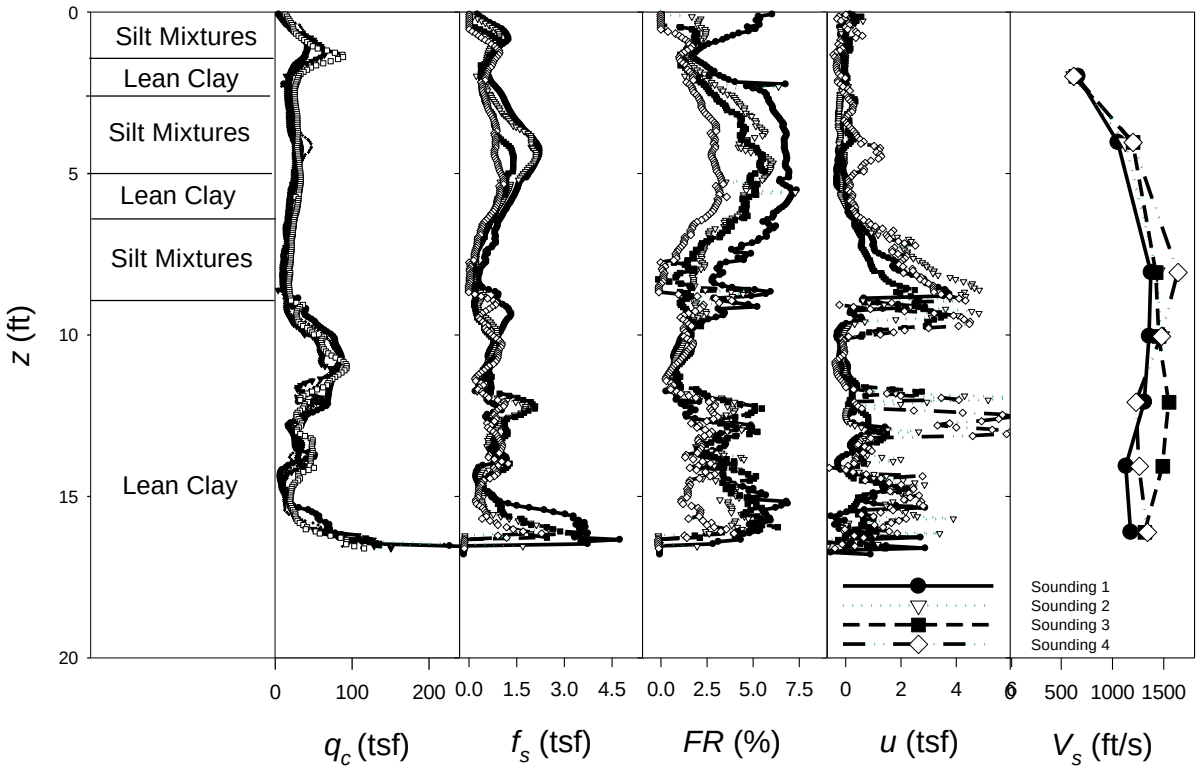

Figure A 25. Full data *for q_c, f_s, u, FR, and V_s* from four soundings conducted on 3/27/2019 for Site 9 (Fears Lab). Note: Soil profiles are based on samples obtained from companion test borings

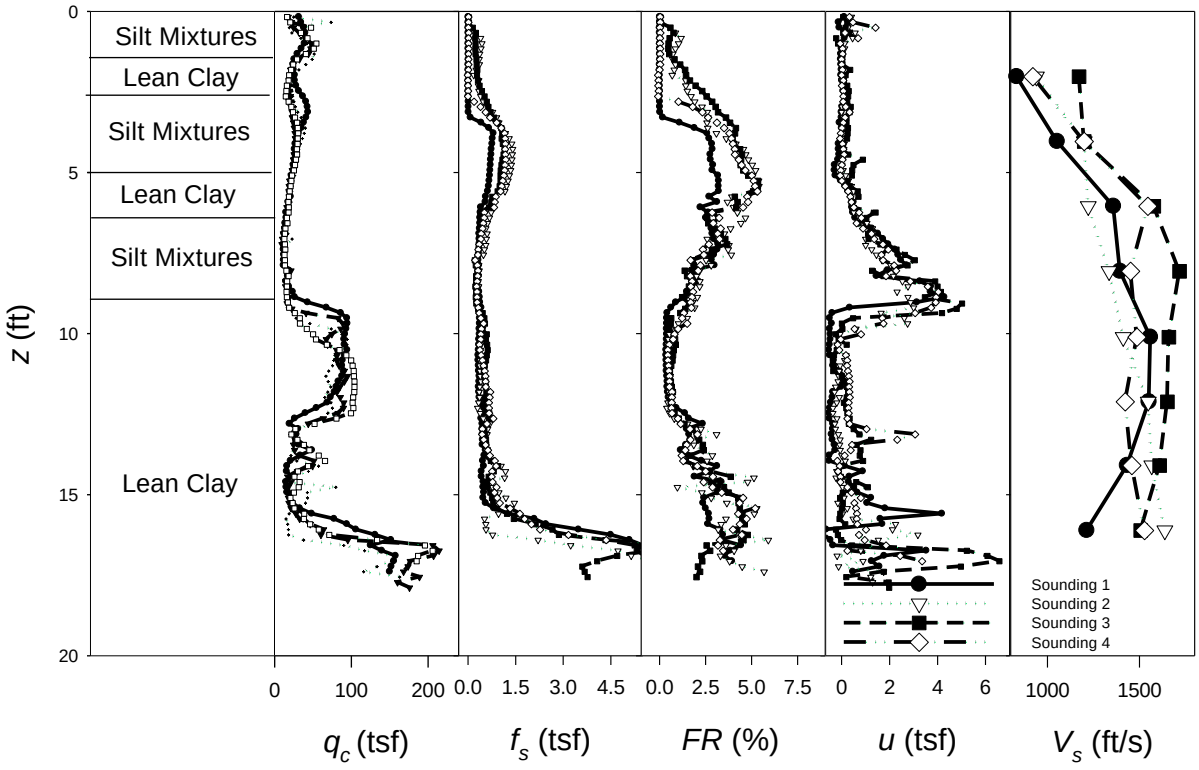

Figure A 26. Full data *for q_c, f_s, u, FR, and V_s* from four soundings conducted on 2/26/2020 for Site 9 (Fears Lab). Note: Soil profiles are based on samples obtained from companion test borings

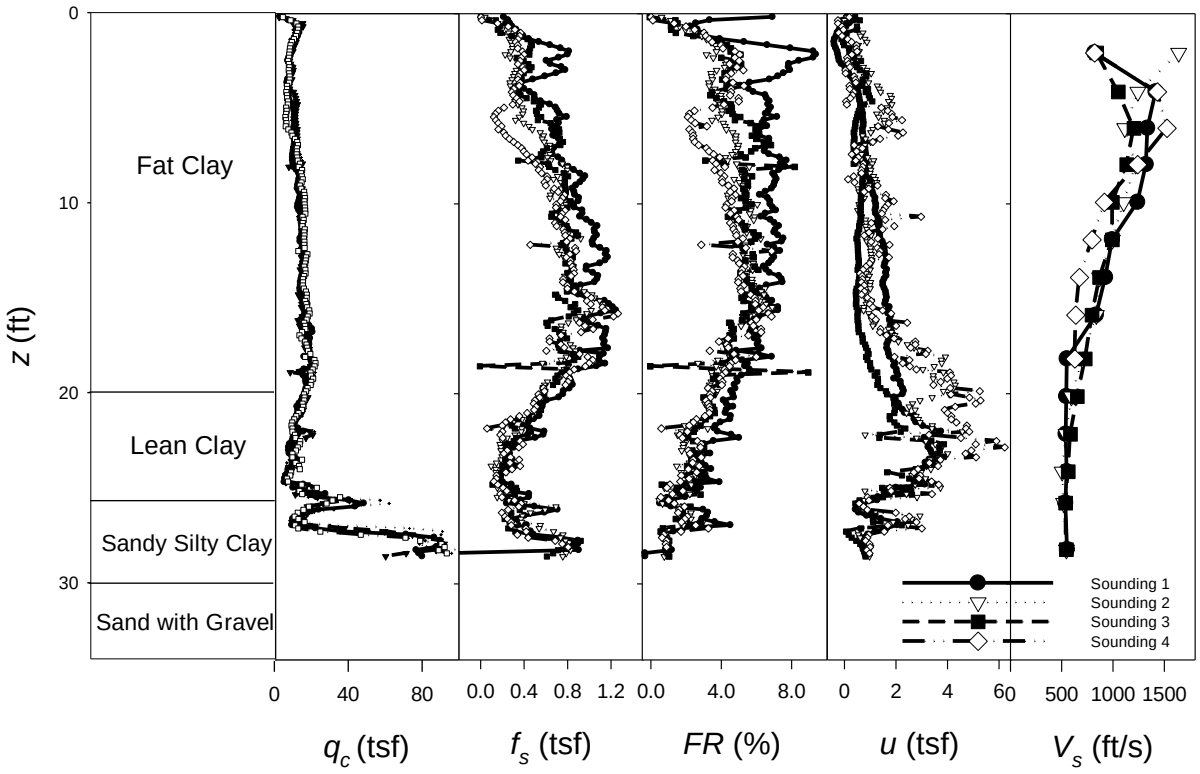

Figure A 27. Full data *for q_c, f_s, u, FR, and V_s* from four soundings conducted on 3/13/2021 for Site 4 (Wagoner). Note: Soil profiles are based on samples obtained from companion test borings

Appendix B: One dimensional consolidation data

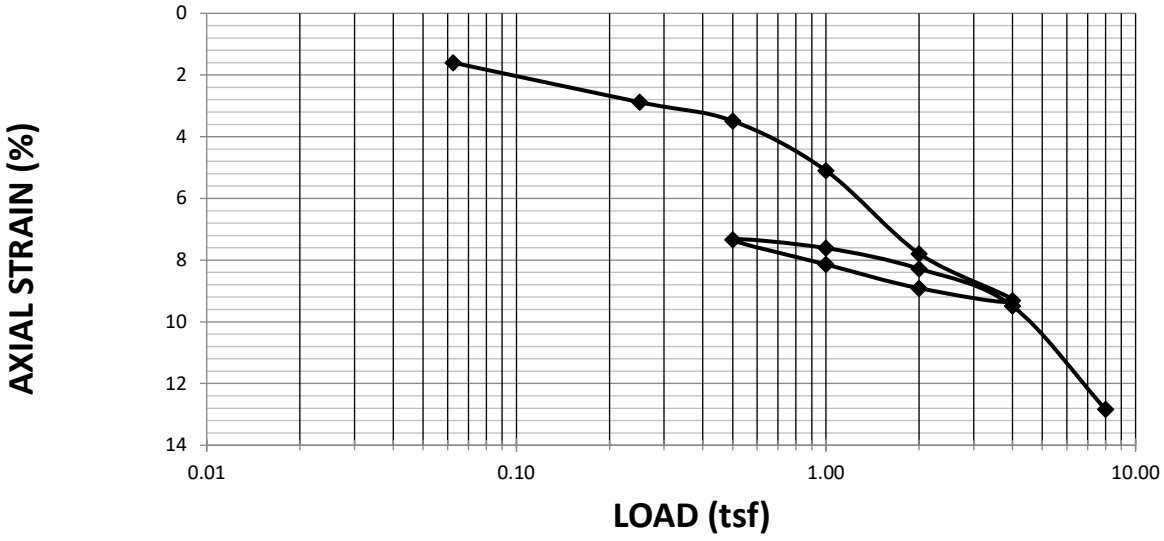

Figure B 1. Site 3- Muskogee 3.6 ft sat Consolidation test results

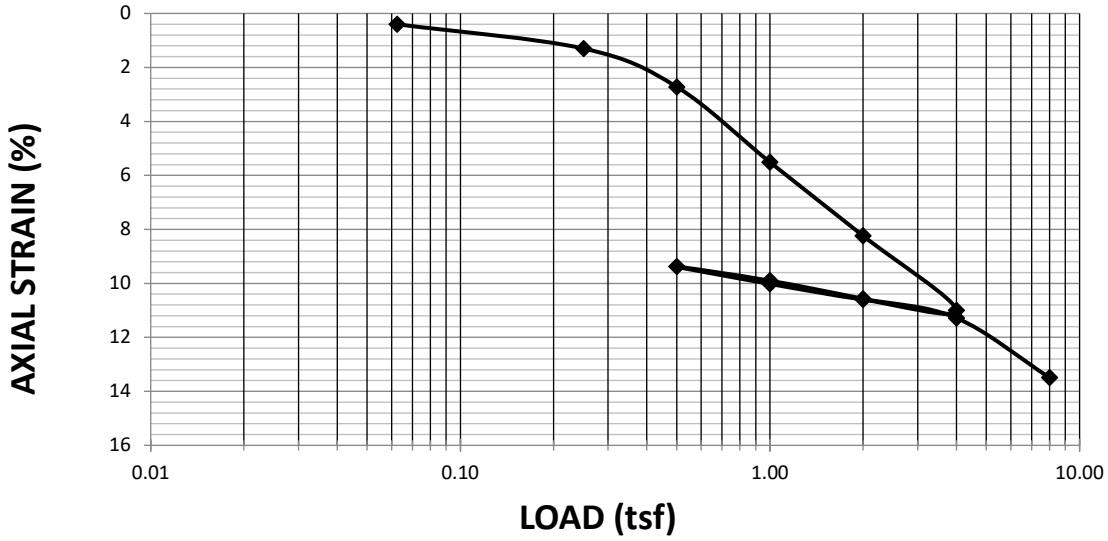

Figure B 2. Site 3- Muskogee 3.5 ft unsat Consolidation test results

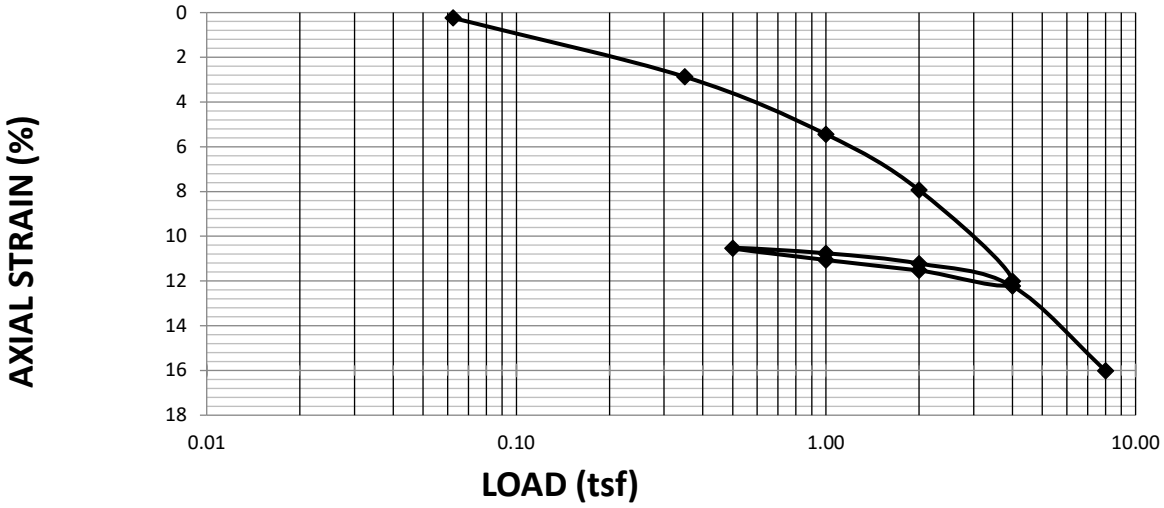

Figure B 3. Site 8- Fairview 6 ft sat Consolidation test results

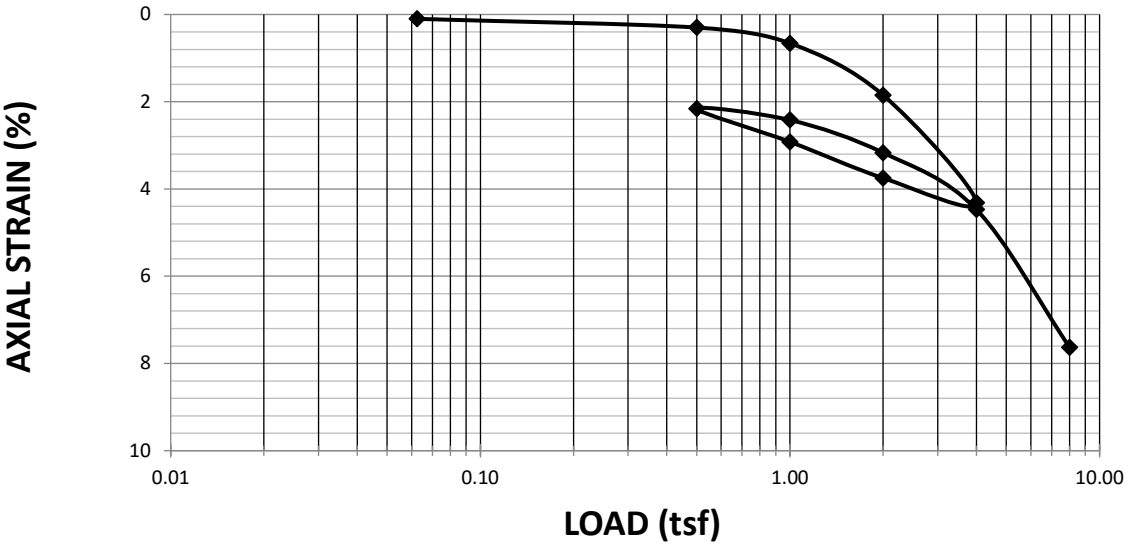

Figure B 4. Site 4- Wagoner 7.7 ft sat Consolidation test results

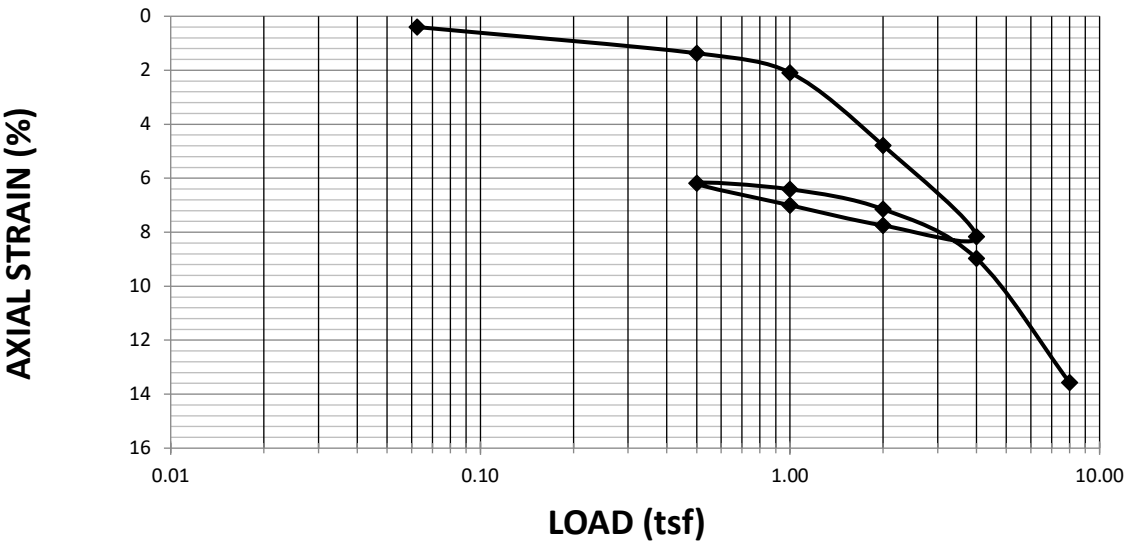

Figure B 5. Site 4- Wagoner 7.8 ft unsat Consolidation test results

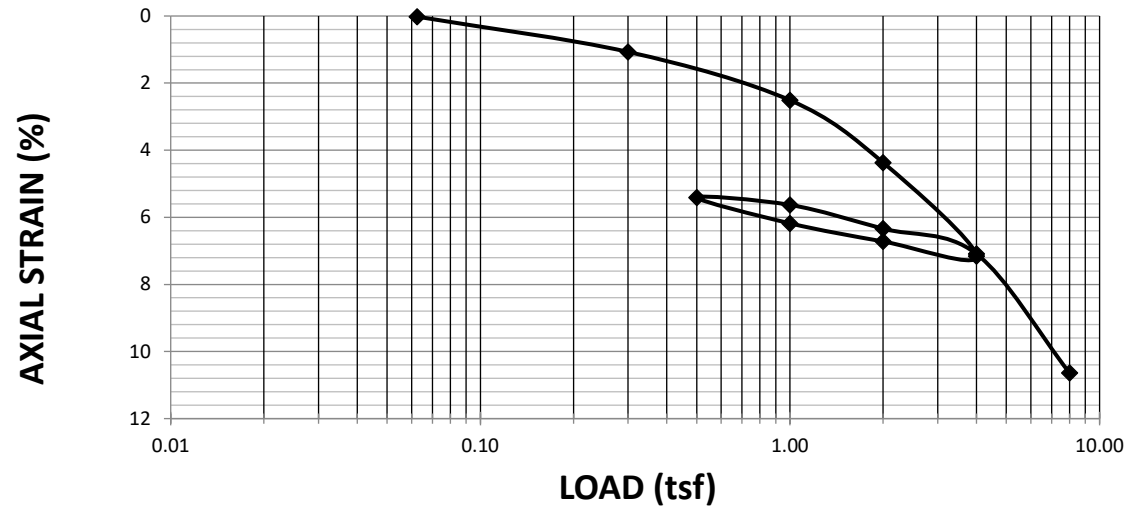

Figure B 6. Site 4- Wagoner 5.6 ft sat Consolidation test results

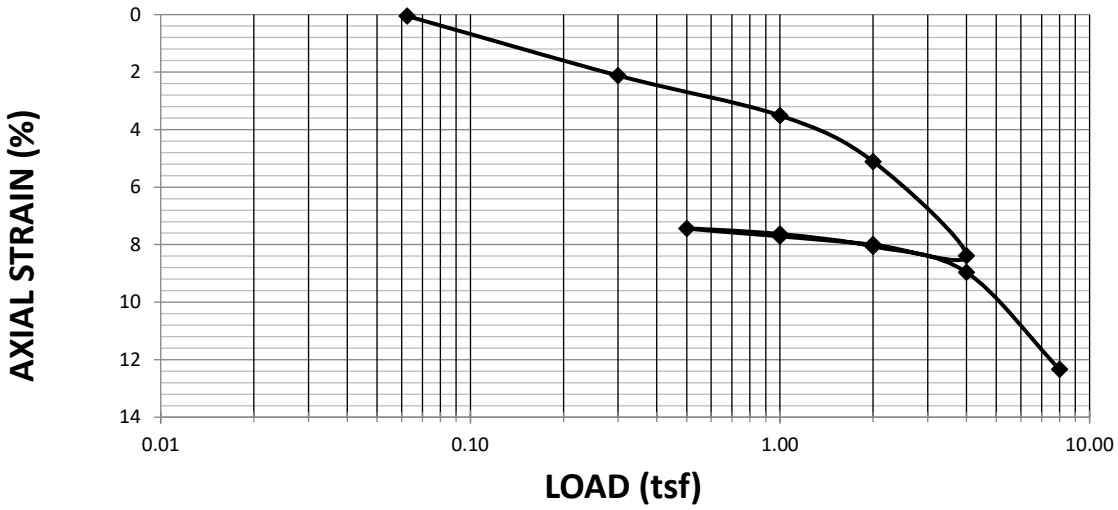

Figure B 7. Site 4- Wagoner 5.7 ft unsat Consolidation test results

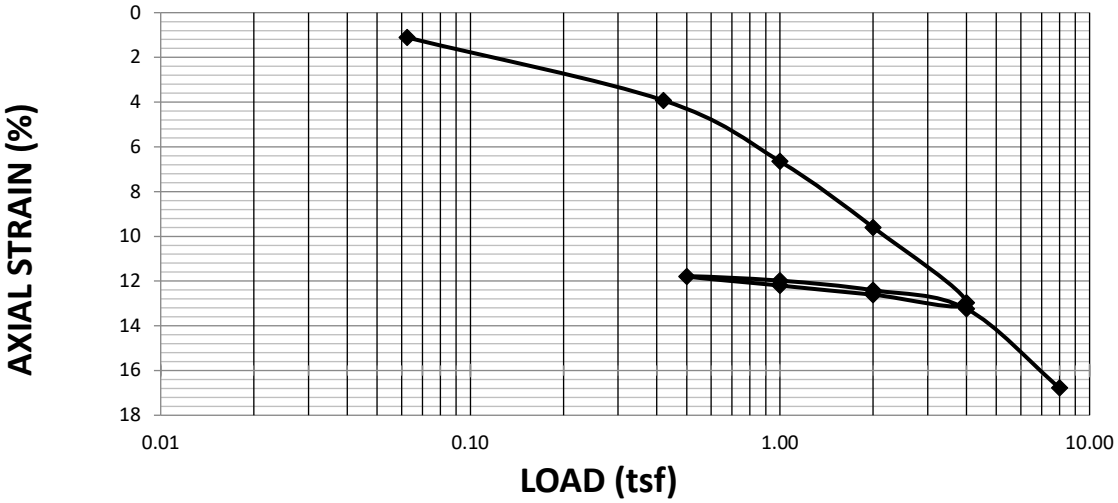

Figure B 8. Site 8- Fairview 7.1 ft sat Consolidation test results

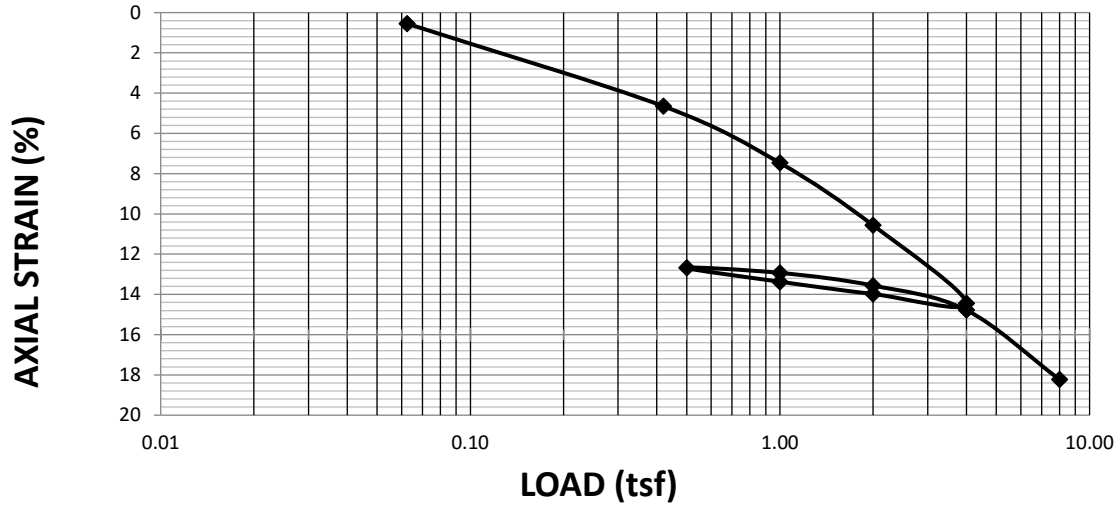

Figure B 9. Site 8- Fairview 7.2 unsat Consolidation test results

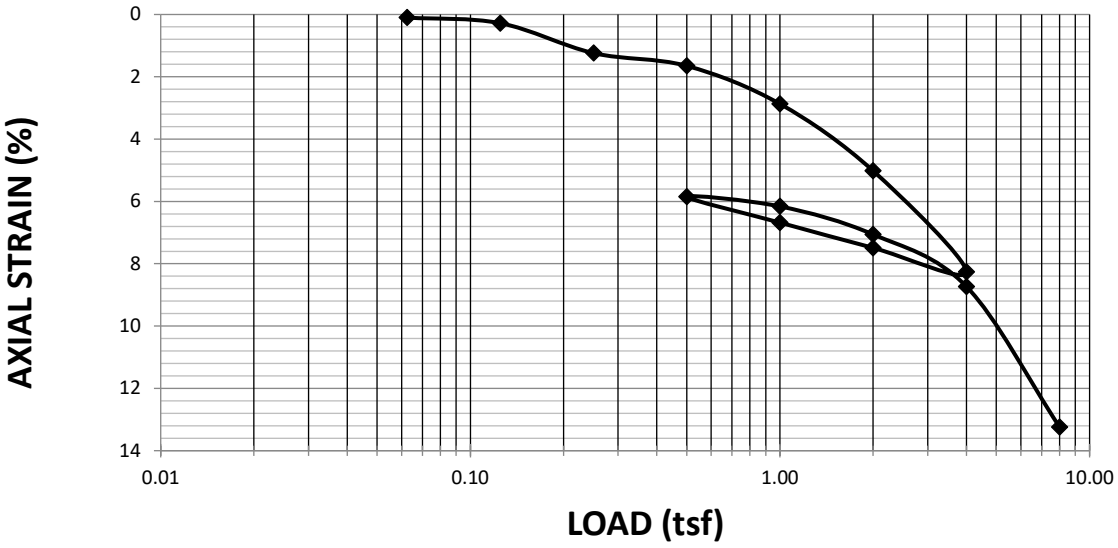

Figure B 10. Site 3- Muskogee 3.9 sat Consolidation test results

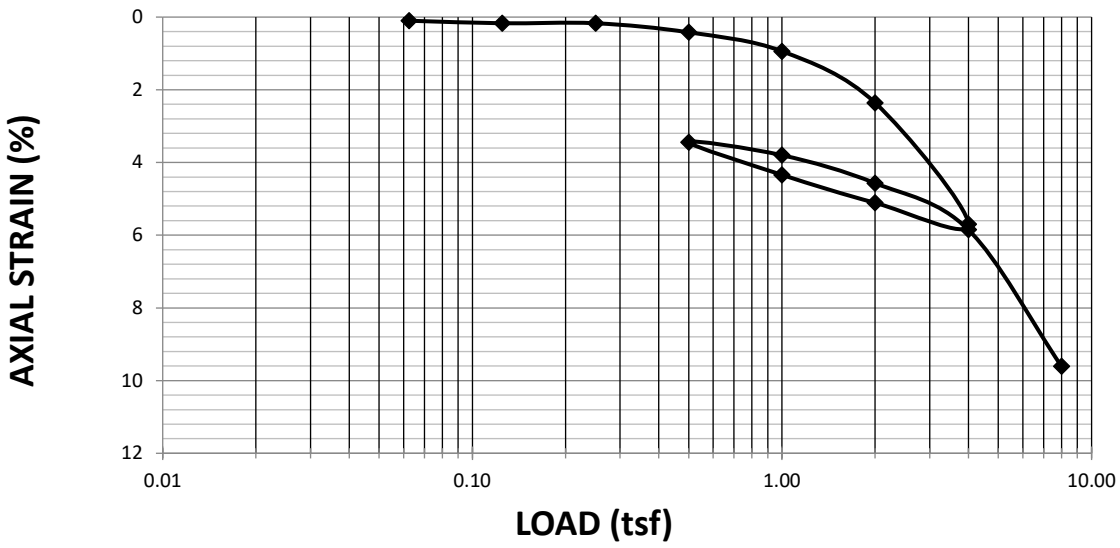

Figure B 11. Site 3-Muskogee 4 ft unsat Consolidation test results

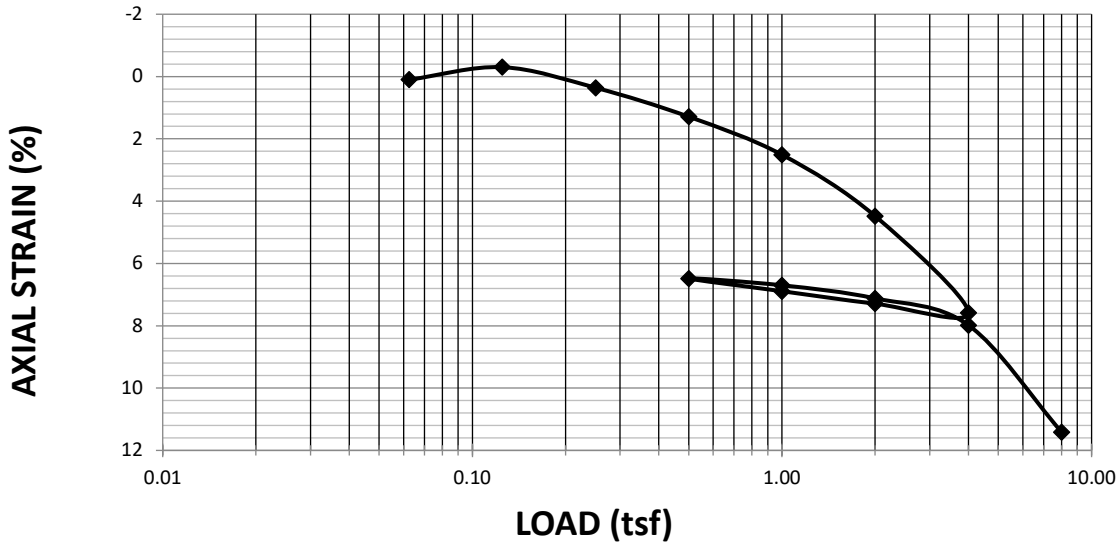

Figure B 12. Site 2- Lake Hefner 0.3 ft sat Consolidation test results

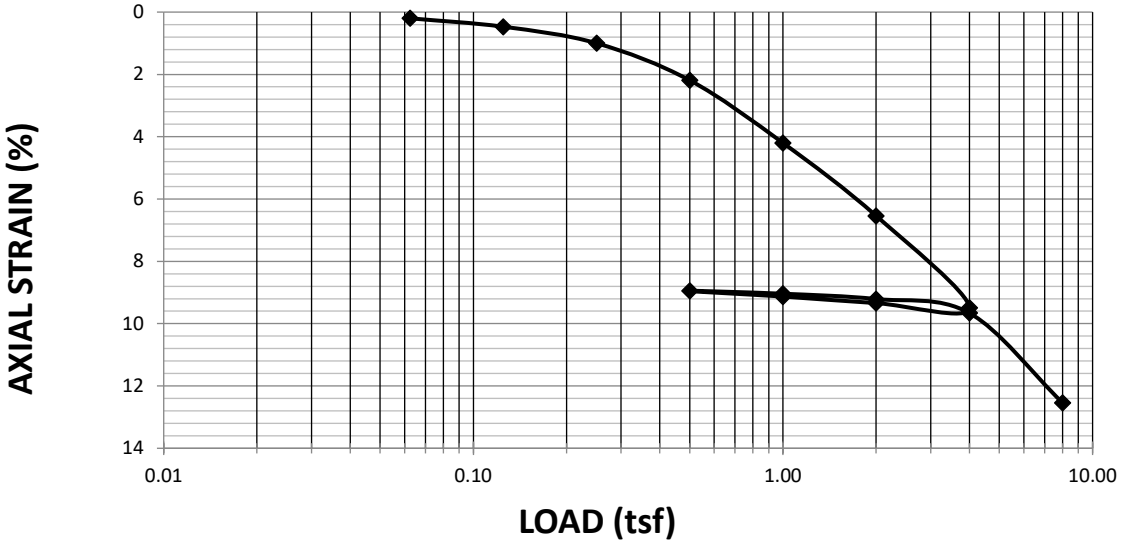

Figure B 13. Site-2 Lake Hefner 0.4 ft unsat Consolidation test results

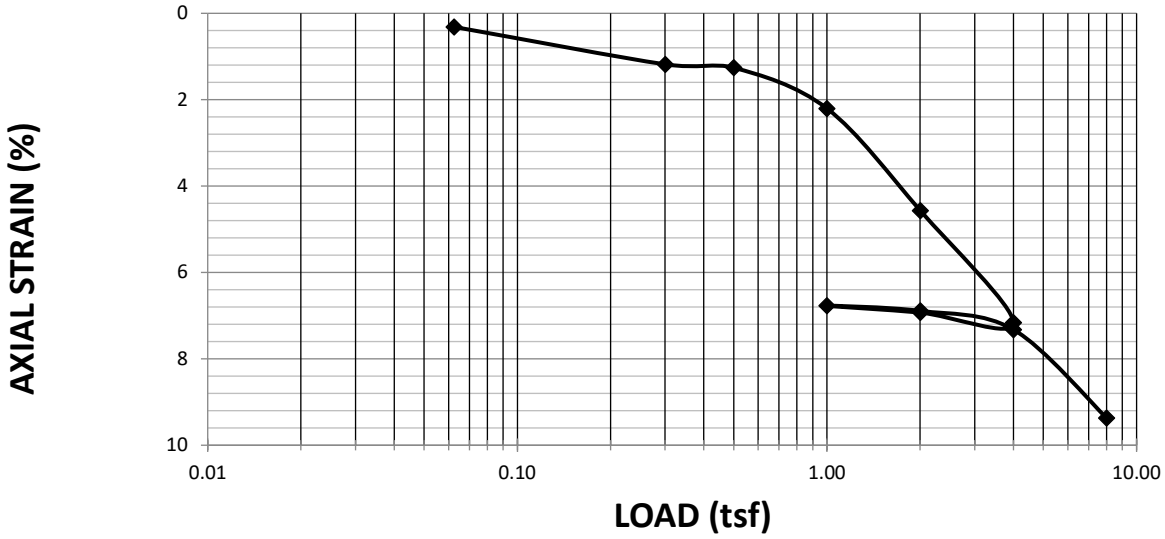

Figure B 14. Site-5 Hobart 4.6 ft unsat Consolidation test results

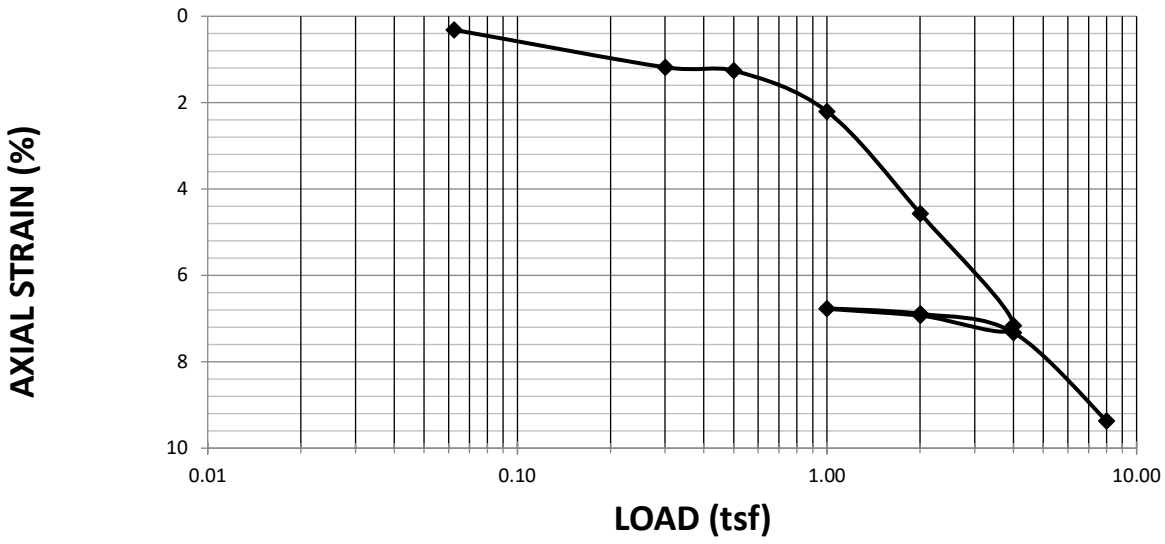

Figure B 15. Site-5 Hobart 4.8 ft sat Consolidation test results

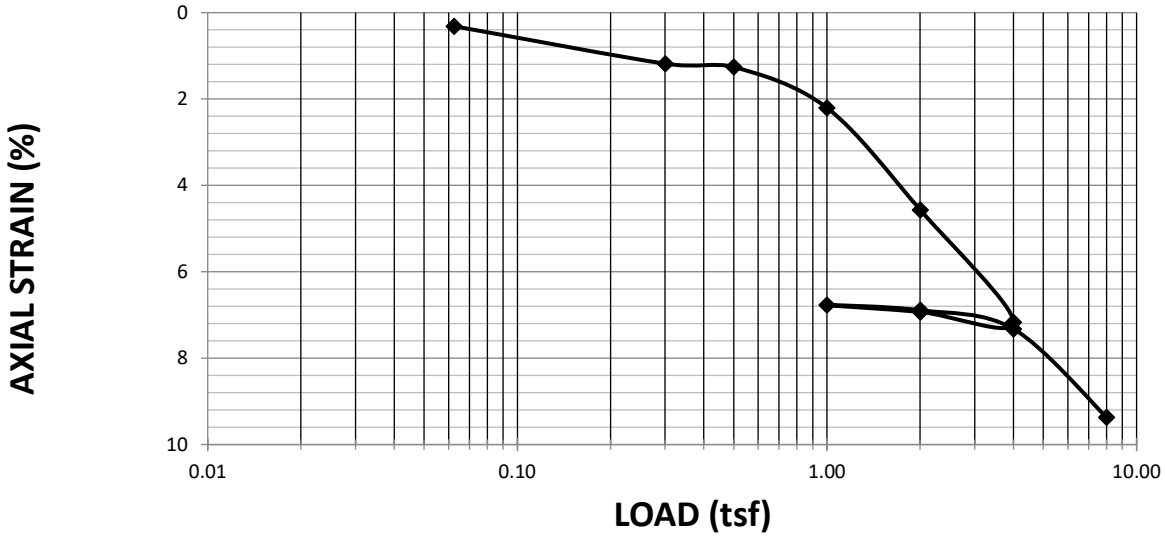

Figure B 16. Site-7 Norman 9.1 ft sat Consolidation test results

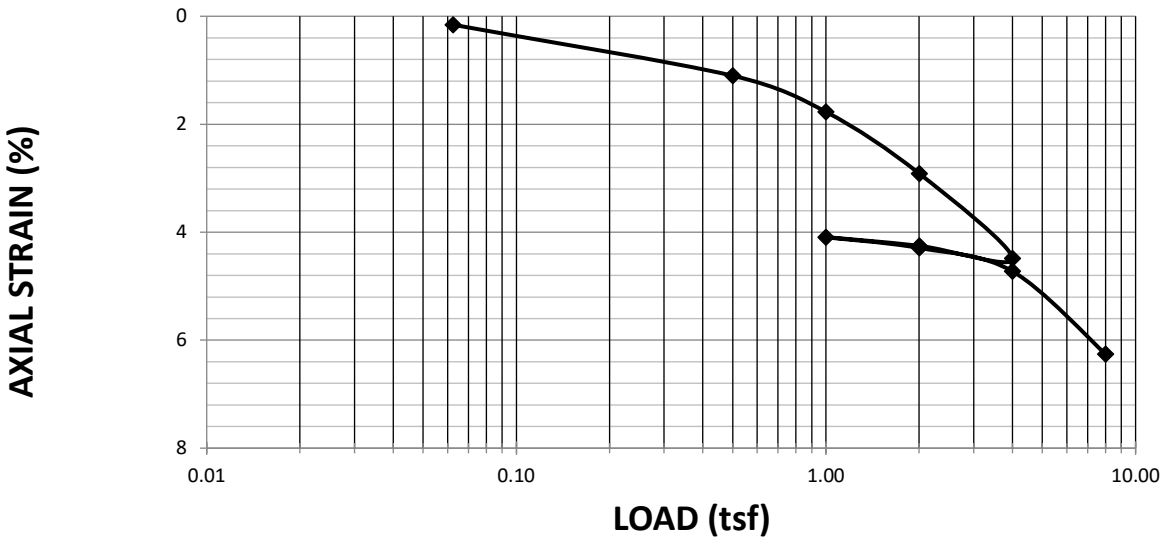

Figure B 17. Site-7 Norman 9.2 ft unsat Consolidation test results

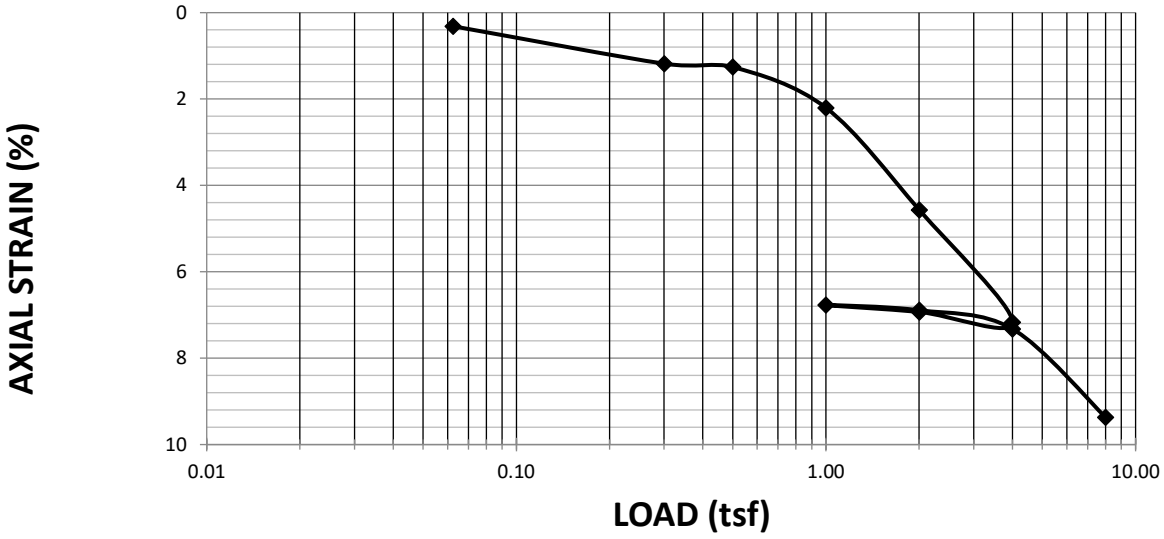

Figure B 18. Site-6 Wewoka 5.6 ft unsat Consolidation test results

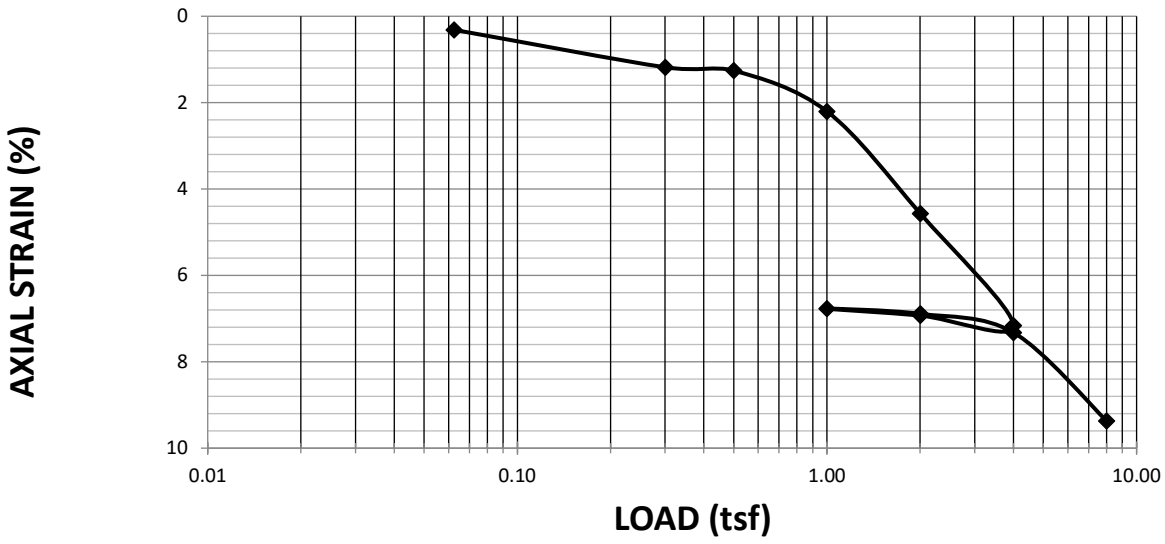

Figure B 19. Site-6 Wewoka 5.5 ft sat Consolidation test results

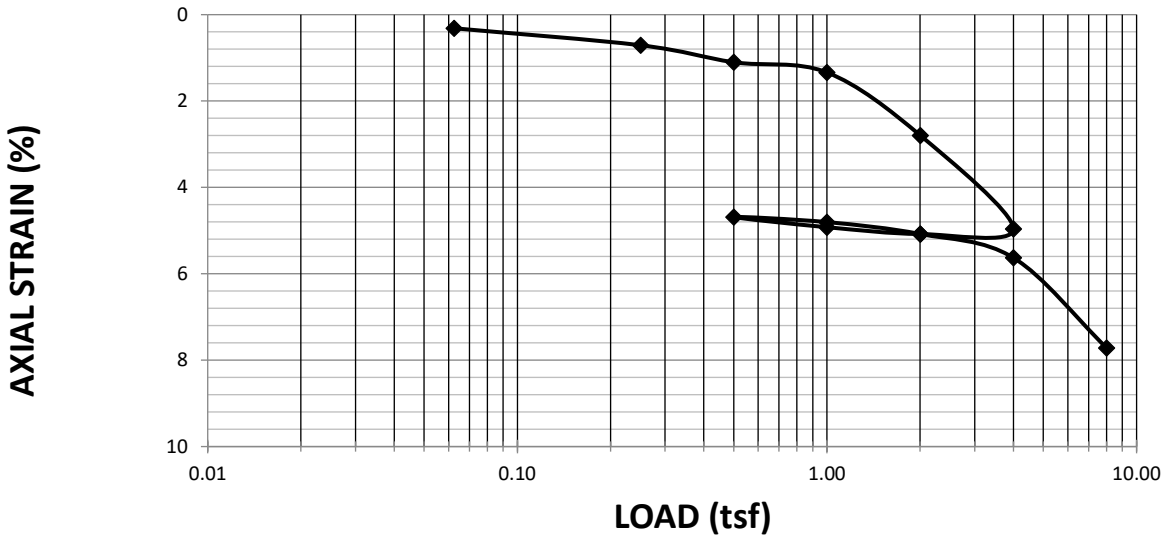

Figure B 20. Site-9 Fears 4.4 ft unsat Consolidation test results

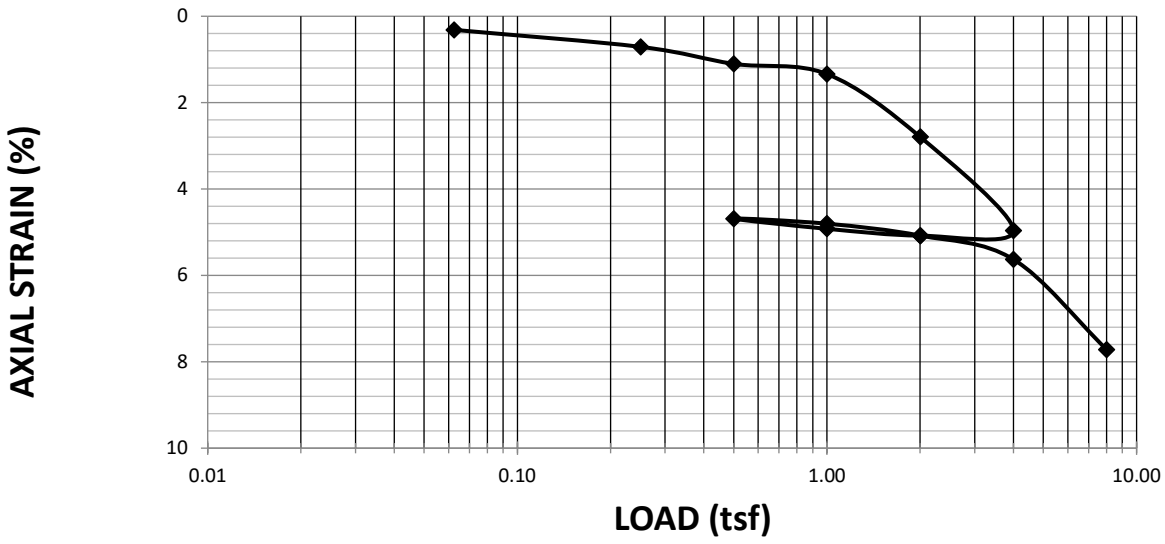

Figure B 21. Site-9 Fears 4.6 ft sat Consolidation test results

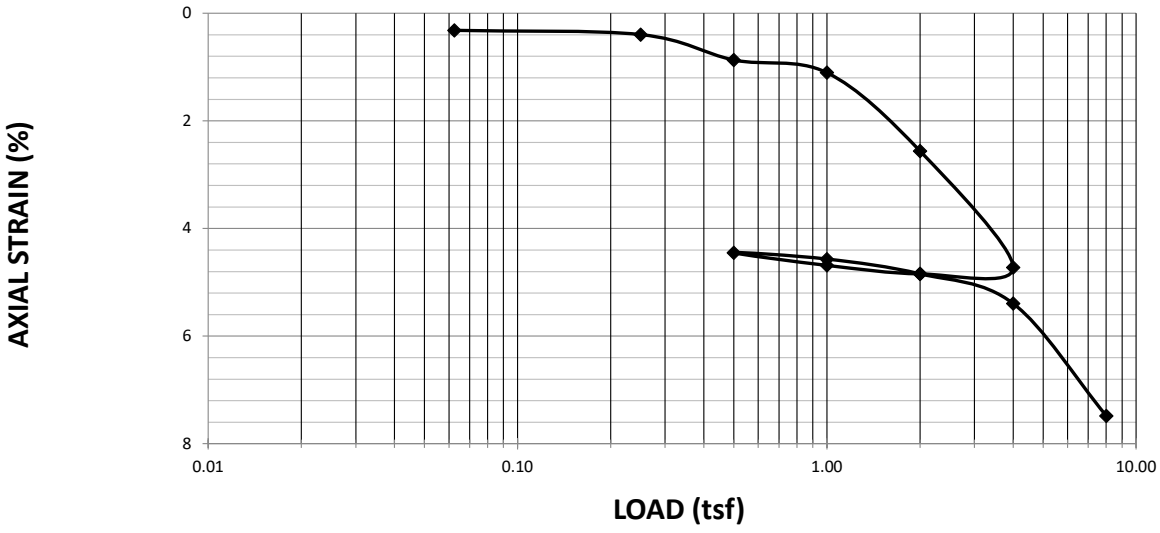

Figure B 22. Site-5 Hobart 7.2 ft sat Consolidation test results

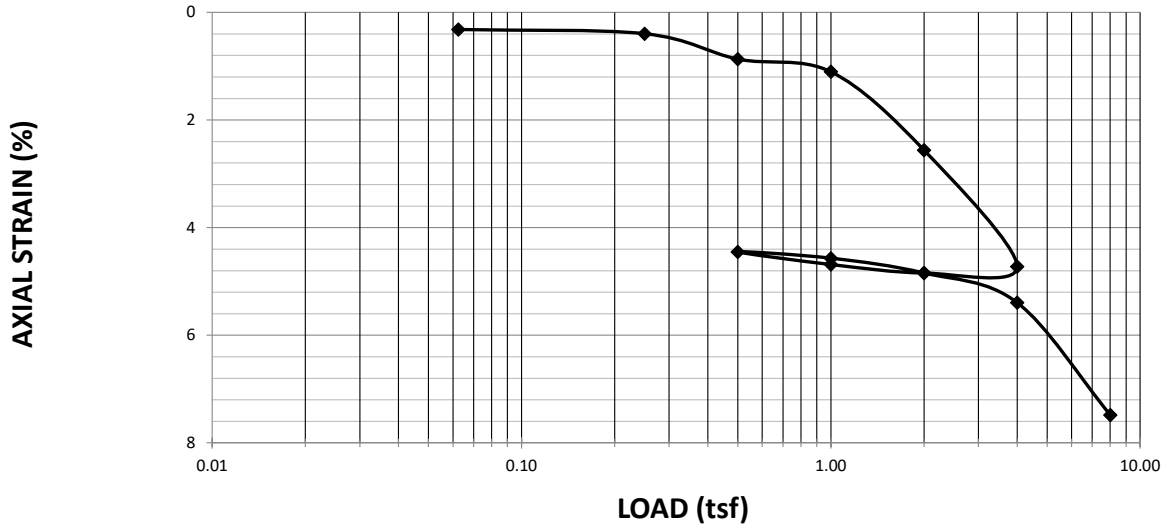

Figure B 23. Site-5 Hobart 7.4 ft unsat Consolidation test results

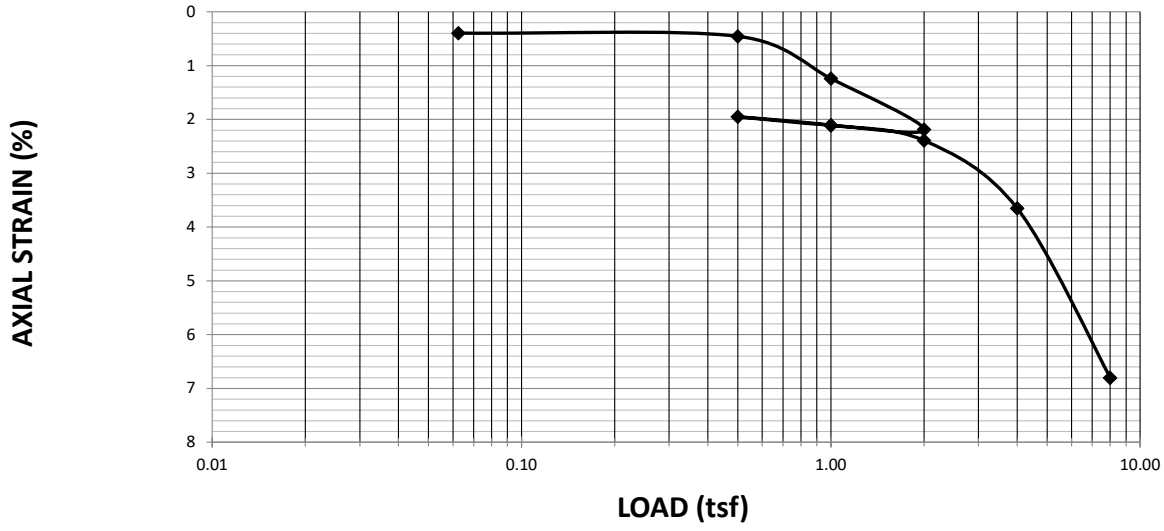

Figure B 24. Site-6 Wewoka 8.1 ft sat Consolidation test results

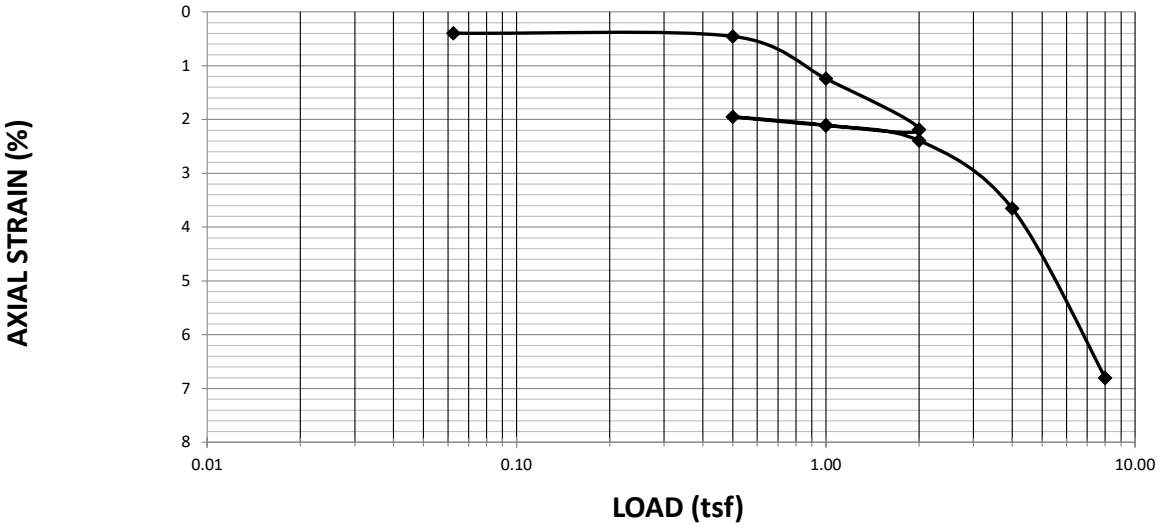

Figure B 25. Site-6 Wewoka 7.9 ft unsat Consolidation test results

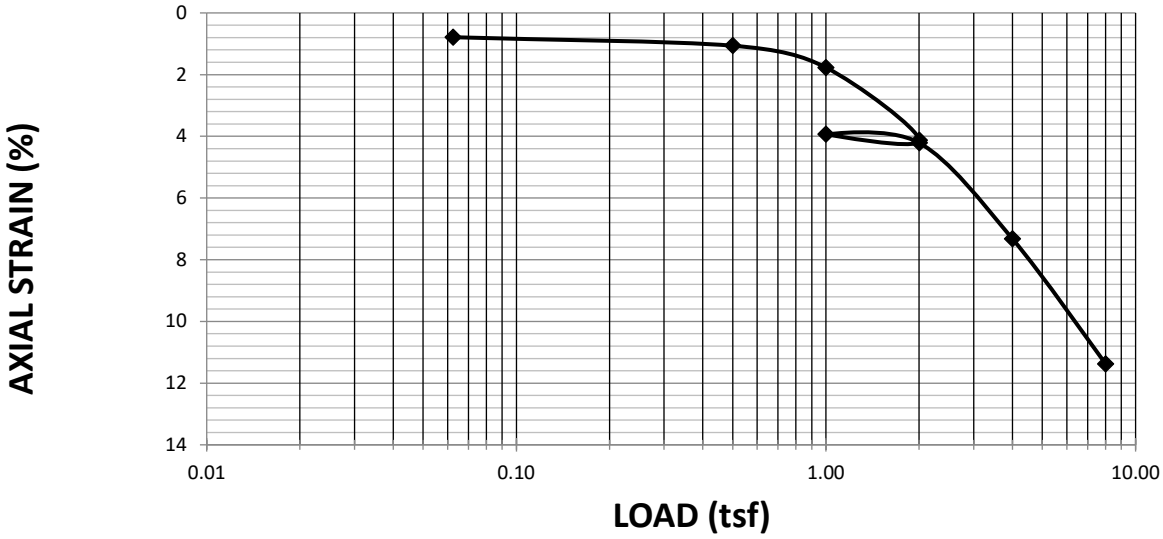

Figure B 26. Site-7 Norman 10.9 ft sat Consolidation test results

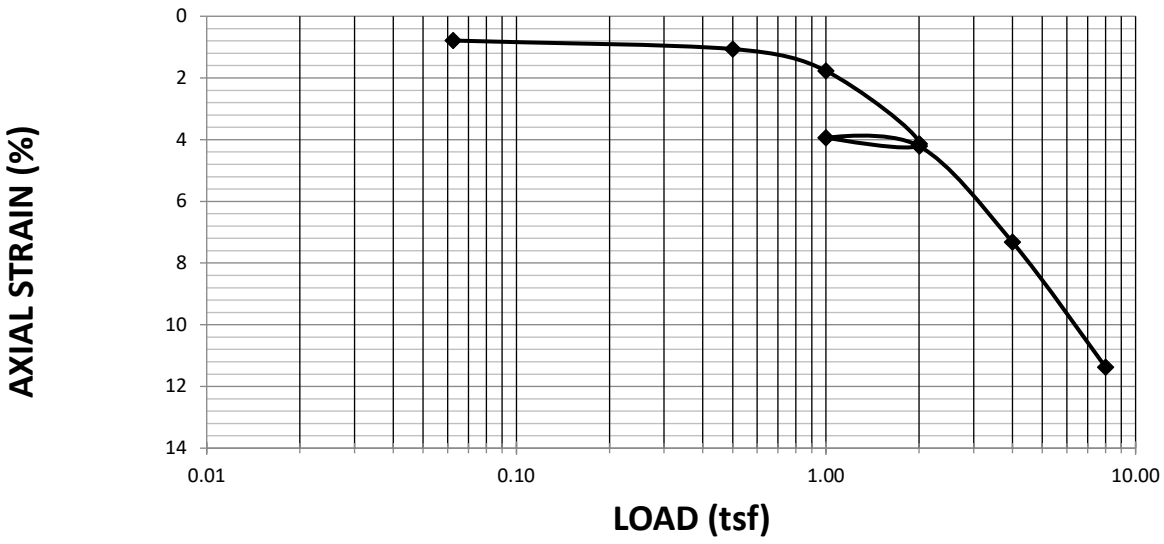

Figure B 27. Site-7 Norman 11.1 ft unsat Consolidation test results

Appendix C: Triaxial data

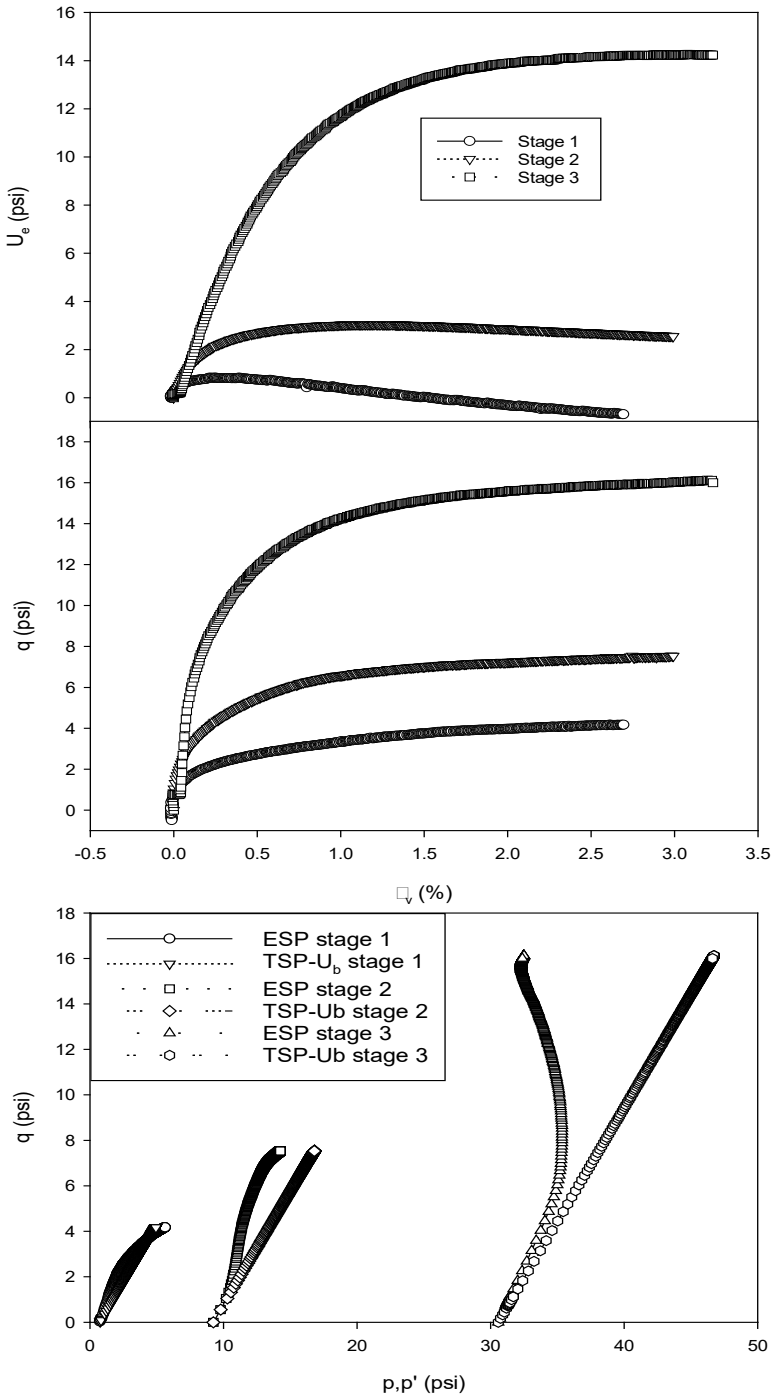

Figure C 1. Triaxial testing results for Site 9 depth 0.7 ft

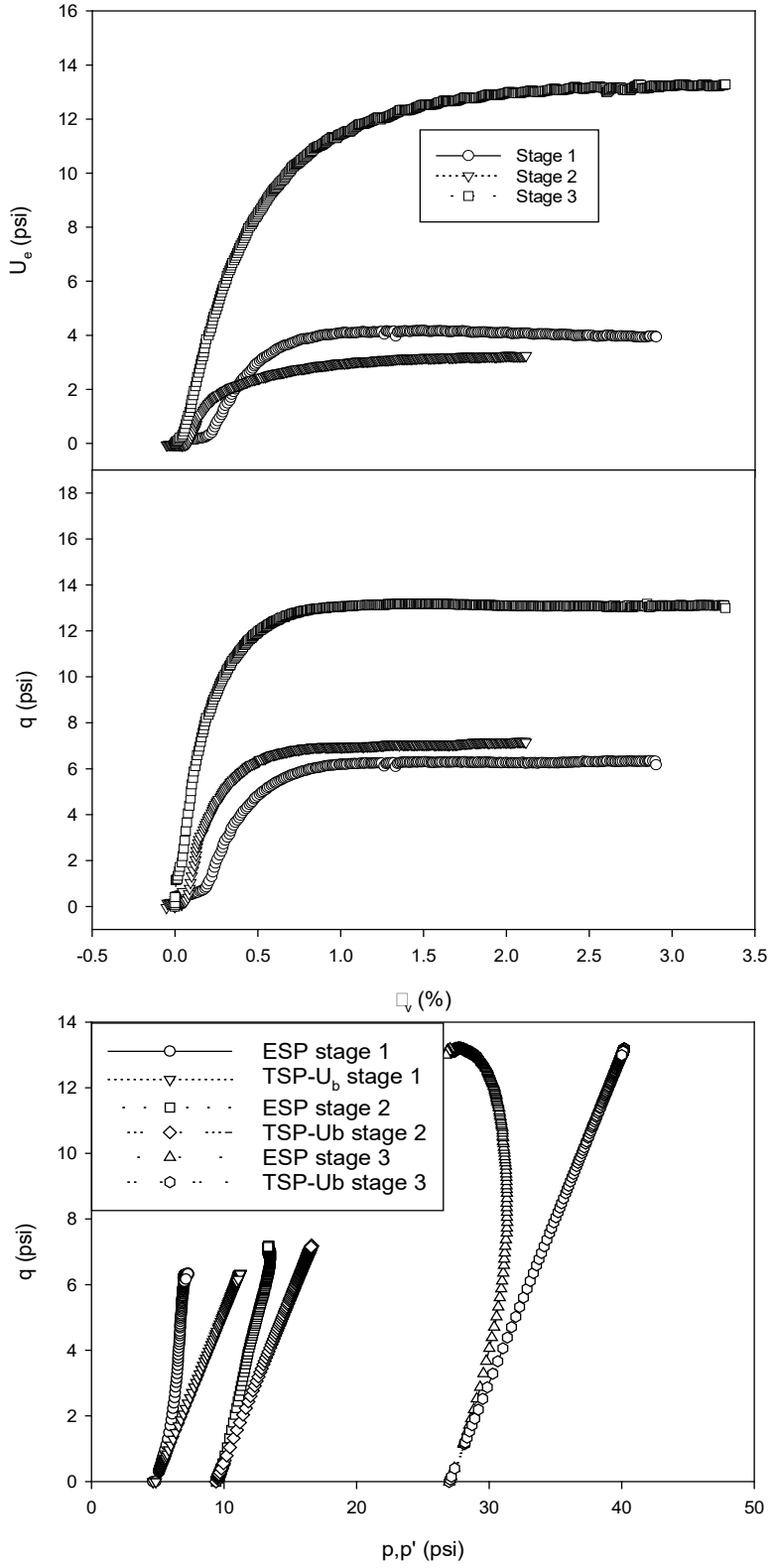

Figure C 2. Triaxial testing results for Site 9 depth 6 ft

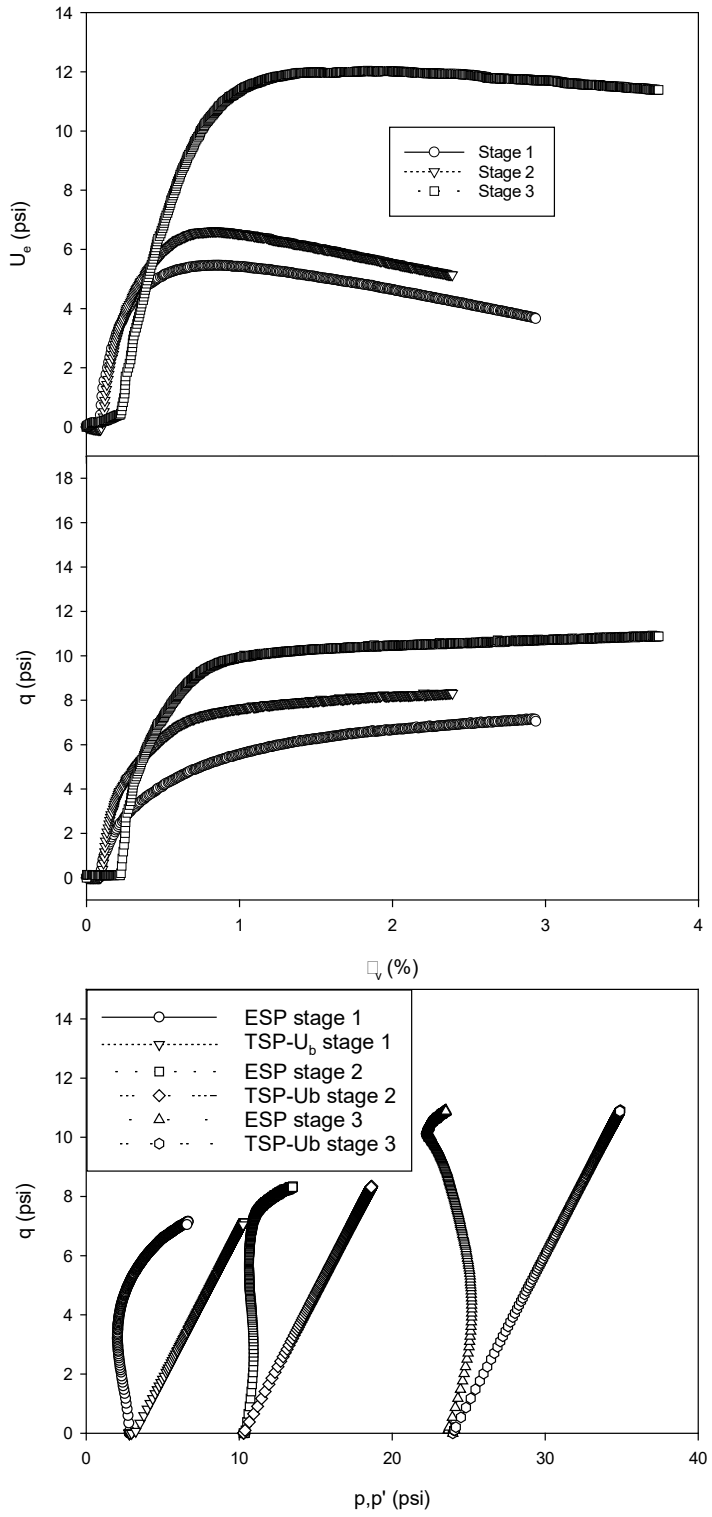

Figure C 3. Triaxial testing results for Site 5 depth 4.2 ft

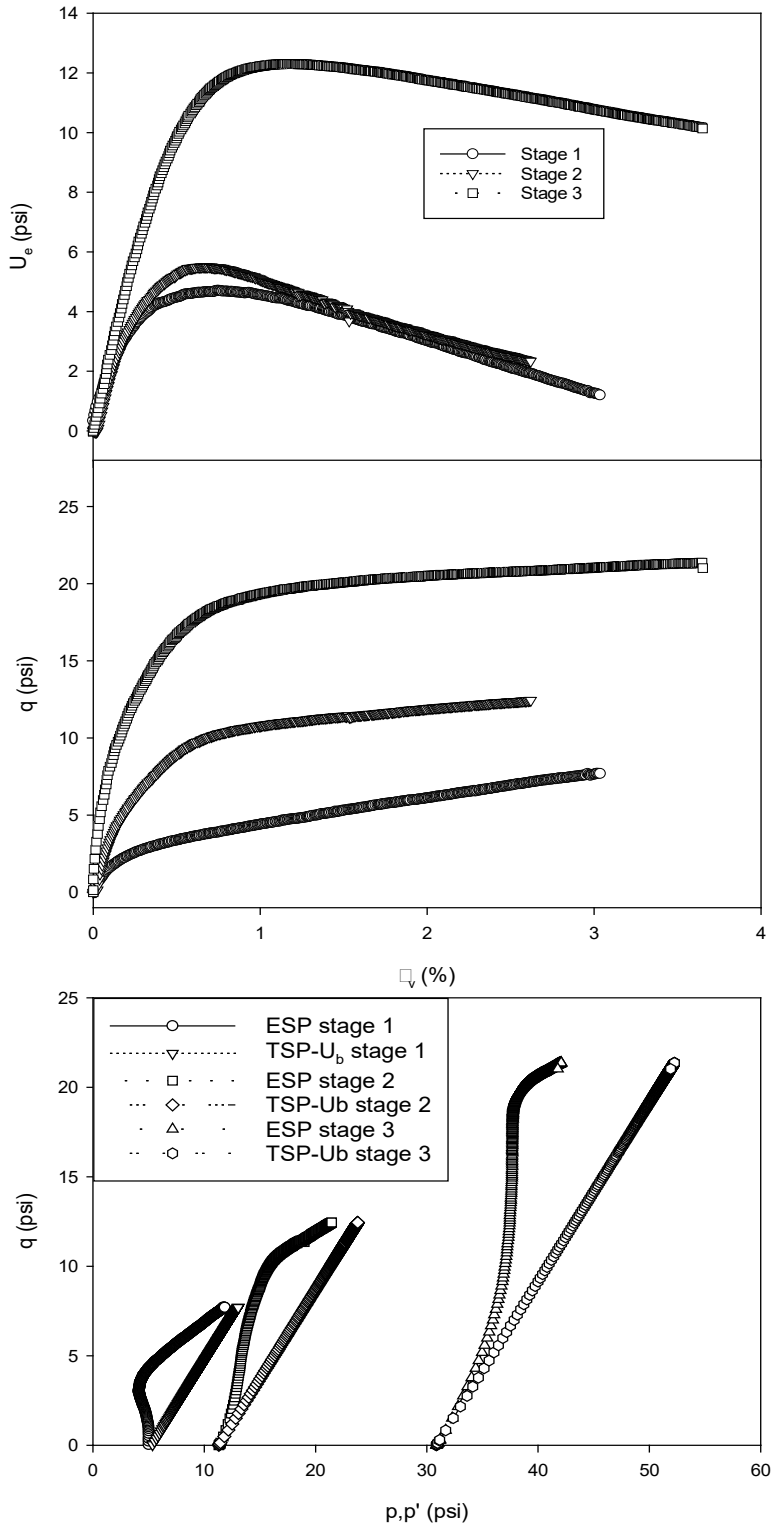

Figure C 4. Triaxial testing results for Site 5 depth 6.6 ft

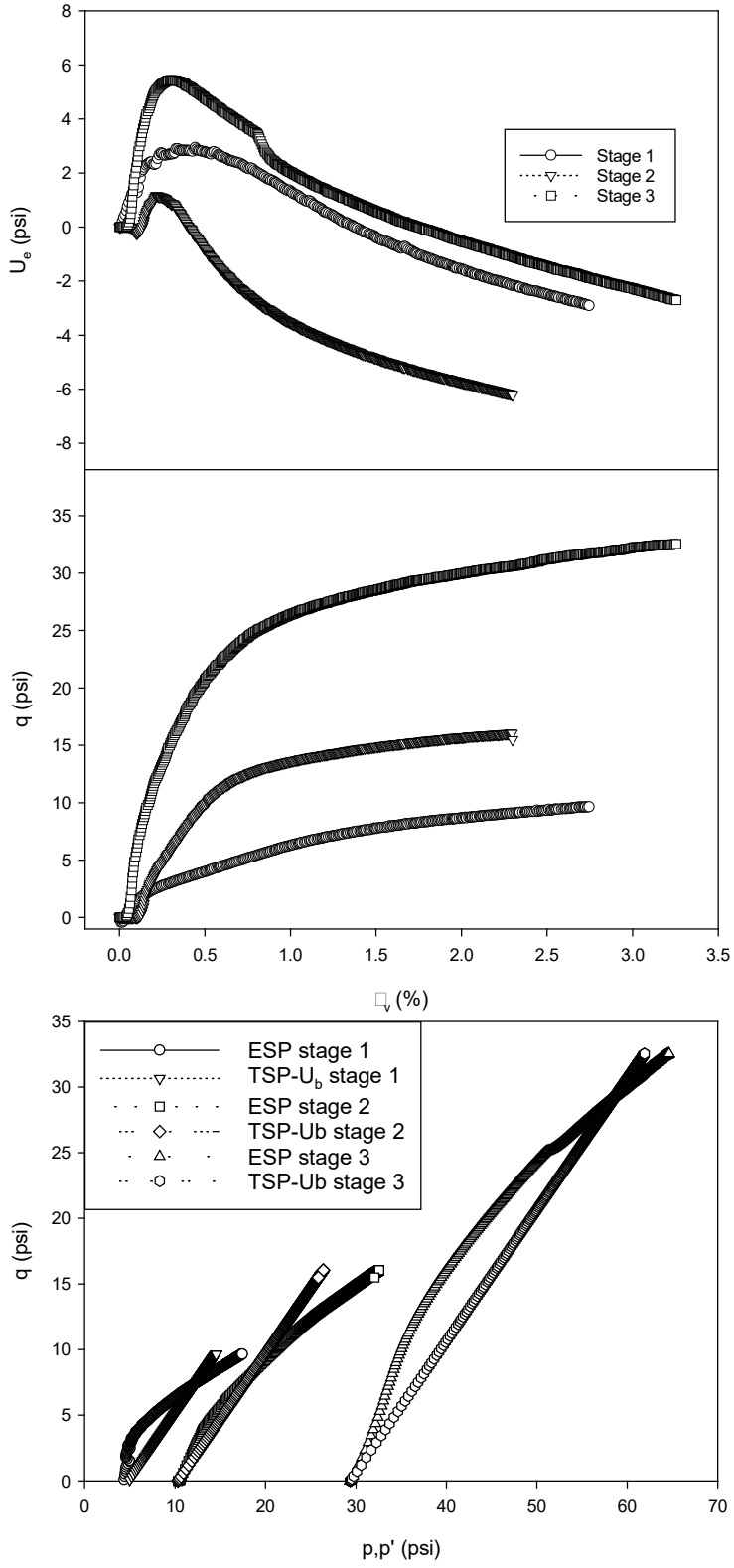

Figure C 5. Triaxial testing results for Site 7 depth 6.1 ft

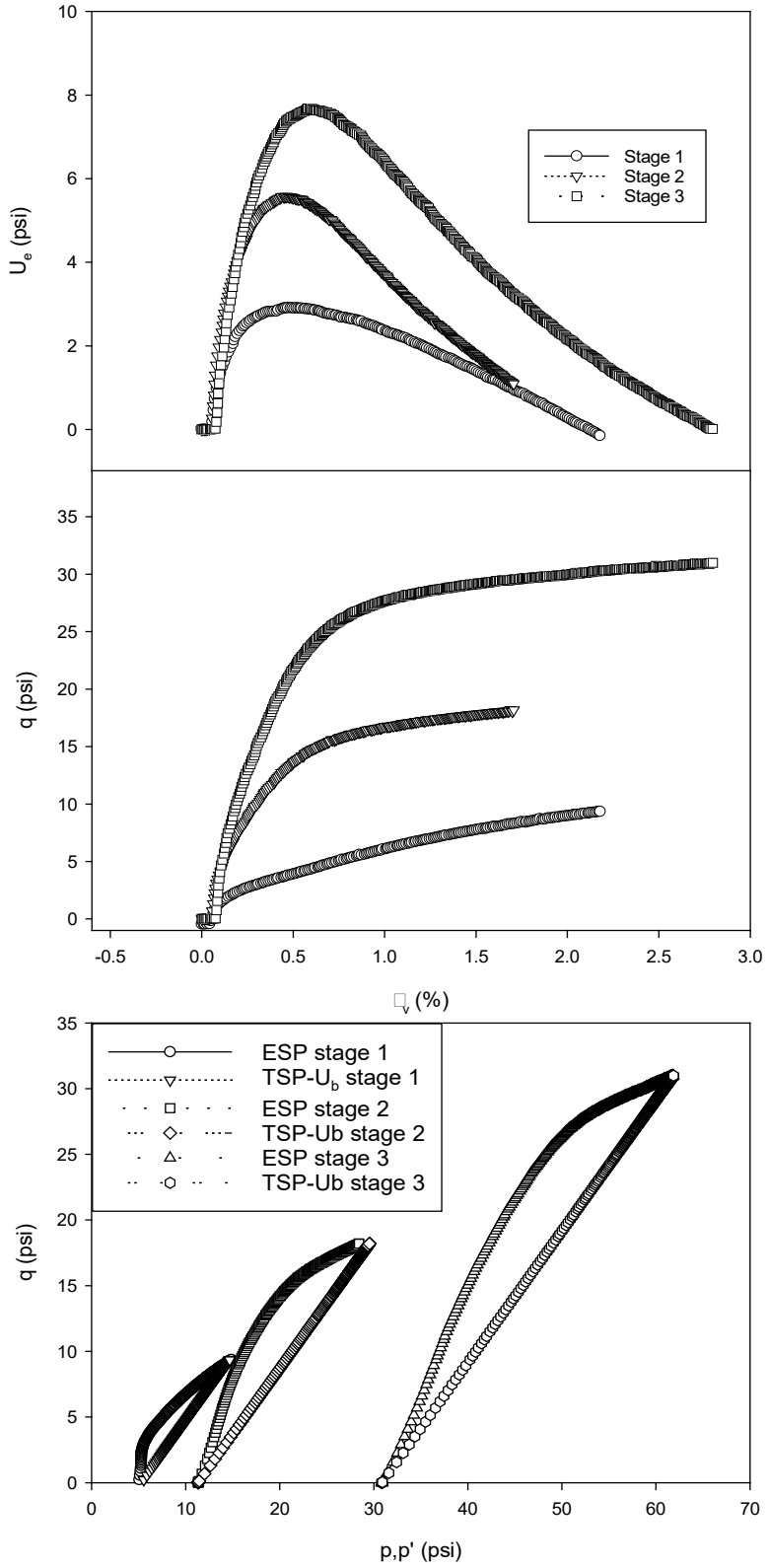

Figure C 6. Triaxial testing results for Site 7 depth 8.4 ft

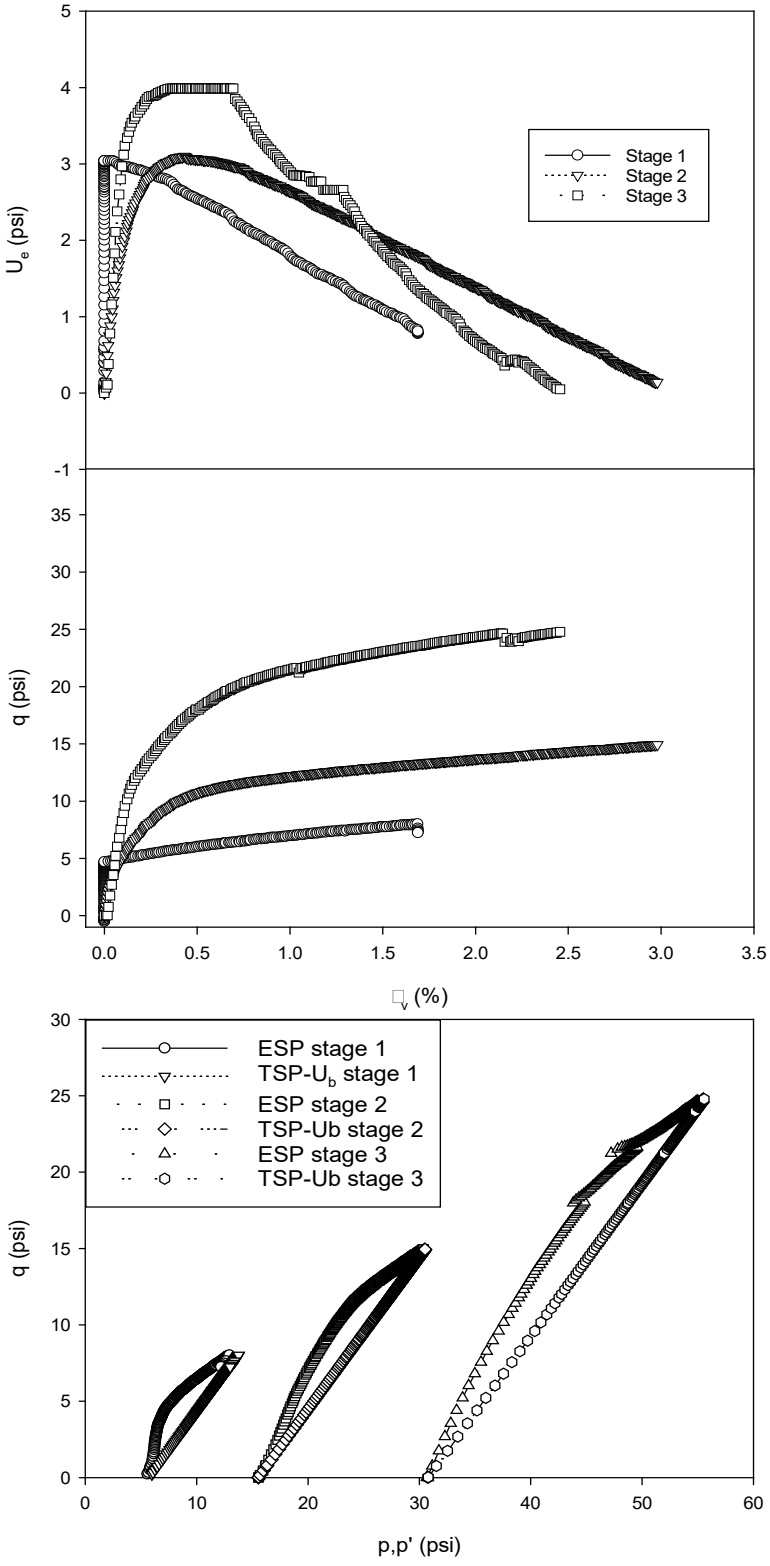

Figure C 7. Triaxial testing results for Site 6 depth 9.1 ft

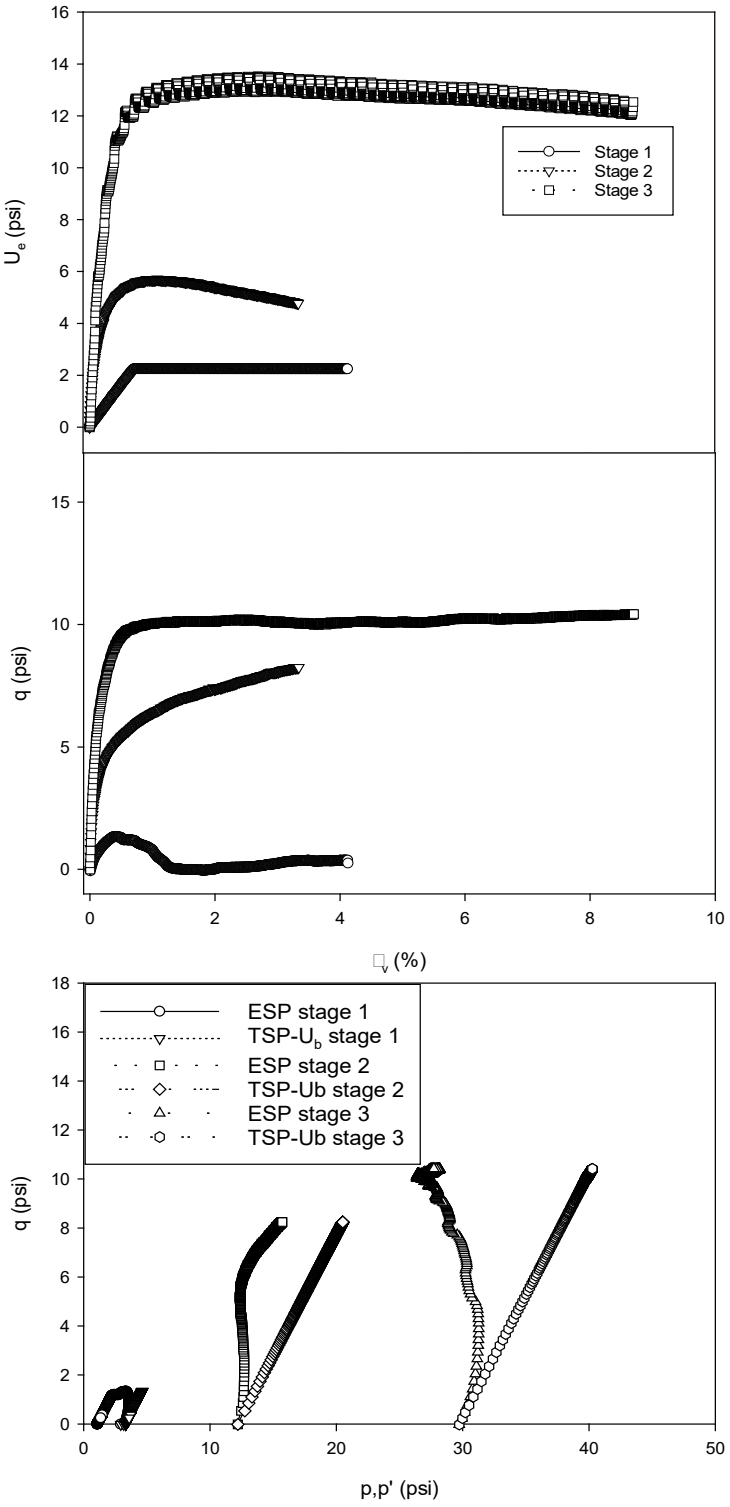

Figure C 8. Triaxial testing results for Site 8 depth 4.1 ft (The triaxial machine stopped working during stage 1 due to a pressure leak which lead to the abnormal behavior in the graph)

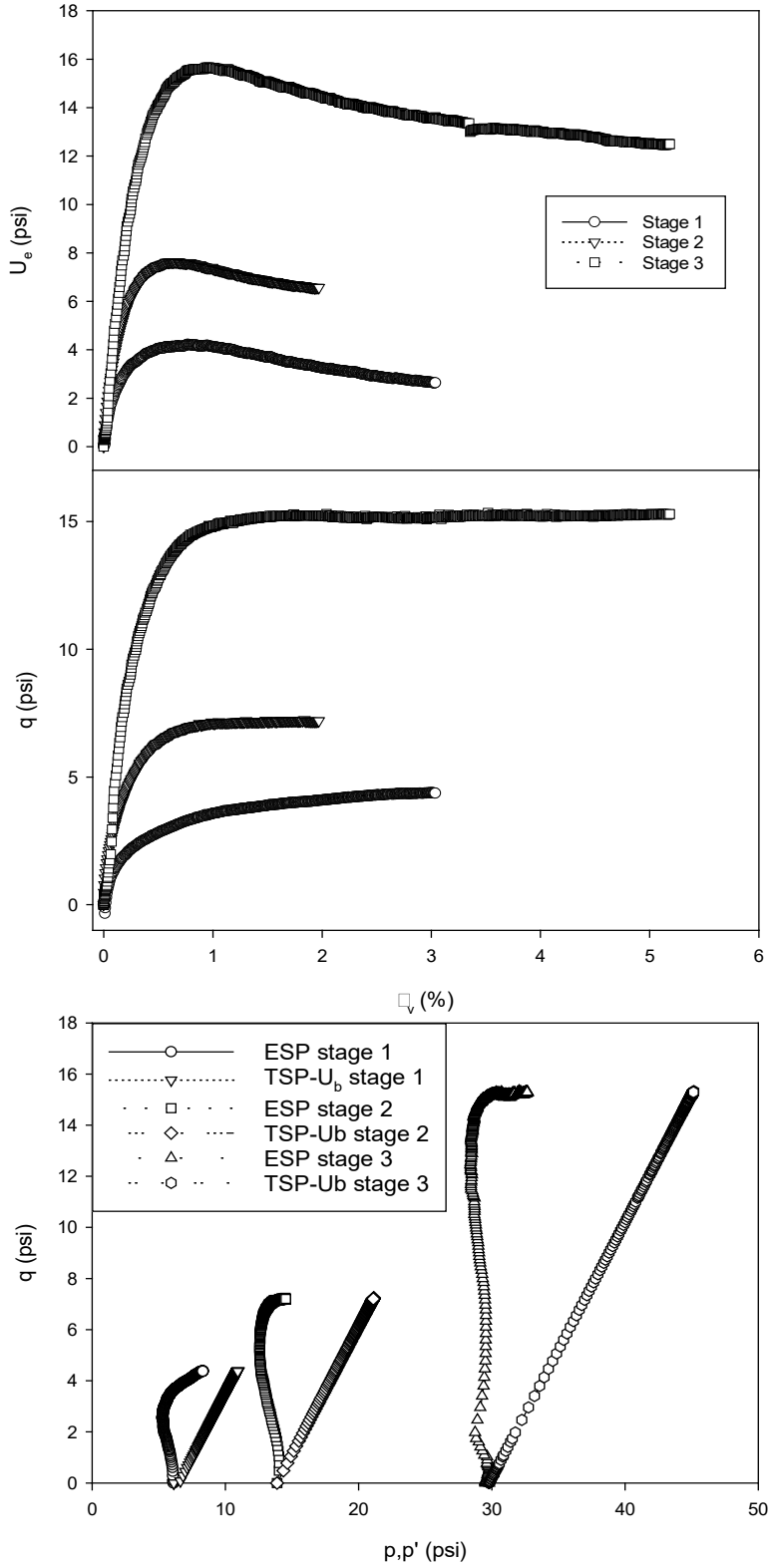

Figure C 9. Triaxial testing results for Site 8 depth 7.8 ft

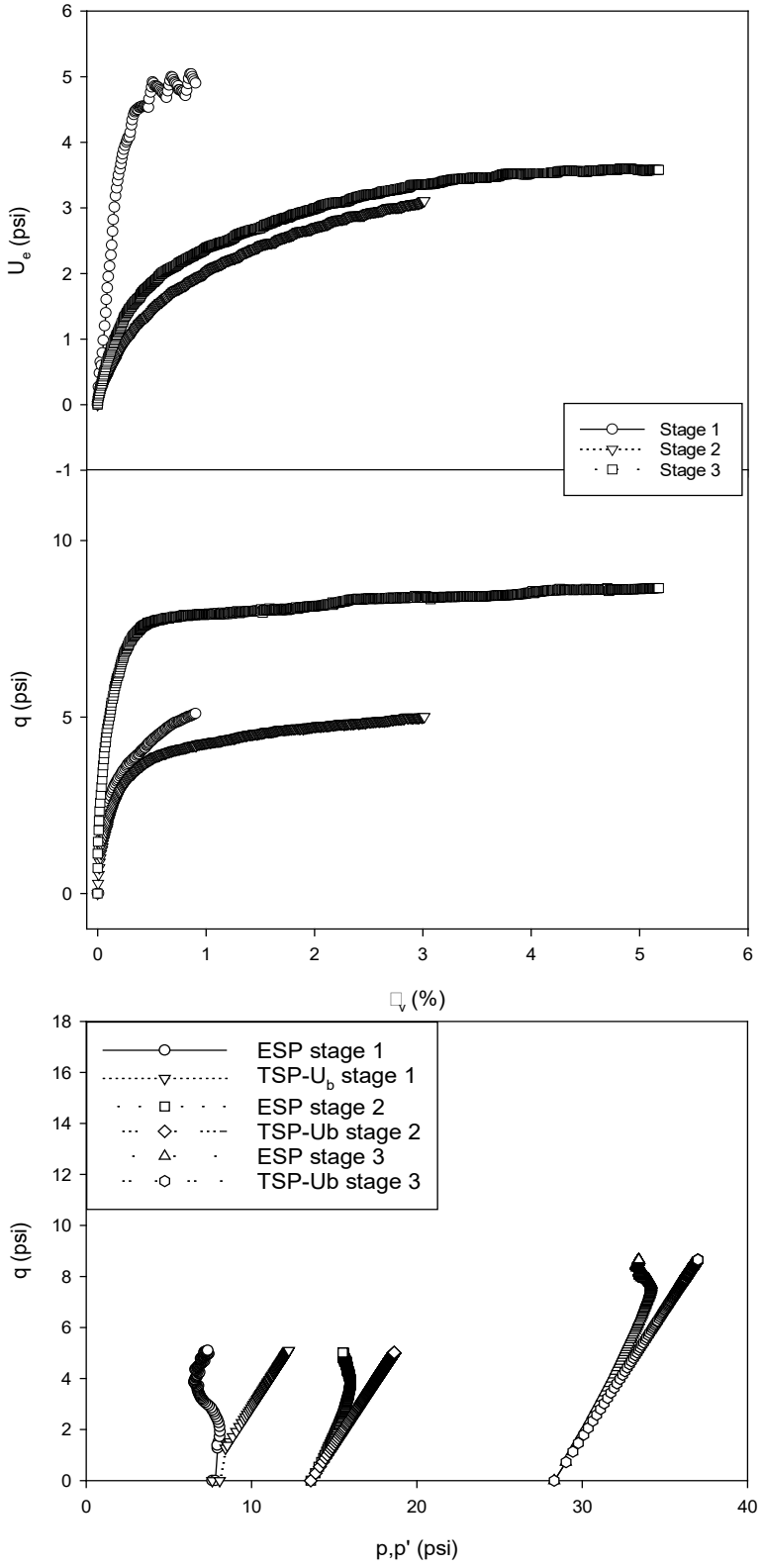

Figure C 10. Triaxial testing results for Site 3 depth 4.5 ft

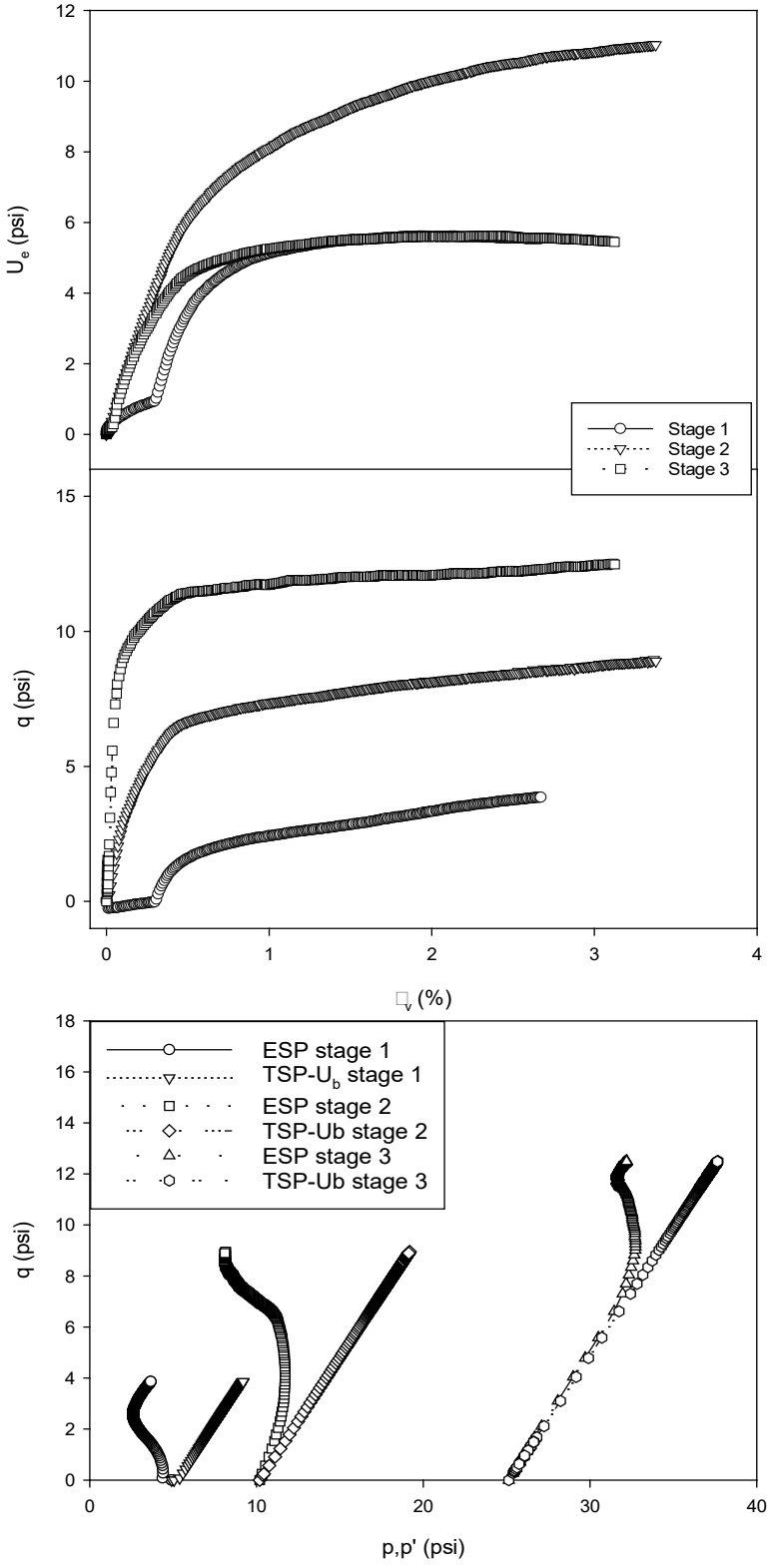

Figure C 11. Triaxial testing results for Site 3 depth 6.3 ft

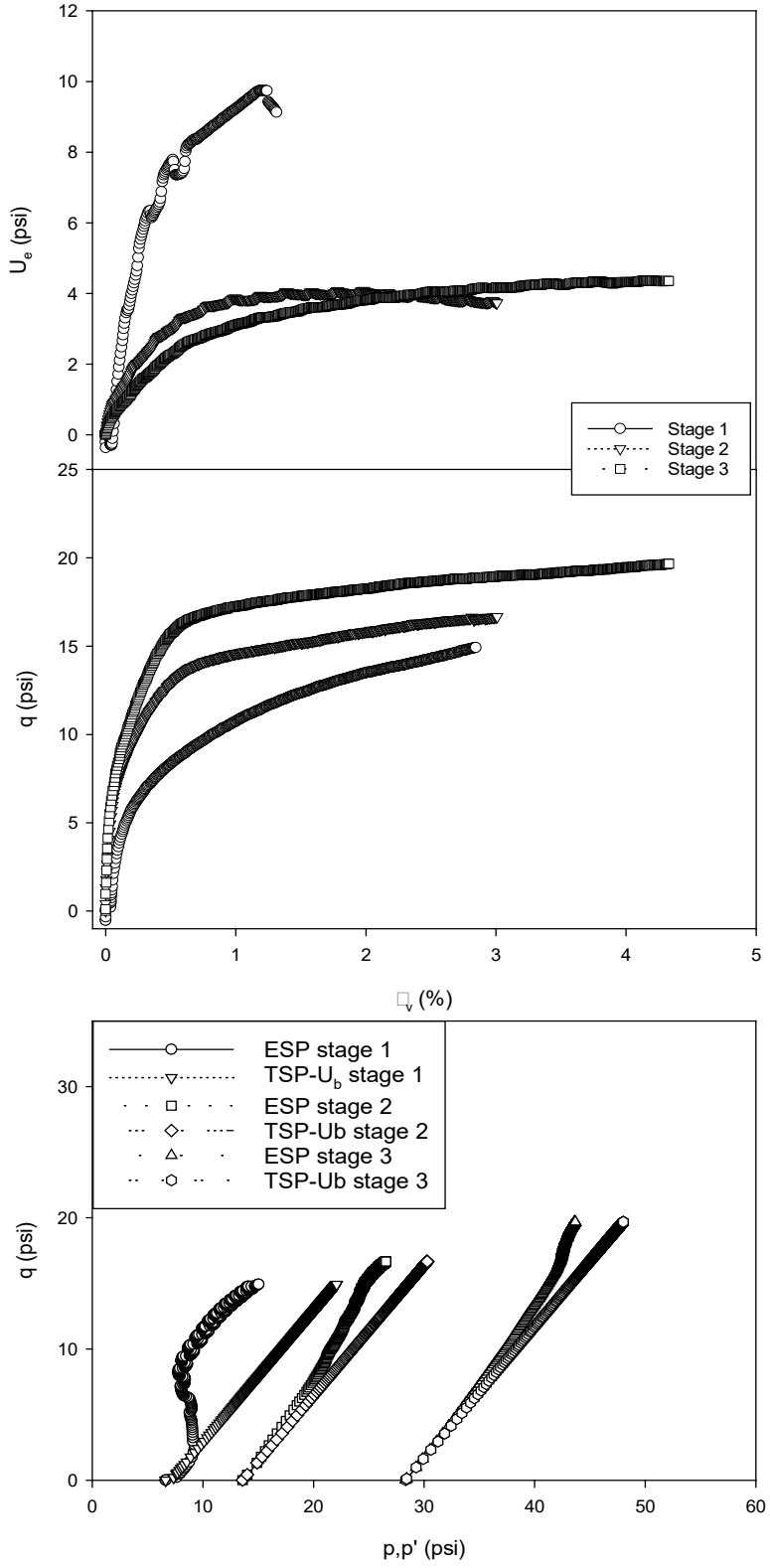

Figure C 12. Triaxial testing results for Site 3 depth 6.3 ft

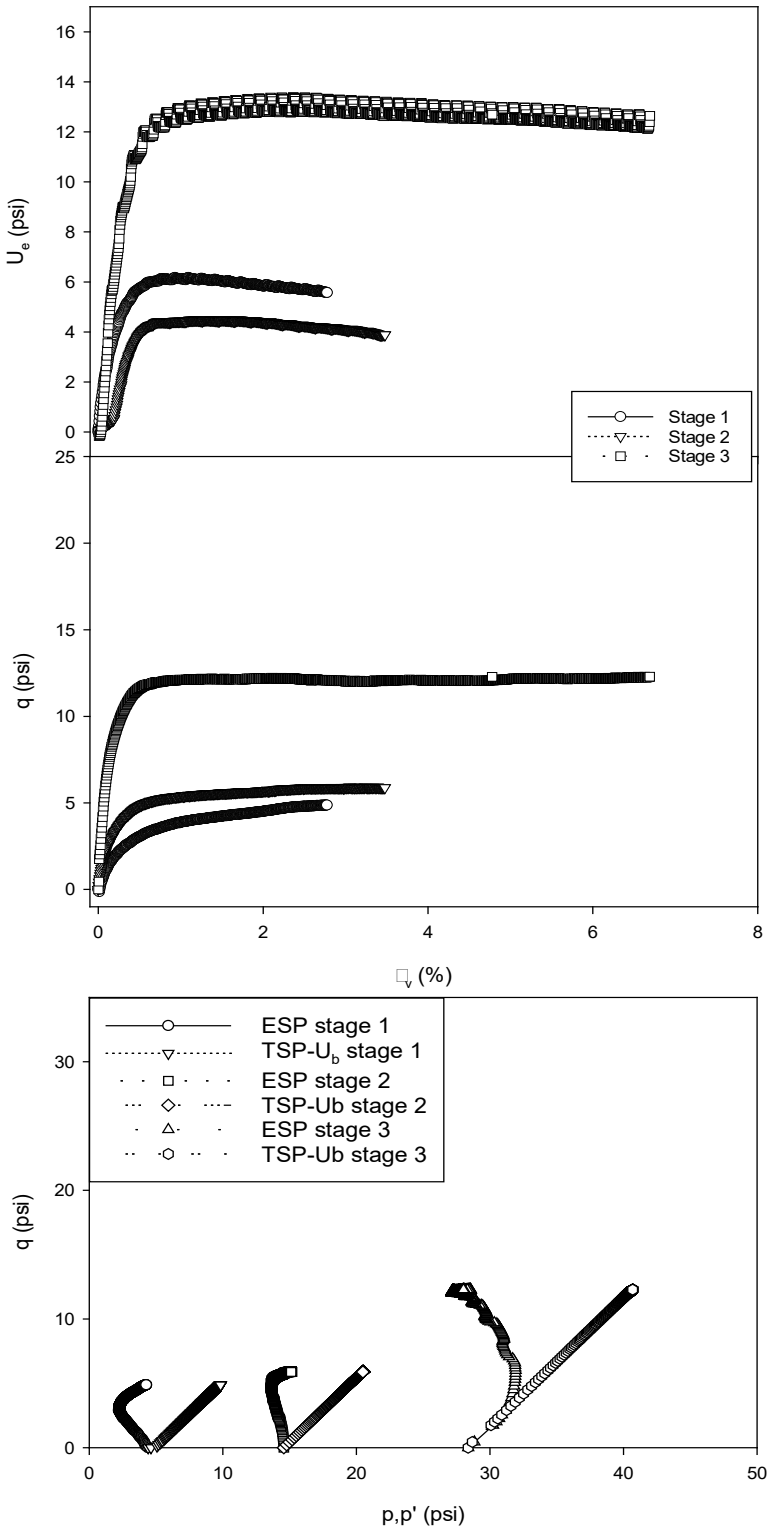

Figure C 13. Triaxial testing results for Site 4 depth 6.3 ft

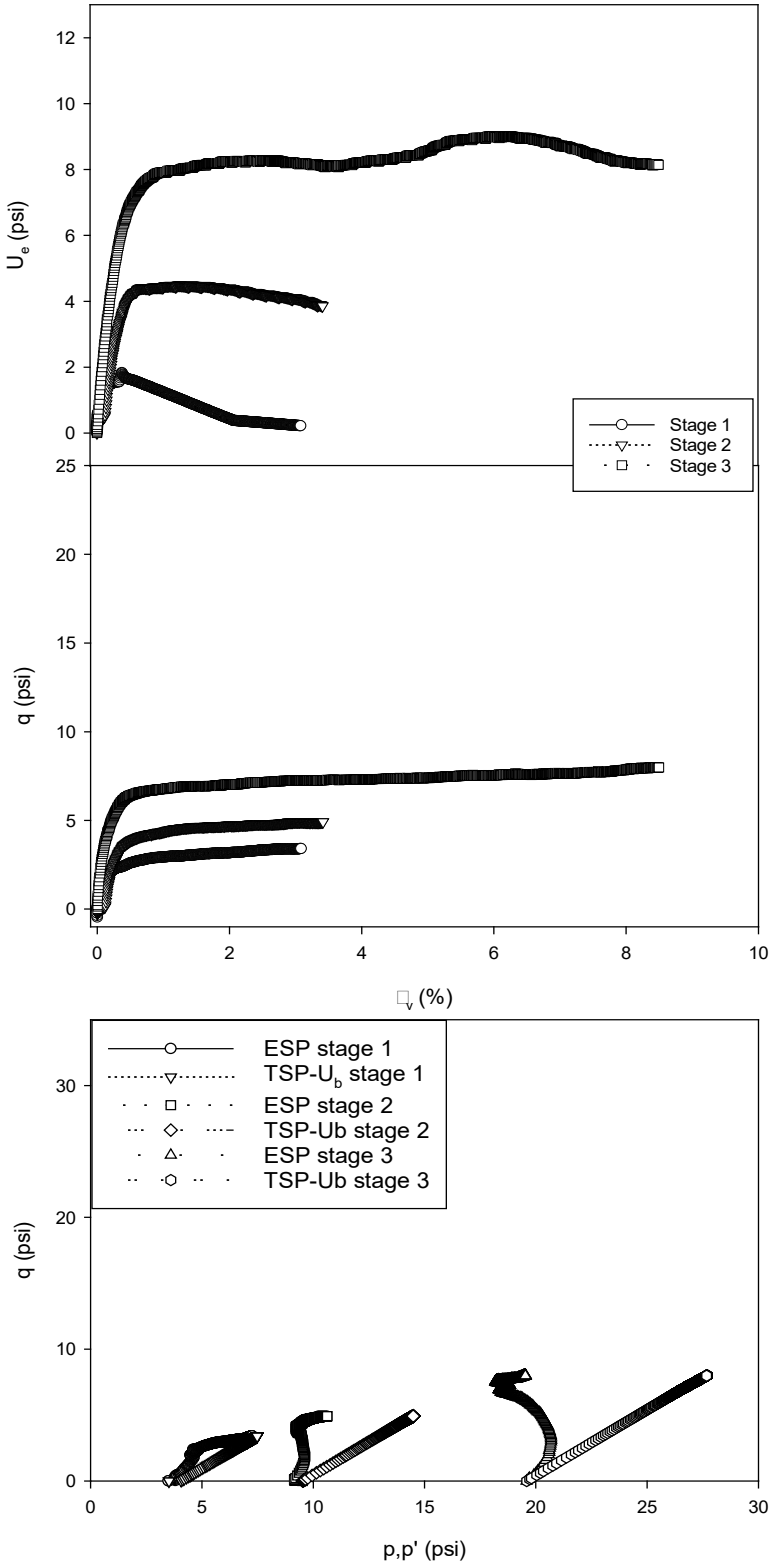

Figure C 14. Triaxial testing results for Site 4 depth 3.8 ft

Appendix D: Tabulated data

Seismic Data:

Table D 1. Summary of shear wave velocity results for test sites 1,2 and 3

Site No	Site Name	Saturation Conditions	Depth Range (ft)	w_n (%)	ΔT_{R2-R1} (ms)	L_{R2}-L_{R1} (ft)	Shear wave velocity (ft/s)
1	Curtis	Dry	6-9	18	2.14	3	1401
1	Curtis	Dry	12-15		3.88	3	773
1	Curtis	Wet	8-10	21	2.39	2	838
1	Curtis	Wet	10-12	23	2.79	2	716
1	Curtis	Wet	28-30		2.14	2	936
1	Curtis	Wet	30-32		2.66	2	751
2	Lake Hefner	Dry	0-2	15	3.38	2	592
2	Lake Hefner	Dry	2-4	18	4.27	2	468
2	Lake Hefner	Dry	4-6	16	3.94	2	508
2	Lake Hefner	Dry	6-8	18	3.10	2	645
2	Lake Hefner	Wet	0-3	22	7.46	3	402
2	Lake Hefner	Wet	3-6	20	5.60	3	536
3	Muskogee	Dry	0-2	11	1.96	2	1020
3	Muskogee	Dry	2-4	23	2.63	2	761
3	Muskogee	Dry	4-6	22	1.55	2	1287
3	Muskogee	Dry	6-8	19	3.57	2	560
3	Muskogee	Dry	8-10		3.06	2	653
3	Muskogee	Dry	10-12		3.58	2	558
3	Muskogee	Dry	12-14		3.71	2	539
3	Muskogee	Wet	0-2	23	4.20	2	476
3	Muskogee	Wet	2-4	26	2.67	2	749
3	Muskogee	Wet	4-6	25	4.42	2	452
3	Muskogee	Wet	6-8	19	3.11	2	644
3	Muskogee	Wet	8-10	18	3.53	2	566
3	Muskogee	Wet	10-12		4.50	2	444
3	Muskogee	Wet	12-14		3.97	2	504
3	Muskogee	Wet	14-16		3.80	2	526

Table D 2. Summary of shear wave velocity results for test sites 4

Site No	Site Name	Saturation Conditions	Depth Range (ft)	w_n (%)	ΔT_{R2-R1} (ms)	$L_{R2}-L_{R1}$ (ft)	Shear wave velocity (ft/s)
4	Wagoner	Dry	0-2	26	2.56	2	782
4	Wagoner	Dry	2-4	26	2.40	2	832
4	Wagoner	Dry	4-6	25	2.20	2	911
4	Wagoner	Dry	6-8	24	2.04	2	978
4	Wagoner	Dry	8-10	25	1.81	2	1106
4	Wagoner	Dry	10-12	26	2.48	2	808
4	Wagoner	Dry	12-14		2.71	2	738
4	Wagoner	Dry	14-16	25	2.54	2	788
4	Wagoner	Dry	16-18		3.08	2	649
4	Wagoner	Dry	18-20		3.28	2	609
4	Wagoner	Dry	20-22		3.47	2	577
4	Wagoner	Dry	22-24		3.54	2	565
4	Wagoner	Dry	24-26		3.58	2	559
4	Wagoner	Dry	26-28		3.47	2	576
4	Wagoner	Wet	0-2	26	1.83	2	1095
4	Wagoner	Wet	2-4	30	2.35	2	850
4	Wagoner	Wet	4-6	27	2.08	2	962
4	Wagoner	Wet	6-8	28	2.35	2	850
4	Wagoner	Wet	8-10	26	2.15	2	931
4	Wagoner	Wet	10-12	27	2.13	2	941
4	Wagoner	Wet	12-14	27	2.33	2	858
4	Wagoner	Wet	14-16		2.87	2	697
4	Wagoner	Wet	16-18	24	3.13	2	638
4	Wagoner	Wet	18-20	25	3.36	2	595
4	Wagoner	Wet	20-22		3.73	2	536
4	Wagoner	Wet	22-24		3.68	2	543
4	Wagoner	Wet	24-26		3.90	2	513
4	Wagoner	Wet	26-28		3.65	2	548

Table D 3. Summary of shear wave velocity results for test sites 5, 6 and 7

Site No	Site Name	Saturation Conditions	Depth Range (ft)	w_n (%)	ΔT_{R2-R1} (ms)	$L_{R2}-L_{R1}$ (ft)	Shear wave velocity (ft/s)
5	Hobart	Dry	0-2	27	3.05	2	655
5	Hobart	Dry	2-4	21	2.15	2	931
5	Hobart	Dry	4-6	22	2.16	2	925
5	Hobart	Dry	6-8	22	1.91	2	1048
5	Hobart	Dry	8-10		1.93	2	1037
5	Hobart	Dry	10-12		1.93	2	1036
5	Hobart	Wet	0-2	27	2.40	2	833
5	Hobart	Wet	2-4	24	2.07	2	964
5	Hobart	Wet	4-6	23	2.33	2	859
5	Hobart	Wet	6-8	23	2.21	2	906
5	Hobart	Wet	8-10		2.11	2	947
5	Hobart	Wet	10-12		2.16	2	928
6	Wewoka	Dry	2-4	18	1.87	2	1070
6	Wewoka	Dry	6-8	10	1.70	2	1174
6	Wewoka	Dry	8-10	20	2.02	2	991
6	Wewoka	Dry	10-12		1.23	2	1632
6	Wewoka	Dry	12-14		1.61	2	1240
6	Wewoka	Wet	2-4	26	5.56	2	360
6	Wewoka	Wet	6-8	21	1.93	2	1035
6	Wewoka	Wet	8-10	22	1.92	2	1041
6	Wewoka	Wet	10-12		4.57	2	438
7	Norman MY	Dry	8-10	19	2.93	2	682
7	Norman MY	Dry	10-12	15	2.42	2	826
7	Norman MY	Wet	6-9	19	4.57	3	657
7	Norman MY	Wet	9-12	19	4.41	3	681

Table D 4. Summary of shear wave velocity results for test sites 8 and 9

Site No	Site Name	Saturation Condition	Depth range (ft)	w_n (%)	ΔT_{R2-R1} (ms)	L_{R2}-L_{R1} (ft)	Shear wave velocity (ft/s)
8	Fairview	Dry	0-2	15	2.75	2	728
8	Fairview	Dry	2-4	18	1.83	2	1090
8	Fairview	Dry	4-6	17	1.72	2	1165
8	Fairview	Dry	6-8	18	1.70	2	1177
8	Fairview	Dry	8-10	21	1.88	2	1066
8	Fairview	Dry	10-12	20	2.25	2	890
8	Fairview	Wet	0-2	21	2.54	2	788
8	Fairview	Wet	2-4	19	1.70	2	1179
8	Fairview	Wet	4-6	23	1.66	2	1205
8	Fairview	Wet	6-8	31	7.58	2	264
8	Fairview	Wet	8-10	22	1.87	2	1067
8	Fairview	Wet	10-12	28	1.88	2	1066
9	Fears	Dry	0-2	17	2.09	2	958
9	Fears	Dry	4-6	13	1.40	2	1425
9	Fears	Dry	8-10	18	2.02	2	991
9	Fears	Wet	0-2	27	3.26	2	614
9	Fears	Wet	4-6	23	3.05	2	655
9	Fears	Wet	8-10	19	1.92	2	1041

Soil Behaviour Type (SBT) Data:

Table D 5. SBT classification based on wet Q_{tn}, F_r and I_c values for site number 1 Curtis

Depth (ft)	Q_{tn} wet period (unitless)	F_r wet period (unitless)	I_c wet period (unitless)	Zone	Classification
1	1323.4	0.56	1.56	7	Gravelly Sands
2	590.1	0.70	1.36	7	Gravelly Sands
3	217.2	0.52	1.74	6	Sands
4	108.3	0.41	1.91	6	Sands
5	96.6	0.45	2.00	6	Sands
6	95.9	0.38	2.03	6	Sands
7	105.7	0.92	1.90	6	Sands
8	58.2	3.12	2.09	5	Sandy Mixtures
9	66.2	3.06	2.06	5	Sandy Mixtures
10	62.1	3.18	2.13	5	Sandy Mixtures
11	84.2	3.33	1.97	5	Sandy Mixtures
12	213.8	1.22	1.59	6	Sands
13	127.2	1.81	1.78	6	Sands
14	85.9	2.01	1.92	5	Sandy Mixtures
15	132.1	1.15	1.75	6	Sands
16	140.9	1.23	1.73	6	Sands
17	124.5	1.23	1.77	6	Sands
18	98.7	1.14	1.85	6	Sands
19	87.2	1.14	1.89	6	Sands
20	88.2	1.37	1.92	5	Sandy Mixtures
21	115.4	1.27	1.80	6	Sands
22	114.9	1.53	1.80	6	Sands
23	42.4	5.00	2.26	4	Silt Mix
24	24.5	3.73	2.42	4	Silt Mix
25	30.2	2.13	2.32	5	Sandy Mixtures
26	33.3	4.23	2.33	4	Silt Mix
27	23.0	5.67	2.50	4	Silt Mix
28	18.3	3.70	2.53	4	Silt Mix
29	19.6	3.79	2.51	4	Silt Mix
30	23.2	4.25	2.46	4	Silt Mix
31	48.2	3.56	2.17	5	Sandy Mixtures

Table D 6 SBT classification based on dry Q_{tn}, F_r and I_c values for site number 1 Curtis

Depth (ft)	Q_{tn} dry period (unitless)	F_r dry period (unitless)	I_c dry period (unitless)	Zone	Classification
1	2060.7	0.46	1.18	7	Gravelly Sands
2	824.8	1.33	1.25	6	Sands
3	181.7	1.04	1.66	6	Sands
4	110.3	0.97	1.81	6	Sands
5	98.6	0.98	1.85	6	Sands
6	73.9	1.08	1.98	5	Sandy Mixtures
7	74.6	1.65	1.97	5	Sandy Mixtures
8	38.2	2.00	2.21	5	Sandy Mixtures
9	28.6	4.57	2.43	4	Silt Mix
10	29.9	3.68	2.36	4	Silt Mix
11	81.0	4.42	2.05	5	Sandy Mixtures
12	186.2	1.64	1.65	6	Sands
13	110.5	2.07	1.84	5	Sandy Mixtures
14	69.8	3.52	2.04	5	Sandy Mixtures
15	111.7	1.52	1.81	6	Sands
16	132.1	1.53	1.75	6	Sands
17	110.5	1.63	1.82	6	Sands
18	96.4	1.46	1.86	6	Sands
19	80.1	1.54	1.93	5	Sandy Mixtures
20	84.9	1.55	1.91	5	Sandy Mixtures
21	93.8	1.49	1.88	6	Sands
22	125.5	1.51	1.77	6	Sands
23	98.9	1.95	1.87	6	Sands
24	21.7	4.86	2.51	4	Silt Mix
25	17.5	4.39	2.57	4	Silt Mix
26	33.1	3.90	2.34	4	Silt Mix
27	38.7	4.02	2.31	4	Silt Mix
28	15.9	3.73	2.59	4	Silt Mix
29	18.2	4.09	2.55	4	Silt Mix
30	28.4	4.95	2.42	4	Silt Mix
31	44.4	3.85	2.21	4	Silt Mix

Table D 7. SBT classification based on wet Q_{tn}, F_r and I_c values for site number 2 Lake Hefner

Depth (ft)	Q_{tn} wet period (unitless)	F_r wet period (unitless)	I_c wet period (unitless)	Zone	Classification
1	271.6	3.76	1.64	8	Very stiff OC sand to clayey sand
2	104.5	4.35	2.1	8	Very stiff OC sand to clayey sand
3	86.3	5.30	1.67	9	Very stiff OC clay to silt
4	316.1	5.30	1.8	9	Very stiff OC clay to silt
5	595.4	5.32	1.97	9	Very stiff OC clay to silt
6	502.8	4.52	1.8	9	Very stiff OC clay to silt
7					

Table D 8 SBT classification based on dry Q_{tn}, F_r and I_c values for site number 2 Lake Hefner

Depth (ft)	Q_{tn} dry period (unitless)	F_r dry period (unitless)	I_c dry period (unitless)	Zone	Classification
1	621.9	1.28	1.97	6	Sands
2	343.4	2.85	1.45	8	Very stiff OC sand to clayey sand
3	210.4	4.32	2.1	8	Very stiff OC sand to clayey sand
4	125.1	3.88	2.1	5	Sandy Mixtures
5	171.5	2.66	2.2	5	Sandy Mixtures
6	323.3	1.81	2.3	6	Sands
7	380.3	2.73	1.96	8	Very stiff OC sand to clayey sand

Table D 9. SBT classification based on wet Q_{tn}, F_r and I_c values for site number 4 Wagoner

Depth (ft)	Q_{tn} wet period (unitless)	F_r wet period (unitless)	I_c wet period (unitless)	Zone	Classification
1	23.5	0.84	1.99	5	Sandy Mixtures
2	23.5	1.29	2.15	4	Silt Mix
3	15.1	1.58	2.52	4	Silt Mix
4	14.1	0.74	2.54	5	Sandy Mixtures
5	7.3	0.86	2.86	4	Silt Mix
6	21.2	1.73	2.35	5	Sandy Mixtures
7	21.1	1.90	2.36	4	Silt Mix
8	14.2	3.77	2.61	4	Silt Mix
9	16.9	2.48	2.50	4	Silt Mix
10	16.9	3.26	2.52	4	Silt Mix
11	17.3	3.24	2.52	4	Silt Mix
12	18.3	3.25	2.50	4	Silt Mix
13	16.4	3.33	2.56	4	Silt Mix
14	17.0	3.02	2.53	4	Silt Mix
15	15.2	3.18	2.60	4	Silt Mix
16	16.1	3.16	2.57	4	Silt Mix
17	15.7	3.95	2.60	4	Silt Mix
18	14.0	3.59	2.65	4	Silt Mix
19	13.9	3.08	2.64	4	Silt Mix
20	13.2	1.94	2.62	4	Silt Mix
21	11.8	1.97	2.69	4	Silt Mix
22	9.8	1.39	2.73	4	Silt Mix
23	15.5	0.73	2.59	5	Sandy Mixtures
24	20.3	0.74	2.49	5	Sandy Mixtures
25	35.7	0.52	2.29	5	Sandy Mixtures

Table D 10 SBT classification based on dry Q_{tn}, F_r and I_c values for site number 4 Wagoner

Depth (ft)	Q_{tn} dry period (unitless)	F_r dry period (unitless)	I_c dry period (unitless)	Zone	Classification
1	204.4	2.39	1.65	6	Sands
2	71.1	5.63	2.09	4	Silt Mix
3	49.9	5.44	2.21	4	Silt Mix
4	32.0	4.53	2.35	4	Silt Mix
5	30.6	4.86	2.38	4	Silt Mix
6	27.2	4.80	2.42	4	Silt Mix
7	25.8	5.31	2.44	4	Silt Mix
8	22.5	6.70	2.53	3	Clays
9	24.2	5.75	2.48	4	Silt Mix
10	22.4	5.96	2.51	4	Silt Mix
11	21.2	5.68	2.53	4	Silt Mix
12	19.8	5.15	2.54	4	Silt Mix
13	18.6	5.98	2.58	4	Silt Mix
14	16.5	6.24	2.63	3	Clays
15	17.1	6.42	2.62	3	Clays
16	15.2	5.96	2.66	3	Clays
17	15.2	5.19	2.64	3	Clays
18	14.8	5.91	2.66	3	Clays
19	15.5	4.36	2.61	3	Clays
20	12.4	4.09	2.69	3	Clays
21	7.8	3.71	2.86	3	Clays
22	8.4	3.01	2.82	3	Clays
23	5.4	3.12	2.99	3	Clays
24	4.4	3.06	3.07	3	Clays
25	11.5	1.66	2.69	4	Silt Mix
26	13.8	2.17	2.62	4	Silt Mix
27	21.4	1.79	2.52	5	Sandy Mixtures
28	50.8	0.95	2.08	5	Sandy Mixtures

Table D 11. SBT classification based on wet Q_{tn}, F_r and I_c values for site number 3 Muskogee

Depth (ft)	Q_{tn} wet period (unitless)	F_r wet period (unitless)	I_c wet period (unitless)	Zone	Classification
1	133.9	1.8	1.3	5	Sandy Mixtures
2	271.1	2.2	1.2	6	Sands
3	50.0	5.5	2.0	4	Silt Mix
4	38.8	4.7	2.1	4	Silt Mix
5	36.4	3.9	2.1	4	Silt Mix
6	40.2	3.0	2.1	5	Sandy Mixtures
7	48.1	3.1	2.1	5	Sandy Mixtures
8	39.7	4.3	2.2	5	Sandy Mixtures
9	43.7	3.1	2.1	5	Sandy Mixtures
10	43.0	4.0	2.2	4	Silt Mix
11	40.1	3.8	2.2	4	Silt Mix
12	42.5	3.8	2.2	4	Silt Mix
13	45.5	4.2	2.2	4	Silt Mix
14	48.2	4.5	2.2	4	Silt Mix

Table D 12 SBT classification based on dry Q_{tn}, F_r and I_c values for site number 3 Muskogee

Depth (ft)	Q_{tn} dry period (unitless)	F_r dry period (unitless)	I_c dry period (unitless)	Zone	Classification
1	306.8	1.30	1.15	6	Sands
2	60.8	5.64	1.87	4	Silt Mix
3	45.9	2.93	2.30	5	Sandy Mixtures
4	42.6	2.97	2.02	5	Sandy Mixtures
5	46.8	2.82	2.00	5	Sandy Mixtures
6	69.4	2.96	1.88	5	Sandy Mixtures
7	66.6	3.01	1.92	5	Sandy Mixtures

Depth (ft)	Q_{tn} dry period (unitless)	F_r dry period (unitless)	I_c dry period (unitless)	Zone	Classification
8	52.0	5.07	2.10	4	Silt Mix
9	63.6	3.31	1.98	5	Sandy Mixtures
10	64.1	3.17	1.97	5	Sandy Mixtures

Table D 13. SBT classification based on wet Q_{tn}, F_r and I_c values for site number 5 Hobart

Depth (ft)	Q_{tn} wet period (unitless)	F_r wet period (unitless)	I_c wet period (unitless)	Zone	Classification
1	38.0	1.05	1.88	5	Sandy Mixtures
2	39.9	0.70	1.99	5	Sandy Mixtures
3	39.7	1.39	2.07	5	Sandy Mixtures
4	45.4	2.17	2.03	5	Sandy Mixtures
5	41.7	2.39	2.06	5	Sandy Mixtures
6	36.2	2.80	2.14	5	Sandy Mixtures
7	19.2	6.45	2.58	4	Silt Mix
8	43.4	3.80	2.16	5	Sandy Mixtures
9	44.3	4.78	2.20	4	Silt Mix
10	22.1	4.40	2.63	4	Silt Mix
11	112.9	4.43	1.86	8	Very stiff OC sand to clayey sand
12	128.4	3.18	1.79	5	Sandy Mixtures

Table D 14 SBT classification based on dry Q_{tn}, F_r and I_c values for site number 5 Hobart

Depth (ft)	Q_{tn} dry period (unitless)	F_r dry period (unitless)	I_c dry period (unitless)	Zone	Classification
1	77.5	0.04	1.43	6	Sands
2	77.3	0.39	1.59	6	Sands
3	73.6	0.81	1.69	6	Sands
4	68.3	1.29	1.96	5	Sandy Mixtures

Depth (ft)	Q_{tn} dry period (unitless)	F_r dry period (unitless)	I_c dry period (unitless)	Zone	Classification
5	55.6	1.06	1.89	5	Sandy Mixtures
6	44.4	1.91	2.08	5	Sandy Mixtures
7	42.6	2.06	2.11	5	Sandy Mixtures
8	33.2	2.48	2.22	5	Sandy Mixtures
9	41.4	2.54	2.18	5	Sandy Mixtures
10	48.6	2.41	2.22	5	Sandy Mixtures
11	101.7	2.29	1.86	5	Sandy Mixtures
12	123.5	1.83	1.95	5	Sandy Mixtures
13	124.0	1.79	1.78	5	Sandy Mixtures
14	93.9	1.86	1.87	5	Sandy Mixtures
15	103.1	2.06	1.86	5	Sandy Mixtures

Table D 15. SBT classification based on wet Q_{tn}, F_r and I_c values for site number 7 Norman Maintenance yard

Depth (ft)	Q_{tn} wet period (unitless)	F_r wet period (unitless)	I_c wet period (unitless)	Zone	Classification
1	809.4	0.02	2.67	7	Gravelly Sands
2	122.7	0.25	2.45	6	Sands
3	117.5	0.25	1.47	6	Sands
4	93.8	0.42	1.58	6	Sands
5	83.2	0.44	1.72	6	Sands
6	69.3	0.46	1.98	6	Sands
7	27.6	0.66	1.90	5	Sandy Mixtures
8	19.6	1.29	2.26	5	Sandy Mixtures
9	12.9	1.15	2.33	5	Sandy Mixtures
10	12.8	0.94	2.59	4	Silt Mix
11	16.8	0.91	2.61	5	Sandy Mixtures
12	37.5	2.88	2.30	4	Silt Mix
13	79.8	3.47	2.21	5	Sandy Mixtures

Depth (ft)	Q_{tn} wet period (unitless)	F_r wet period (unitless)	I_c wet period (unitless)	Zone	Classification
14	34.3	3.48	2.19	4	Silt Mix
15	37.1	4.24	2.27	4	Silt Mix
16	49.4	2.33	1.99	5	Sandy Mixtures
17	86.3	1.83	1.99	5	Sandy Mixtures
18	89.3	1.47	2.39	5	Sandy Mixtures
19	16.3	1.96	2.45	4	Silt Mix
20	26.6	2.67	2.45	4	Silt Mix
21	24.1	1.05	1.96	5	Sandy Mixtures
22	68.3	2.48	2.64	5	Sandy Mixtures
23	100.3	1.58	2.57	6	Sands
24	14.9	0.98	2.06	5	Sandy Mixtures
25	11.5	0.70	1.91	5	Sandy Mixtures
26	44.8	0.71	1.75	5	Sandy Mixtures
27	44.9	0.61	1.69	5	Sandy Mixtures
28	74.7	0.52	1.71	5	Sandy Mixtures
29	199.5	0.52	1.66	6	Sands
30	197.7	0.44	1.74	6	Sands

Table D 16 SBT classification based on dry Q_{tn}, F_r and I_c values for site number 7 Norman Maintenance yard

Depth (ft)	Q_{tn} dry period (unitless)	F_r dry period (unitless)	I_c dry period (unitless)	Zone	Classification
1	199.8	0.64	1.20	6	Sands
2	279.8	1.01	1.20	6	Sands
3	142.5	1.08	1.41	6	Sands
4	84.5	0.98	1.66	6	Sands
5	75.3	0.86	1.75	6	Sands
6	80.2	0.83	1.77	6	Sands
7	63.7	1.29	1.88	5	Sandy Mixtures

Depth (ft)	Q_{tn} dry period (unitless)	F_r dry period (unitless)	I_c dry period (unitless)	Zone	Classification
8	25.6	2.39	2.33	4	Silt Mix
9	19.0	2.08	2.44	4	Silt Mix
10	10.9	2.94	2.72	3	Clays
11	18.7	1.97	2.45	4	Silt Mix
12	35.9	2.03	2.20	5	Sandy Mixtures
13	37.9	2.79	2.21	5	Sandy Mixtures
14	25.6	2.85	2.39	4	Silt Mix
15	25.6	2.23	2.36	4	Silt Mix
16	43.1	1.67	2.15	5	Sandy Mixtures
17	35.2	1.02	2.26	5	Sandy Mixtures
18	15.2	1.51	2.58	4	Silt Mix
19	20.3	1.19	2.49	5	Sandy Mixtures
20	13.3	1.69	2.62	4	Silt Mix
21	52.9	0.70	2.13	5	Sandy Mixtures
22	14.9	2.20	2.59	4	Silt Mix
23	50.4	0.87	2.24	5	Sandy Mixtures
24	52.9	0.75	2.12	5	Sandy Mixtures
25	121.1	1.14	1.88	6	Sands

Table D 17. SBT classification based on wet Q_{tn}, F_r and I_c values for site number 9 Fears Lab

Depth (ft)	Q_{tn} wet period (unitless)	F_r wet period (unitless)	I_c wet period (unitless)	Zone	Classification
1	649.1	1.90	1.30	8	Very stiff OC sand to clayey sand
2	148.9	2.60	1.75	5	Sandy Mixtures
3	104.3	4.47	1.94	8	Very stiff OC sand to clayey sand
4	121.1	5.08	1.93	9	Very stiff OC clay to silt

Depth (ft)	Q_{tn} wet period (unitless)	F_r wet period (unitless)	I_c wet period (unitless)	Zone	Classification
5	83.5	5.58	2.04	9	Very stiff OC clay to silt
6	50.9	5.16	2.20	5	Sandy Mixtures
7	31.6	3.38	2.32	4	Silt Mix
8	18.6	1.87	2.51	4	Silt Mix
9	34.9	2.77	2.28	4	Silt Mix
10	99.4	1.36	1.85	6	Sands
11	115.5	0.78	1.79	6	Sands
12	59.4	3.02	2.12	5	Sandy Mixtures
13	30.1	3.76	2.35	4	Silt Mix
14	33.7	2.91	2.30	5	Sandy Mixtures
15	13.3	4.42	2.68	3	Clays
16	52.8	4.94	2.20	4	Silt Mix

Table D 18 SBT classification based on dey Qtn, Fr and Ic values for site number 9 Fears Lab

Depth (ft)	Q_{tn} dry period (unitless)	F_r dry period (unitless)	I_c dry period (unitless)	Zone	Classification
1	735.3	0.33	2.01	7	Gravelly Sands
2	153.1	1.45	2.06	6	Sands
3	155.4	2.27	1.79	6	Sands
4	116.6	3.78	1.88	8	Very stiff OC sand to clayey sand
5	73.1	4.57	2.06	5	Sandy Mixtures
6	46.9	3.80	2.19	4	Silt Mix
7	31.9	3.19	2.33	4	Silt Mix
8	35.1	1.89	2.24	5	Sandy Mixtures
9	40.4	1.53	2.22	5	Sandy Mixtures
10	124.9	0.63	1.79	6	Sands

Depth (ft)	Q_{tn} dry period (unitless)	F_r dry period (unitless)	I_c dry period (unitless)	Zone	Classification
11	128.2	0.51	1.78	6	Sands
12	112.8	0.56	1.82	6	Sands
13	28.9	2.26	2.32	4	Silt Mix
14	47.5	2.29	2.18	5	Sandy Mixtures
15	26.3	3.65	2.42	5	Sandy Mixtures
16	61.9	3.75	2.16	5	Sandy Mixtures

Table D 19. SBT classification based on wet Q_{tn}, F_r and I_c values for site number 8 Fairview

Depth (ft)	Q_{tn} wet period (unitless)	F_r wet period (unitless)	I_c wet period (unitless)	Zone	Classification
1	350.7	1.0	1.8	6	Sands
2	223.3	2.3	1.6	6	Sands
3	108.1	2.8	2.0	5	Sandy Mixtures
4	74.3	3.7	2.0	5	Sandy Mixtures
5	32.2	3.1	2.3	4	Silt Mix
6	21.7	2.0	2.5	4	Silt Mix
7	13.9	2.0	2.7	4	Silt Mix
8	13.6	3.2	2.8	3	Clays
9	13.6	1.6	2.7	4	Silt Mix
10	18.1	1.6	2.5	4	Silt Mix
11	41.9	4.4	2.2	4	Silt Mix
12	141.4	4.5	1.8	8	Very stiff OC sand to clayey sand

Table D 20 SBT classification based on dry Q_{tn}, F_r and I_c values for site number 8 Fairview

Depth (ft)	Q_{tn} dry period (unitless)	F_r dry period (unitless)	I_c dry period (unitless)	Zone	Classification
1	182.3	0.3	1.7	6	Sands
2	66.2	2.2	2.0	5	Sandy Mixtures
3	77.4	3.7	2.0	5	Sandy Mixtures
4	28.6	6.2	2.4	3	Clays
5	72.2	2.9	2.0	5	Sandy Mixtures
6	45.6	3.6	2.2	5	Sandy Mixtures

Depth (ft)	Q_{tn} dry period (unitless)	F_r dry period (unitless)	I_c dry period (unitless)	Zone	Classification
7	41.3	2.5	2.2	5	Sandy Mixtures
8	18.2	2.4	2.5	4	Silt Mix
9	29.5	2.7	2.3	4	Silt Mix
10	44.3	2.9	2.2	5	Sandy Mixtures
11	45.5	4.1	2.2	4	Silt Mix
12	101.5	4.7	2.0	8	Very stiff OC sand to clayey sand
13	73.7	4.8	2.1	5	Sandy Mixtures

Table D 21. SBT classification based on wet Q_{tn}, F_r and I_c values for site number 6 Wewoka

Depth (ft)	Q_{tn} wet period (unitless)	F_r wet period (unitless)	I_c wet period (unitless)	Zone	Classification
1	350.2	1.7	1.5	6	Sands
2	36.2	3.2	2.0	5	Sandy Mixtures
3	14.1	1.9	2.5	4	Silt Mix
4	10.0	4.3	2.7	3	Clays
5	15.0	4.0	2.5	3	Clays
6	31.7	4.5	2.3	4	Silt Mix
7	33.2	5.3	2.3	4	Silt Mix
8	29.1	5.7	2.4	4	Silt Mix
9	25.3	5.5	2.4	4	Silt Mix
10	25.9	3.5	2.4	4	Silt Mix
11	25.5	3.7	2.4	4	Silt Mix

Table D 22 SBT classification based on dry Q_{tn}, F_r and I_c values for site number 6 Wewoka

Depth (ft)	Q_{tn} dry period (unitless)	F_r dry period (unitless)	I_c dry period (unitless)	Zone	Classification
1	906.4	0.1	2.3	7	Gravelly Sands
2	529.3	0.1	2.3	7	Gravelly Sands
3	104.3	1.7	1.6	5	Sandy Mixtures
4	75.0	4.5	1.9	4	Silt Mix
5	63.7	5.3	2.0	4	Silt Mix
6	48.2	3.7	2.1	4	Silt Mix
7	50.9	3.0	2.1	5	Sandy Mixtures
8	40.1	3.4	2.2	5	Sandy Mixtures
9	50.2	3.2	2.1	5	Sandy Mixtures
10	50.6	3.5	2.1	5	Sandy Mixtures

Depth (ft)	Q_{tn} dry period (unitless)	F_r dry period (unitless)	I_c dry period (unitless)	Zone	Classification
11	88.2	2.8	1.9	5	Sandy Mixtures
12	74.7	3.3	2.0	5	Sandy Mixtures

Triaxial Testing Data:

Table D 23. Shelby tube samples results for Multi-Stage CIUC Triaxial test

Site Name	Depth (ft)	c' (psi)	ϕ' (°)	γ (pcf)	s_{u1} (psi)	s_{u2} (psi)	s_{u3} (psi)	σ_{31} (psi)	σ_{32} (psi)	σ_{33} (psi)
Wewoka	8.8	3.21	23.2	130.8	16.4	31.0	50.9	6	15	30
Norman	6.6	0.81	29.3	125.1	13.4	32.9	67.4	5	10	30
Norman	8.0	1.10	25.9	127.4	22.3	37.0	67.0	5	10	30
Fears	0.2	2.04	23.8	118.1	7.4	15.6	33.4	1	10	30
Fears	7.1	3.93	17.2	122.7	13.1	14.2	27.0	5	10	30
Hobart	4.0	5.83	11.8	127.7	14.8	17.2	22.7	3	10	25
Hobart	6.3	2.87	26.7	127.4	15.9	25.6	44.4	5	10	30
Fairview	0.5	1.61	40.3	109.5	10.1	15.5	45.5	1	5	15
Fairview	2.2	0.81	39.1	128.7	11.0	15.0	45.0	3	6	15
Fairview	6.5	0.20	14.2	125.5	3.0	7.0	14.0	3	15	30
Fairview	4.3	0.48	24.0	126.7	2.7	17.1	22.9	4	13	30
Wagoner	8.2	5.10	7.2	108.2	11.6	13.5		5	15	30
Wagoner	1.4	3.16	11.0	119.3	4.5	16.1	36.2	1	9	29
Wagoner	7.8	0.05	28.5	110.5	9.1	15.7	32.2	7	14	30
Lake Hefner	0.8	0.41	37.0	128.4	2.2	6.5	8.9	1	6	15
Fairview	2.0	3.50	12.2	125.3	4.1	7.5	10.0	1	10	29
Lake Hefner	6.3	4.08	16.5	110.0	12.5	14.0	20.5	5	10	25
Lake Hefner	8.1	0.71	26.6	115.7	9.3	15.3	33.5	7	15	30
Muskogee	2.6	1.37	25.2	111.2	3.6	10.3	18.6	3	10	21
Fairview	6.4	3.02	16.2	106.1	10.1	12.3	25.9	6	15	30
Wewoka	4.7	3.75	7.9	109.1	11.0	13.2	18.4	4	14	29
Wagoner	8.6	12.5	9.6	111.2	30.7	34.4	41.1	8	15	30